UNIVERSITÀ
DEGLI STUDI
FIRENZE

Corso di Dottorato in Fisica e Astronomia
Dipartimento di Fisica e Astronomia
S.S.D. FIS/03 (Fisica della Materia)

# Perturbation theory for the dynamics of mean-field systems


*Candidate*
Aurelio Patelli

*Supervisor*
Prof. Stefano Ruffo

*PhD Coordinator*
Prof. Roberto Livi



ciclo XXVI, 2011-2013

Università degli Studi di Firenze, Dipartimento di Fisica e Astronomia.

Thesis submitted in partial fulfilment of the requirements for the degree of PhilosophæDoctor in Fisica e Astronomia.

# Acknowledgements

I would like to acknowledge all the people who helped me so much in my research work and in laying the foundations of my PhD project.. A special effort was made for my supervisor, Prof. Stefano Ruffo. He motivated me to study new and interesting fields and encouraged me to interact with other scientists. Moreover, he spent a lot of time in checking the language of this manuscript.

I'm also grateful to the Laboratoire de Physique of the École Normale Supérieure de Lyon for the warm hospitality and to all the professors, visitors, researchers, post-docs and Phd students I had the chance to meet there, especially to the Dr. Thierry Dauxois for being always available. To Cesare Nardini and Rachele Nerattini I would like to reserve my deep gratitude for the long and interesting discussions about science and life.

A special thank goes to the researcher with whom I have collaborated, hoping that this fruitful interaction will continue: Shamik Gupta, Yoshiyuki Yamaguchi, Shun Ogawa, Hugo Touchette, Duccio Fanelli and Pierre de Buyl. I would like also to acknowledge the contribution of all the community at the Center for Complex Systems Dynamics (CSDC) and at the CNR Institute for Complex Systems (ISC).

# Contents


Acknowledgements iii

Contents v

Journal publications 1

Introduction 3

1 Long-range interactions 7
- 1.1 Overview on long-range interacting systems . . . 7
- 1.2 Equilibrium properties of LRI . . . 11
- 1.3 Out of equilibrium properties: the phenomenology . . . 17
  - 1.3.1 Dynamical definition of long-range interactions . . . 20
- 1.4 A paradigmatic model: the Hamiltonian Mean Field model . . . 21

2 Kinetic Theory 29
- 2.1 Introduction . . . 29
- 2.2 Liouville equation . . . 31
- 2.3 BBGKY hierarchy . . . 32
- 2.4 The Vlasov equation . . . 34
- 2.5 Relaxation mechanism of the Vlasov dynamics . . . 36
  - 2.5.1 Non interacting particles . . . 37
  - 2.5.2 Landau damping . . . 40
- 2.6 Lenard-Balescu equation . . . 45
  - 2.6.1 Properties of the Lenard-Balescu equation . . . 48

3 Linear response theory of homogeneous systems 51
- 3.1 Introduction . . . 51
- 3.2 Some introductory remarks . . . 52

3.2.1 Initial homogeneous distribution . . . 53
3.3 Linear Vlasov equation . . . 55
3.3.1 Solution of the homogeneous state in the Fourier-Laplace space . . . 58
3.4 Solution for real times and the time asymptotic regime . . . 59
3.4.1 The water-bag case . . . 62
3.4.2 The long time regime . . . 63
3.5 Numerical results . . . 65
3.5.1 Simulations for single realizations . . . 66
3.5.2 Ensemble average over different realizations . . . 68
3.5.3 Relaxation towards equilibrium . . . 70
3.6 Perturbative theory at second order . . . 70
3.6.1 The HMF case . . . 73
3.7 Conclusions . . . 74

**4 Linear response theory of inhomogeneous systems 77**
4.1 Introduction . . . 77
4.2 Derivation of the response formula . . . 78
4.3 Time asymptotic behaviour . . . 81
4.4 Constraints . . . 83
4.4.1 Mass constraint . . . 84
4.4.2 Energy constraint . . . 84
4.4.3 Implementation of the constraints . . . 85
4.5 Application of the response formula . . . 87
4.5.1 Equilibrium without constraints . . . 88
4.5.2 Equilibrium with the mass constraint . . . 90
4.5.3 Equilibrium with both energy and mass constraints . . . 90
4.5.4 The Fermi-Dirac initial distribution . . . 91
4.6 Numerical comparison . . . 92
4.6.1 Methods . . . 92
4.6.2 Equilibrium . . . 94
4.6.3 Fermi-Dirac distribution . . . 94
4.7 Critical exponents of a mean-field system . . . 94
4.7.1 Dielectric function for inhomogeneous states . . . 97
4.7.2 Jeans initial distribution functions . . . 99
4.7.3 Numerical comparison for the equilibrium distribution . . . 101
4.8 Conclusions . . . 103

**5 Small systems interacting with bigger systems 105**
5.1 Introduction . . . 105
5.2 The model . . . 107
5.3 Leading-order dynamics . . . 110
5.4 Next-to leading order dynamics . . . 112
5.5 Application to the HMF model and corresponding numerical experiments . . . 113
5.6 Conclusions . . . 117

**6 Conclusions 119**
6.1 Summary of contributions . . . 119
6.2 Directions for future work . . . 121

**A 123**
A.1 BBGKY Hierarchy . . . 123
A.2 Fourier and Laplace transform . . . 124
A.3 Riemann-Lebesgue lemma . . . 126
A.3.1 Analytic functions . . . 127
A.4 Principal Value integral . . . 129

**B 131**
B.1 Normalization, energy density, and stability criterion for the Fermi-Dirac distribution (3.7) . . . 131

**C 135**
C.1 Asymptotic time limit of $J_\omega$ . . . 135
C.2 Energy-Casimir considerations . . . 137

**Bibliography 139**

# Journal publications

This work is the result of a research activity that led to the following publications. The specific Chapter in which the paper will be presented is indicated below the references.

Published papers:

- **Linear response theory for long- range interacting systems in quasi-stationary states**
  A. Patelli, S. Gupta, C. Nardini and S. Ruffo
  Physical Review E, 85, 021133, (2012).
  Presented in Chapter 3

- **Absence of thermalization for systems with long-range interactions coupled to a thermal bath**
  P. de Buyl, G. De Ninno, D. Fanelli, C. Nardini, A. Patelli, F. Piazza and Y. Y. Yamaguchi
  Physical Review E, 87, 042110, (2013).
  Presented in Chapter 5

- **Statistical mechanics and dynamics of long-range interacting systems**
  A. Patelli and S. Ruffo
  Rivista di Matematica della Universitá di Parma, 4, (2013), 345-396.
  Part of Chapter 1

- **Large deviations techniques for long-range interactions**
  A. Patelli and S. Ruffo
  *Deviations in physics: the legacy of the law of large numbers three centuries after*, Lecture Notes in Physics, Springer (2013).
  (Eds) F. Cecconi, M. Cencini, A. Puglisi, D. Vergni and A. Vulpiani.
  Part of Chapter 1

- **Non-mean-field critical exponent in a mean-field model: Dynamics versus statistical mechanics**
  S. Ogawa, A. Patelli and Y. Y. Yamaguchi
  arXiv preprint arXiv:1304.2982, (2013), submitted to Physics Review E.
  Presented in Chapter 4

Papers in preparation:

- **Linear response theory for inhomogeneous long-range interacting systems**
  A. Patelli and S. Ruffo
  work in preparation
  Presented in Chapter 4

# Introduction

This work concerns the study of perturbations of the dynamics of mean-field systems. A mean-field system is a many-body system that belongs to the class of systems with long-range interaction, whose dynamics is governed by the Vlasov equation and by kinetic equations like Landau and Lenard-Balescu equations. The time-scale in which long-range interactions converge to equilibrium diverges on system size, $N$. The process which causes thermalization is governed by energy exchange, such as collisions, and this process occurs on time-scales depending algebraically on the size of the system. Consequently, the early dynamics of long-range interacting systems is ruled by the Vlasov equation and in the $N \to \infty$ limit this equation becomes exact. Vlasov equation shows an infinity of stable and stationary solutions which are related to long-living states for finite systems, called Quasi-Stationary States (QSSs).

Our interest in this work is to study the stability and the response with respect to an external field which perturbs the dynamics of QSSs, as shown in Chapters 3, 4 and 5. For finite Hamiltonian systems this study is usually carried out by using Kubo linear response theory for the Liouville equation. This theory describes the variation of observables due to the perturbation when the unperturbed state is the thermal equilibrium. Such variation is related to equilibrium fluctuations through the celebrated fluctuation-dissipation theorem. Indeed, Kubo formula for the response shows that equilibrium statistical fluctuations are proportional to the response to external perturbations.

Having in mind this procedure, in Chapters 3 and 4 we derive the analogue of Kubo linear response theory starting from the Vlasov equation instead of the Liouville equation. The non linear nature of Vlasov equation brings to a more involved linear response formula. The external perturbation induces two sources of response: the first one is the usual Kubo term which relates the variation of the observable to statistical fluctuations, while the second term arises from fluctuations induced in the mean-field interaction.

Vlasov stationary solutions can be either homogeneous or inhomogeneous and this property will play an important role in the solution of the linear response theory. The dynamics of homogeneous states is the dynamics of free particles because the mean-field interaction is zero. Actually, this property ensure a separations of modes of the systems and the theoretical description of the linear Vlasov response can be carried out by using Fourier-Laplace technique, shown in Chapter 3. In this framework Landau shown a form of relaxation of the Vlasov dynamics, called Landau damping. However, modes of inhomogeneous states are coupled and their contribution can be easily separated only for integrable interactions, as shown in Chapter 4. In this case the infinity of constants of motion of the Vlasov dynamics, called Casimirs, constrain the time evolution of the system. For generic interactions we consider an approximate linear theory in which only some of these constants of motion are constrained. However, the dynamics of states close to transition points is strongly affected by the presence of Casimirs, i.e., critical exponents in the Vlasov regime of a mean-field integrable system can be different to classical mean-field critical exponents.

Finally, we will extend in Chapter 5 the linear response theory of the Vlasov equation to different kind of perturbations, such as the action of a big system to a small one.

This manuscript is organized as follows.

In Chapter 1 we will introduce the field of long-range interactions focusing on both equilibrium and out-of-equilibrium features. Specifically, we will expose the main properties of equilibrium states, for which the lack of additivity induces phenomena absent for short-range interacting systems. Moreover, we will argue about out-of-equilibrium features, such as the birth of Quasi-Stationary States. These states motivate the present study, indeed we will perturb a QSS in order to evaluate qualitatively and quantitatively the response of the system and its stability. In the last Section of Chapter 1 we will describe a paradigmatic mean-field model, the Hamiltonian Mean-Field model, which will be used in the following Chapters to verify the theory introduced in our work.

In Chapter 2 we will present a brief survey of Kinetic Theory for long-range interactions. We will justify the range of validity of this theory and the separation of time-scales that allows the definition and the study of QSSs. In detail, we will show the standard procedure used to obtain the Vlasov equation for mean-field systems. On top of that, we will describe the relaxation mechanism which leads to Landau damping. After that, we will comment on the process

which rules relaxation to equilibrium on time-scales that diverge with system size and the properties of the Lenard-Balescu equation, the kinetic equation which governs such process of equilibration.

In Chapter 3 we will discuss the linear response theory of the Vlasov equation for homogeneous initial conditions with respect to an external perturbation. In the first part of this Chapter we will study the theory at the linear order in the size of the perturbation and we will compare the theoretical results with numerical simulations on some representative QSS. In the last part of Chapter 3 we will describe the theory at successive orders in the perturbation, with an emphasis on the second order.

In Chapter 4 we will treat the linear response theory for inhomogeneous states. For such states, the solution of the linear Vlasov equation becomes more complicated due to the coupling of different modes of the system. Linear response theory can be exactly performed for integrable systems, for which a transformation of coordinates separates the contributions of different modes. In this work we will introduce an approximation of linear response theory which can be used for non-integrable systems. We will compare this linear response theory with numerical simulations and with the exact one for an integrable system. In the last Section of Chapter 4 we will discuss a feature of the exact linear response theory for the Hamiltonian Mean-Field model: a broad class of initial states settles down on perturbed QSSs where a conveniently defined susceptibility diverges close to the instability threshold, similarly to second order phase transitions at equilibrium. The study of critical exponents shows a non trivial result induced by Vlasov dynamics.

In Chapter 5 we will discuss the coupling of two mean-field systems interacting via a mean-field term. Specifically, we will study the evolution of a small system coupled to a large one. This latter system will play the role of a reservoir, in analogy with the thermal bath for short-range interactions.

# Chapter 1

# Long-range interactions

*This work concerns the study of many-body systems with Long Range Interactions (LRI). A long range interaction is a two-body conservative interaction whose amplitude goes to zero weakly as the distance between the two bodies increases. This feature introduces peculiar and counter-intuitive properties both in equilibrium and in out-of-equilibrium statistical mechanics. Long range interactions are common in different areas of physics, such as in plasma physics, in astrophysics and in fluid dynamics. They can also appear as effective macroscopic interactions in elasticity, capillarity, etc. While specific behaviors in these different areas seem unrelated, there are some universal features arising from the nature itself of the long range interaction. The first Section is devoted to an introduction to the equilibrium properties of LRI while in the following Sections we discuss the non-equilibrium ones.*

## 1.1 Overview on long-range interacting systems

Long-Range Interacting (LRI) systems are common in nature [32, 44, 97]. Examples come from different areas of study; electromagnetic [48, 72, 88] and gravitational [17, 90, 94, 107] forces are fundamental interactions with a long-range behavior in some regimes. Other kinds of LRI systems are given by coarse grained interactions, such as mean-field [44], elastic [32] or hydrodynamic [24] ones.

There are different definitions of LRI, depending on the properties on which

one focuses the analysis. For instance, in the context of statistical mechanics it is useful to require that the energy is extensive. Extensivity implies that for large systems the energy has to grow linearly with the number of degrees of freedom. Therefore, the potential has to be an integrable function and one assumes that for large distances between the two bodies the LRI decay with a power-law behaviour.

Calling $V(r)$ the potential describing the interaction and $r = |r_1 - r_2|$ the distance between two bodies labelled 1 and 2 we have

$$V(r) \approx \frac{J}{r^\alpha}, \tag{1.1}$$

where $J$ is the coupling constant and $\alpha \geq 0$. This power-law decaying potential determines the extensive properties of the energy of the system. Assuming spherical symmetry. we can write, for a homogeneous system, the energy per volume as

$$e = \frac{E}{\mathrm{V}} = \Omega_{d-1} \int_\delta^R \rho \frac{r^{d-1} dr}{r^\alpha} = \frac{\Omega_{d-1}\rho}{d-\alpha}[R^{d-\alpha} - \delta^{d-\alpha}] \tag{1.2}$$

where $\delta$ is a cut-off at small distances, $R$ is a cut-off at large distances and $\mathrm{V}$ is the volume. $d$ is the dimension of the embedding space for the motion of the particles and $\Omega_d$ is the angular volume in such a $d$-dimensional space. Moreover, $\rho$ is a mass (or charge) density, which becomes a constant in the usual thermodynamic limit. It is then straightforward to check that

- if $\alpha > d$ then $e \to const$ when $R \to \infty$,
- if $0 \leq \alpha \leq d$ then $e \sim \mathrm{V}^{1-\alpha/d}$ ($\mathrm{V} \sim R^d$) .

In terms of the extensive energy $E = e\mathrm{V}$, we find

$$\alpha > d \quad E \sim \mathrm{V} \tag{1.3}$$

$$\alpha \leq d \quad E \sim \mathrm{V}^{2-\alpha/d} , \tag{1.4}$$

and the free energy

$$F = E - TS \quad , \quad S \sim \mathrm{V} , \tag{1.5}$$

with $T$ the intensive temperature and $S$ the entropy, that typically scales linearly with the volume. Therefore, thermodynamic properties of long-range systems are dominated by the energy $E$, which scales with volume $\mathrm{V}$ faster than linear.

A way out from this energy dominance was proposed by Marc Kac. It consists in scaling the coupling constant as

$$J \to J\mathrm{V}^{\alpha/d-1} \ . \tag{1.6}$$

In this way the free energy turns out to be extensive in the volume

$$F \sim \mathrm{V} \ . \tag{1.7}$$

However, this is a "mathematical trick" and doesn't correspond to any physical effect: no interaction that changes its strength when varying the volume is known.

Kac's trick can be adopted only for the sake of performing a meaningful large volume limit. Once the free energy per particle is obtained, the physical description can be retrieved by scaling back the coupling constant.

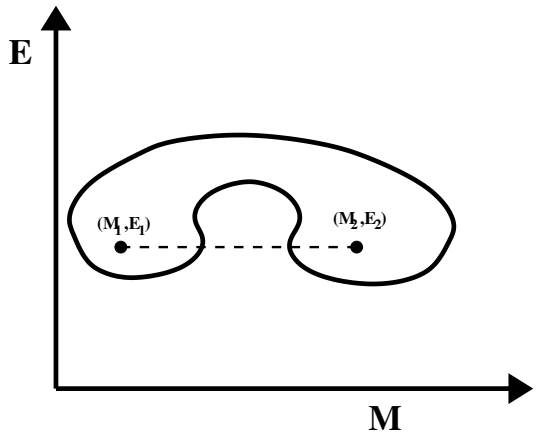


Figure 1.1: Non convex shape of the region of accessible macrostates in the magnetization/energy plane for long-range systems.

Alternatively, one can rescale temperature

$$T \to T\mathrm{V}^{1-\alpha/d} \tag{1.8}$$

and then the free energy scales superlinearly in the volume

$$F \sim \mathrm{V}^{2-\alpha/d} \ . \tag{1.9}$$

Although one can get an extensive energy using Kac's trick, this is not necessarily additive [111]. The violation of additivity is crucial in determining

the thermodynamic properties of systems with long-range interactions [79, 80]. For instance, it determines a violation of convexity of the domain of accessible macrostates. An example is shown in Fig. 1.1, where the boundary of the region of accessible macrostates is represented by the thick line with the shape of a bean. In standard thermodynamics, for short range interactions, all states satisfying

$$E = \lambda E_1 + (1-\lambda)E_2 \quad , \quad M = \lambda M_1 + (1-\lambda)M_2 \quad , \quad 0 \leq \lambda \leq 1 \quad (1.10)$$

must be present at the macroscopic level, because additivity is satisfied. This is in general not true for long-range interactions. This property could determine a violation of ergodicity in the microcanonical ensemble [84], where some configuration cannot be visited.

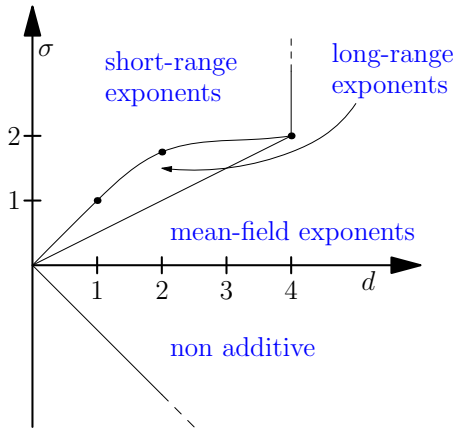


Figure 1.2: Different behaviors of LRI depending on dimension $d$ and the exponent $\sigma = \alpha - d$.

Let us consider power-law potentials, such as (1.1). Defining $\alpha = d + \sigma$ one can identify different regions in the $d, \sigma$ plane (see Fig. 1.2) [52]. The non additive long-range region has $-d \leq \sigma \leq 0$. However, the long-range behavior extends to $\sigma > 0$, although the energy is here additive and Kac's trick is not necessary. It can be shown that, if $0 < \sigma \leq d/2$, the critical behavior is characterized by mean-field (classical) exponents, exactly as for the full region $d > 4$ (any value of $\sigma$). Moreover, in a region $\sigma > d/2$ and below a given line which is only partially known, the system maintains some long-range features, but with non classical $\sigma$-dependent critical exponents. Some points along this line are known. At $d = 1$ the line passes through $\sigma = 1$: indeed in the whole range $0 \leq \sigma \leq 1$ one can have phase transitions in one dimension.

For $d = 2$, numerical simulations show that the line passes through $\sigma = 7/4$. Finally, renormalization group techniques suggest that the line reaches $\sigma = 2$ from below at $d = 4$. Above this line and below $d = 4$ the system becomes short-range.

Another way of implementing the $V \to \infty$ limit is obtained by using Kac potentials [65,99,115]. The length scale of the interaction is finite for any finite system but it grows with the system size. In parallel, the magnitude of the interaction decreases with system size, such as for the Kac's trick. Calling $\lambda$ the length scale, the Kac potential is defined as

$$V(q) = \lambda^{-d}\phi(\lambda q), \tag{1.11}$$

with $\phi$ a smooth function. The thermodynamic limit is hence given by $V = \lambda^d \to \infty$ and leads to the mean-field description [99].

Another kind of definition of LRI comes from dynamical reasons: the force has to be intensive in order to get a mean-field description of the dynamics [25]. For instance, power-law interactions with an exponent $d - 1 < \alpha < d$ have a long-range behavior of the energy, but a mean-field force which scales linearly with the volume without any trick. Hence, requiring a mean-field dynamics is different from requiring a mean-field statistical mechanics [54].

## 1.2 Equilibrium properties of LRI

Long-range interacting systems show intriguing equilibrium features that are not present for short-range ones, such as ensemble inequivalence [113] that implies, for example, negative specific heat [77] in the microcanonical ensemble. Moreover, one-dimensional short-range models cannot have phase transition [103], while LRI contradict this statement and allow phase transition in one dimension [21,47].

The use of canonical ensemble in system with long-range interactions is doubtful, because its classical derivation from the microcanonical ensemble is based on additivity. In the following, we will consider both the microcanonical and the canonical ensemble. In order to justify the use of the canonical distribution for systems with LRI, that are non additive, one must resort to an alternative physical interpretation. For instance, one can consider that the system is in interaction with an external bath of a different nature, e.g. stochastic.

Let us discuss ensemble inequivalence and its most notable feature related to the negative specific heat in the microcanonical ensemble in the case of the

gravitational interaction. In Section 1.4 we will discuss a model which presents a second order phase transition in one dimension.

### Ensemble inequivalence

For systems with long-range interactions statistical ensembles can be inequivalent. For instance, the temperature-energy relation might not be the same in the microcanonical and canonical ensemble. In the microcanonical ensemble specific heat can be negative.

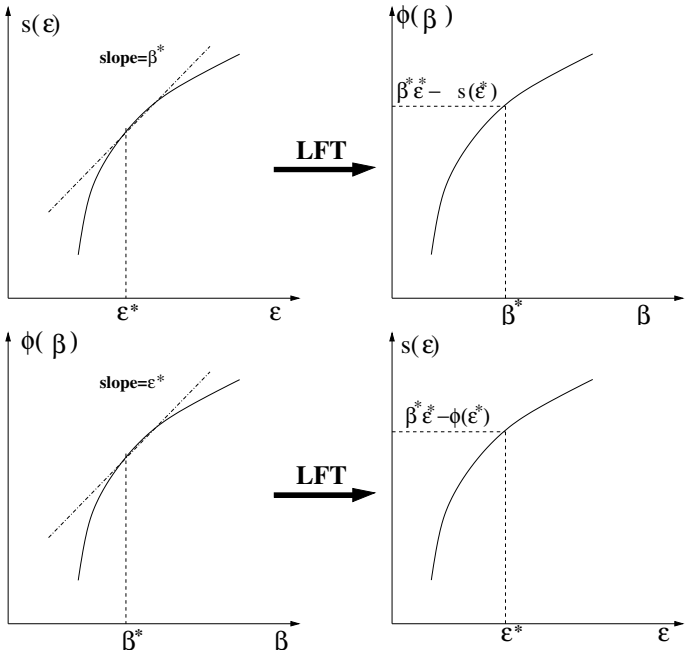


Figure 1.3: Upper panel: Free energy from entropy by a Legendre-Fenchel transform. Lower panel: Entropy from free energy.

Let us first illustrate the case in which ensembles are indeed equivalent. It means that free energy can be obtained by a Legendre-Fenchel transform of entropy and that entropy is itself the Legendre-Fenchel transform of free energy

$$\phi(\beta) = \beta f(\beta) = \inf_{\varepsilon} \left[\beta\varepsilon - s(\varepsilon)\right] \quad , \quad s(\varepsilon) = \inf_{\beta} \left[\beta\varepsilon - \phi(\beta)\right] \ , \tag{1.12}$$

where $f(\beta)$ is the free energy and $\phi(\beta)$ the Massieu potential. This involutive property is shown graphically in Fig. 1.3.

This relation is a consequence of a saddle-point limit $N \to \infty$

$$\begin{aligned} \exp(-\beta N f(\beta)) &= Z(\beta) = \int dE \int \frac{dq^{3N} dp^{3N}}{h^{3N}} \, \delta(H(p,q) - E) \exp(-\beta E) \\ &= \int dE \, \Omega(E) \exp(-\beta E) = N \int d\varepsilon \, \exp\left(-N\left[\beta\varepsilon - s(\varepsilon)\right]\right) \ , \end{aligned} \tag{1.13}$$

where $Z(\beta)$ is the partition function.

At a first order phase transition, entropy has a constant slope in the energy range $[\varepsilon_1, \varepsilon 2]$ (the phase coexistence region), resulting into a free energy with a cusp at the transition inverse temperature $\beta_t$, see Fig. 1.4.

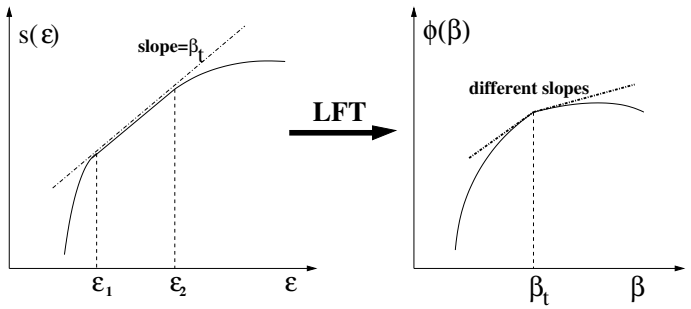


Figure 1.4: Relation between entropy and free energy at a first order phase transition.

A system with a first order phase transition is an extreme case of ensemble equivalence, since there is a continuum of microcanonical states with different energy having the same temperature, specific heat is ill defined and one must introduce the concept of latent heat.

If entropy becomes non concave, as shown in Figs. 1.5 and 1.6, microcanonical and canonical ensemble are not equivalent. The Legendre-Fenchel transform is no more involutive: if applied to the entropy it returns the correct free energy. However, the Legendre-Fenchel transform of free energy does not coincide with entropy but rather with its concave envelope. This is the basic feature causing ensemble inequivalence.

As a side remark, let us observe that Maxwell's equal area condition

$$\int_{\varepsilon_1}^{\varepsilon_2} d\varepsilon(\beta(\varepsilon) - \beta_t) = 0 \tag{1.14}$$

implies (and is a consequence of) free energy continuity at $\beta_t$.

In the case of a phase transition with symmetry breaking, entropy can have two branches, a high energy and a low energy one. For instance, for a ferromagnetic system, the high energy paramagnetic phase with magnetization $m = 0$ and the low energy ferromagnetic phase with $m \neq 0$, see Fig. 1.5. The two branches of the entropy generically cross with two different slopes, i.e. two different temperatures. At a given energy $\varepsilon_t$ two different microcanonical temperatures can coexist, we find a temperature jump. This is not conceptually different from the energy jump (latent heat) found in the canonical ensemble. A temperature jump can only appear in an energy range where entropy is globally convex. In Fig. 1.5 we show a situation where also a region of negative specific heat is present, but this is not necessary for the existence of a temperature jump. The whole region where these peculiar phenomena appear is completely washed out in the canonical ensemble. As shown in Fig. 1.5, after Legendre-Fenchel transform, one obtains a free energy which has the same features as the one modeling a first-order phase transition. It has indeed been conjectured that a necessary condition in order to have negative specific heat and temperature jumps in the microcanonical ensemble is the presence of a first-order transition in the canonical ensemble.

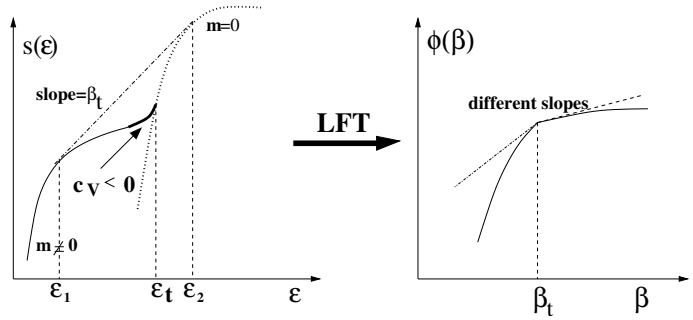


Figure 1.5: Left panel: Microcanonical entropy with negative specific heat and temperature jump in a system with symmetry breaking. Right panel: Corresponding free energy in the canonical ensemble.

In order to better understand the origin of negative specific heat, it is useful to introduce the constrained entropy

$$s(\varepsilon, m) = \lim_{N\to\infty} \frac{\ln \sum_{\{S_i\}} \delta\left(E - H(\{S_i\})\right) \delta\left(Nm - M(\{S_i\})\right)}{N} \,, \qquad (1.15)$$

where $S_i$ is a discrete spin variable (e.g. $S_i = \pm 1$), $M = \sum_i S_i$ is the extensive magnetization and $m = M/N$ the magnetization per spin. In terms of the

constrained entropy, we define the corresponding free energy as

$$\beta f(\beta, \varepsilon, m) = \beta\epsilon - s(\varepsilon, m) \ . \tag{1.16}$$

The microcanonical and canonical variational problems can be defined as follows

$$s(\varepsilon) = \sup_m s(\varepsilon, m) \quad , \quad f(\beta) = \inf_{m,\varepsilon} f(\beta, \varepsilon, m). \tag{1.17}$$

In the canonical extremal problem we seek for values of $\varepsilon$ and $m$ that realise an extremum of $f(\beta)$, while in the microcanonical problem we only maximize over $m$. It can be easily checked that the extrema are the same for the two problems. However, the stability is different. In the microcanonical problem the only condition for stability is $s_{mm} < 0$ (the subscript $mm$ indicates a double derivative with respect to $m$), while in the canonical problem the trace and determinant of the Hessian must be positive, implying that $s_{\varepsilon\varepsilon}$ and $s_{mm}$ are both negative and $s_{\varepsilon m}^2 - s_{\varepsilon\varepsilon}s_{mm} > 0$. The canonical problem is more constrained. It can be shown that the specific heat has the following expression in both the ensembles

$$c_V = \frac{\beta^2 s_{mm}}{(s_{\varepsilon m}^2 - s_{\varepsilon\varepsilon}s_{mm})}, \tag{1.18}$$

which implies that specific heat is always positive in the canonical ensemble, while it can be negative in the microcanonical ensemble at free energy saddles $s_{\varepsilon\varepsilon} > 0$, $s_{mm} < 0$.

### Negative specific heat

The most notable and fundamental example of long-range interaction is gravity, for which the potential energy is

$$U(\overrightarrow{r}_1, \ldots, \overrightarrow{r}_N) = -Gm^2 \sum_{1 \le i < j \le N} \frac{1}{|\overrightarrow{r}_i - \overrightarrow{r}_j|} \tag{1.19}$$

In order to get a finite microcanonical partition sum, one has to confine the self-gravitating system in a box of volume $V$. This is necessary also when doing the statistical mechanics of the perfect gas. Hence,

$$\Omega(E) = \int_V \prod_i d\overrightarrow{r}_i d\overrightarrow{p}_i \delta(E - K - U) \propto \int_V \prod_i d\overrightarrow{r}_i (E-U)^{(3N-2)/2} \ , \tag{1.20}$$

where $K$ is kinetic energy and a first integration over momenta has been performed. The integral in (1.20) behaves as $r_{ij}^{4-3N/2}$ when $r_{ij} = |\overrightarrow{r}_i - \overrightarrow{r}_j| \to 0$, i.e. when two bodies get close. Hence, it diverges for $N \geq 3$, determining a divergence of microcanonical entropy $S(E) = k_B \ln \Omega(E)$ (similarly, the canonical partition function diverges). There is no way to prevent this short-distance divergence other than regularizing Newtonian potential. This can be done in different ways: softening, hard-core, Pauli exclusion. Irrespective of the way gravitational potential is regularized, the non-additive features related to the long-range nature of the interaction persist. These are significantly represented by the presence of negative specific heat. This phenomenon can be heuristically justified using virial theorem, which for the gravitational potential reads

$$< K >= -\frac{1}{2} < U > \quad , \quad < K >= -E \tag{1.21}$$

where $< \cdot >$ denotes a temporal average. Since kinetic energy $K$ is always positive, it is clear that this theorem can only be valid for bound states, for which $E$

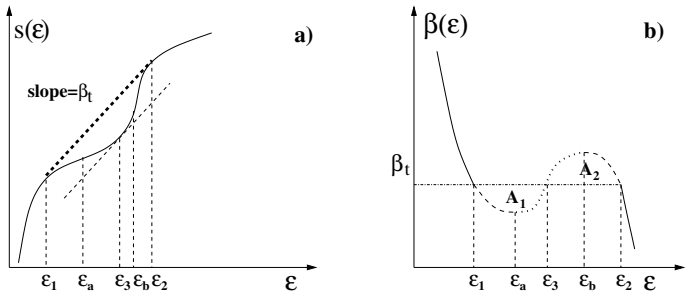


Figure 1.6: Schematic shape of microcanonical entropy per particle $s = S/N$ as a function of energy per particle $\varepsilon = E/N$ (solid line) showing a "globally" convex region in the range $[\varepsilon_1, \varepsilon_2]$, the thick dashed line realizes the "concave envelope". b) Inverse temperature $\beta$ as a function of $\varepsilon$. According to the Maxwell's constructions the areas $A_1$ and $A_2$ are equal. The curve $\beta(\varepsilon)$ represents states that are stable (solid line), unstable (dotted line) and metastable (dashed lines).

is negative. Using equipartition theorem, average kinetic energy is proportional to temperature and, hence, the second identity in (1.21) tells us that specific heat $c_V$, which is proportional to $dE/dT$, is indeed negative. However, this is just handwaving and this type of argument uses plenty of hypotheses. More rigorously, it can be shown that regularized self-gravitating systems confined in a box have an entropy that is a non concave function of the energy, as shown

in Fig. 1.6a. Since specific heat is related to the second derivative of entropy with respect to energy

$$\partial^2 s/\partial \varepsilon^2 = -(c_V T^2)^{-1} \ , \tag{1.22}$$

it follows that in the energy range $[\varepsilon_a, \varepsilon_b]$, where the entropy is convex, specific heat must be negative. For short-range additive interactions all states within the wider range $[\varepsilon_1, \varepsilon_2]$ would have an entropy that is represented by thick dashed line in Fig. 1.6a. In Fig. 1.6b, the inverse temperature $\beta$ is plotted as a function of $\varepsilon$. In the negative specific heat region, temperature decreases as energy increases.

## 1.3 Out of equilibrium properties: the phenomenology

Numerical simulations for a simple mean-field model, the HMF model which will be introduced in Section 1.4 [4, 117], have shown an unusual behavior of the relaxation of the system towards the equilibrium predicted by statistical mechanics. Further numerical experiments on other models have shown that this property in not a peculiarity of the HMF model but, actually, it is a general feature of LRIs. For instance, in plasma theory it has been known since many years [45, 102] that the relaxation time-scale of systems for which the Vlasov approximation is valid, grows with the system size. Actually, a one-dimensional neutral plasma model, the plasma sheet model, shows that the relaxation time grows as $n_d^2$, where $n_d = \rho \lambda_D$ is the number of particles inside a region with a typical length of the order of Debye's length. Inside this range the Vlasov equation gives a good approximation of the dynamics. These phenomena have led to the discovery of long-living states, called *Quasi-Stationary States* (QSS).

In figure 1.7 (such as in figure 3.5) we observe a typical behavior, here shown for a prototypical long-range model, the HMF model, that will be discussed in Section 1.4. The system is initially sampled in a homogeneous state called Water-Bag[1] and with an energy such that the homogeneous phase is not thermodynamically stable. However, the qualitative behavior shown in that figure is representative of many different homogeneous initial states and it is not only a peculiarity of the Water-Bag distribution. Since, the HMF model describes a

[1] See Section 3.2.1 for a precise definition of the Water-Bag distribution

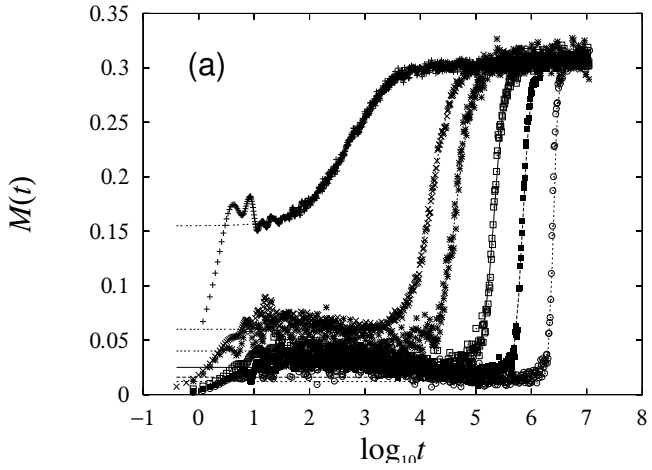


Figure 1.7: Magnetization of the HMF model vs. time (in logarithmic scale) at energy $\varepsilon = 0.69$. From left to right the system size $N$ are $N = 10^2, 10^3, 2 \times 10^3, 5 \times 10^3, 10^4, 2 \times 10^4$.

ferromagnetic system and we monitor the magnetization which probes the homogeneity of the state. In figure 1.7 we plot magnetization versus the logarithm of time. Increasing system size $N$ (here the number of particles), we observe different phases, well represented by the following diagram:

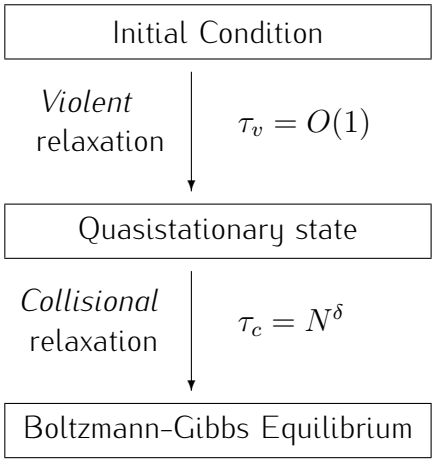


In the first step the system undergoes a fast evolution called *violent relaxation*, in which the state might change brutally. This phase does not seem to depend on system size and, moreover, it does not depend on the initial homogeneity of the state. It can be shown rigorously [25, 46, 87] that for early times the system

is well described by Vlasov dynamics[2], for which the time evolution is ruled by mean-field effects.

Violent relaxation originates from the search at early times of a stable state. Until now there isn't a convincing theoretical description of this phenomenon. Numerically it is confirmed that Vlasov dynamics fully describes violent relaxation. Whenever the initial datum is very close (in some sense) to a Vlasov stable state violent relaxation is described by linear Landau damping [71]. However, when the initial state is not close to a stable state, the system should visit others stable states and up to now it is not clear which one is preferred. A mathematical work of Villani and co-workers [83] shows that an initial state at a finite but small distance to a stable state, remains close to such stable state and its marginal density[3] converges exponentially in time to a limit distribution. Unfortunately, both the relation between the initial datum and the the stable state and how large can be the distance between them is not known. Using a statistical mechanics approach, Lynden-Bell [76] proposed a trial description of the relaxed state starting from the knowledge of the initial datum. He argued that Vlasov evolution is conservative, hence each region of the single particle phase space conserves its volume. This conservation induces an "exclusion" principle on every region of the phase space. Partitioning the single particle phase space in microscopic cells, one can use Fermi-Dirac statistic on the cells with a weight given by the initial datum. That approach does not consider some effects, such as strong oscillations in the mean-field, which change the energy of each cell and change the initial weight. A more fine tuned approach is given by Levin and co-workers [95].

After violent relaxation the system settles down in a state, the QSS, whose life-time increases with system size; therefore it diverges in the thermodynamics limit. On a much longer time-scale the system undergoes a process of *collisional relaxation* in analogy with collisional relaxation of short-range systems. Rigorously [25], the presence of a diverging life-time of QSS is due to Vlasov dynamics and its growth is at least logarithmic in $N$. However, simulations show that stationary states survive for longer time-scales whenever they are stable under Vlasov dynamics, and their life-time $\tau_c$ increases algebraically with $N$, thus $\tau_c = N^\delta$. In principle the life-time exponent should depend on the particular choice of the initial condition. In the case of the HMF model and with a water-bag initial condition, the one of figure 1.7, the scaling exponent $\delta$ was first

[2]See Chapter 2 for the derivation of the Vlasov equation.

[3]Marginal density is the integral over the velocities of the phase-space distribution.

evaluated as $\delta \approx 1.7$ [117]. That exponent was confirmed numerically by other studies [33, 118], in which the number of particles of the system was increased up to $10^3 - 10^4$. An analytical approach to explain this non trivial exponent was proposed in Ref. [49]. More recently, Ref. [51] provides strong numerical evidence with simulations performed with $N \sim 10^5$, that the scaling exponent might be $\delta \approx 2$. That result is compatible with Kinetic Theory, as shown in Chapter 2, but should be confirmed by simulation performed with larger number of particles. However, finer phase space effects reveal even larger time-scales of the order $e^N$ in the process of the approach to the final state, as found by Campa et al. [33] and Chavanis [35].

On a longer time-scale, compared to the QSS' life-time, the system goes towards Boltzmann-Gibbs equilibrium, which is described by standard statistical mechanics. The way in which the system relaxes to equilibrium is ruled by collective phenomena where the energy is exchanged between all the constituents of the system.

How can we explain this behavior? A way to characterize it is given by Kinetic Theory, which describes the evolution of a many particle systems without any assumption of relaxation. Indeed, long-living out of equilibrium states can be outlined in a general framework. In Chapter 2 we briefly describe that theory, while in the next subSection we argue about a definition of long-range interactions starting from out-of-equilibrium features instead of equilibrium ones.

### 1.3.1 Dynamical definition of long-range interactions

QSSs depend on the particular kind of long-range interaction, i.e. figure 1.7 shows the relaxation time-scale of a mean-field model. However, power-law interactions (1.1) show a scaling in time that depends on the parameter $\sigma$ of the power-law. Let us consider a different definition of long-range interactions, valid for power-law potentials, based on the presence of QSSs and a finite virial ratio [36, 54].

Actually, power-law interactions present a crossover from small to large scales. Small scales are governed by collisions in which two particles scatter, while large scales feel the truly long-range features, such as collective effects. In figure 1.8 we summarize different regions in the $(d, \sigma)$ plane corresponding to different scaling laws.

When the exponent $\sigma > 0$, ($\alpha > d$) the energy exchange is driven by collisions, therefore, by the small scale behavior. No long-range features are

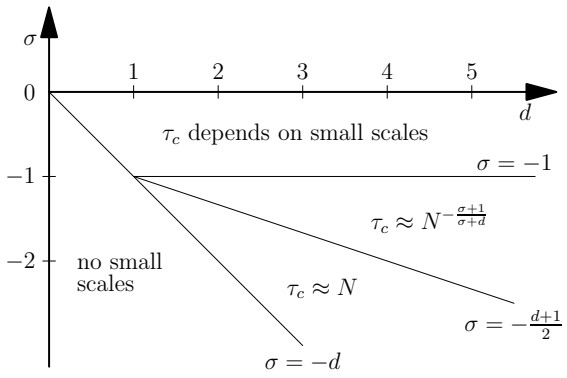


Figure 1.8: Different dynamical behavior of LRI.

present, such as QSSs, and the relaxation, as for dilute gases, is ruled by the Boltzmann equation. An example of such interaction is the Lenard-Jones potential.

When $\sigma < -d$, ($\alpha > 0$) the interaction is not divergent on small scales and, moreover, does not go to zero for large distances. An example of such power-law interaction is the harmonic oscillator for which the potential energy is quadratic with the distance. We do not consider these cases.

A critical exponent $\sigma_c = -\frac{d+1}{2}$ exists, below which the system is well described by soft collisions and mean-field effects. Therefore, small scales can be neglected and large scales dominate the dynamics. For instance, in this regime the kinetic equation that describes the relaxation is Lenard-Balescu equation, discussed in Chapter 2. The relaxation time-scale can increase even slower than linear in the size of the systems, e.g., in figure 1.7 we find $\tau_c \gtrsim N^{1.7}$.

In the regime $-\frac{d+1}{2} < \sigma < -1$, both small and large scales contribute to the dynamics of the system and the relaxation time-scale diverges algebraically but with an exponent smaller then one.

Finally, in the range $-1 < \sigma < 0$, dynamics strongly depends on the small scales features and no general results exists to the best of our knowledge.

## 1.4 A paradigmatic model: the Hamiltonian Mean Field model

Long-range interacting systems are systems in which the interaction is all to all. This feature induces a difficulty in the numerical simulations of such systems,

because the CPU time needed to perform an integration step increases with the size of the system. Therefore, the time necessary to perform a simulation increases generically as $N^2$, preventing the study of big systems.

In this perspective, the study of mean-field interactions overcomes the problem of the wild increase of simulation time, because $N$-body molecular dynamics simulations need a CPU time that grows only linearly with system size. We focus in this Section on a paradigmatic mean-field model: the Hamiltonian Mean-Filed (HMF) model [3,43,59]. This model has captured a lot of attention, because it is a simple model showing a lot of peculiarities of long-range interacting systems [32]. Moreover, the HMF model is relevant for the study of the free electron laser [20,39] and for recoil atomic systems [19].

The Hamiltonian function of the $N$ particle HMF system is

$$H_N = \sum_{i=1}^{N} \frac{p_i^2}{2} + \frac{J}{2N} \sum_{i \neq j}^{N \times N} \left(1 - \cos(q_i - q_j)\right), \tag{1.23}$$

where the interaction among particles is ruled by a single mode cosine potential. The coordinates $q_i$ are angles and their embedding space is the circle, hence $[-\pi, \pi]$. The momenta $p_j$ are the conjugate momenta of the angles and can take any real value. The particles have unitary mass and $J$ is the coupling constant. The HMF Hamiltonian shows a global translational symmetry of the angles and the dynamics conserves total momentum.

The HMF model can be seen in two different ways: from one point of view, it is an isolated Hamiltonian system in which $N$ particles move on a unitary circle and interact with a strength that depends on their relative angle. From another point of view, it can be seen as a system of $N$ spins on a lattice without any notions of distance. Here, two spins in two sites of the lattice interact via an XY potential.

This analogy allows us to define the *magnetization vector* $\mathbf{m} = (m_x, m_y)$, where

$$m_x = \frac{1}{N} \sum_{i=1}^{N} \cos(q_i), \quad m_y = \frac{1}{N} \sum_{i=1}^{N} \sin(q_i). \tag{1.24}$$

Using this vector the Hamiltonian function (1.23) becomes

$$H_N = \sum_{i=1}^{N} \frac{p_i^2}{2} + \frac{JN}{2} \left(1 - m^2\right), \qquad m^2 = m_x^2 + m_y^2, \tag{1.25}$$

for any $N$. The quantity $m$ is the modulus of the magnetization vector (1.24).

A negative coupling constant, $J < 0$, gives a repulsive interaction (or antiferromagnetic interaction) and the equilibrium state is homogeneous at all energies (temperatures). However, the dynamics induces the growth of biclusters in the low energies phase [13]. These clusters are stable on some time-scale.

Hereafter, we are interested in the ferromagnetic case, where $J > 0$, since this case presents both homogeneous and inhomogeneous phases at the thermodynamics level where QSSs can be characterized more easily. The interaction strength, $J$, can be set to $J = 1$ without loss of generality.

Let us discuss the equilibrium features and the continuum description of the HMF model.

### Equilibrium statistical mechanics of the HMF model

The HMF model is a system with a continuous phase transition from a disordered (homogeneous) phase where magnetization is zero $m = 0$, to an ordered (inhomogeneous) phase where magnetization is different from zero, $m \neq 0$. Therefore, the modulus of the magnetization plays the role of the order parameter of a second order phase transition. Such a transition shows ensemble equivalence: microcanonical and canonical ensembles are equivalent. Consequently, we consider the simpler canonical ensemble to treat the equilibrium statistical mechanics of the HMF model.

The partition function of the HMF model at a given inverse temperature $\beta$ and number of particles $N$ is

$$Z(\beta, N) = \left(\frac{2\pi}{\beta e^{\beta}}\right)^{N/2} \int \left(\prod_{i=1}^{N} dq_i\right) \exp\left\{\frac{\beta}{2N}\left[\left(\sum_{j=1}^{N}\cos q_j\right)^2 + \left(\sum_{j=1}^{N}\sin q_j\right)^2\right]\right\}. \tag{1.26}$$

This integral can be computed using the Hubbard-Stratonovic transformation and the saddle point method [32,58]. The result is

$$Z(\beta, N) \approx e^{-N\phi(\beta)}, \tag{1.27}$$

$$\phi(\beta) = \frac{\beta}{2} - \frac{1}{2}\ln 2\pi + \frac{1}{2}\ln\beta + \inf_{x\geq 0}\left\{\frac{\beta x^2}{2} - \ln I_0(\beta x)\right\}, \tag{1.28}$$

where $I_0$ is the modified Bessel function of order 0 and the value of $x$ that minimizes the term between the brackets in the formula above gives the equilibrium

magnetization. Actually, the modulus of magnetization solves a self-consistence equation

$$m = \frac{I_1(\beta m)}{I_0(\beta m)}, \tag{1.29}$$

where $I_1$ is the modified Bessel function of order 1, the derivative of $I_0$. The upper panel of Figure 1.9 shows the magnetization as a function of microcanonical energy.

In the microcanonical ensemble the equilibrium state of the HMF model is parametrized by the energy instead of the inverse temperature. The relation between the two is the energy formula in the canonical ensemble

$$e(\beta) = \frac{1}{2\beta} + \frac{1}{2}\left(1 - m(\beta)^2\right), \tag{1.30}$$

and inverting this one-to-one relation one gets the temperature as a function of energy, as shown in the lower panel of Figure 1.9. At the critical energy $e_c = 0.75$ there is a phase transition and the magnetization becomes non zero at lower energies. This critical energy corresponds to the critical canonical temperature $T_c = 0.5$ and to the critical inverse temperature $\beta_c = 2$.

Let us discuss the response to an external field in equilibrium. This will be important for a comparison with the results of Chapters 3 and 4. The size of the external field is $h$ and the magnetic susceptibility, $\chi$, is the variation of the magnetization for vanishing perturbations. The equilibrium magnetization in presence of an external field, along the spontaneous magnetization direction, is given by the solution of

$$m'(\beta, h) = \frac{I_1}{I_0}\Big(\beta(m'(\beta, h) + h)\Big)\ . \tag{1.31}$$

We develop this expression in Taylor series around the unperturbed state ($h = 0$)

$$m' = m + h\chi + \mathcal{O}(h^2), \tag{1.32}$$

to get the thermodynamic response

$$\chi_{can} = \frac{1/\beta + I_2/I_0 - m^2}{m^2 - I_2/I_0}. \tag{1.33}$$

This formula gives canonical susceptibility. It describes the response of the system to an external field in the thermodynamic limit in the canonical ensemble.

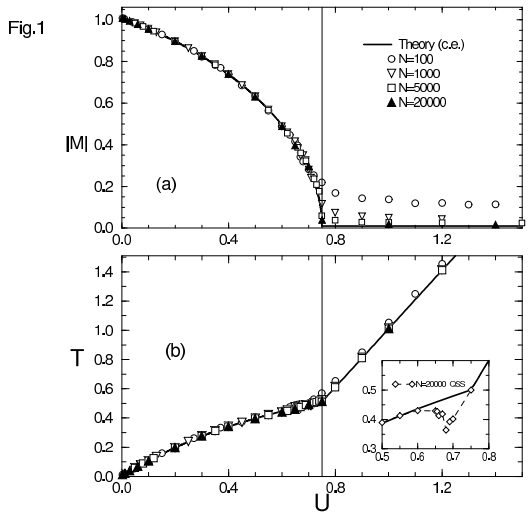


Figure 1.9: Upper panel: magnetization vs. energy. Lower panel: Caloric curve of the HMF model (1.4). In the snapshot of the lower panel the behavior of the temperature as a function of the energy shows a negative slope: historically, this was the first hint to the presence of QSSs. The points are the results of numerical simulations, the full lines are obtained analytically from statistical mechanics.

The microcanonical ensemble gives a different result. We must now consider that the energy remains constant when the external field is coupled adiabatically. As a consequence, inverse temperature changes as follows

$$\beta \to \beta' = \beta + h\delta\beta + \mathcal{O}(h^2). \tag{1.34}$$

The energy is the sum of kinetic and potential energies. Hence, a variation of the magnetization induces a variation of the temperature in order to maintain the energy constant, as follows

$$\frac{1}{2\beta} + \frac{1}{2}(1 - m^2) = \frac{1}{2\beta'} + \frac{1}{2}(1 - m'^2). \tag{1.35}$$

Using expansion (1.34) and comparing order by order in $h$, one gets the relation

$$\delta\beta = -2m\beta^2\chi, \tag{1.36}$$

at linear order. The self-consistency equation of the equilibrium magnetization becomes

$$m'(\beta, h) = \frac{I_1}{I_0}\Big(\beta'(m'(\beta', h) + h)\Big) \ , \tag{1.37}$$

and the thermodynamic response of magnetization reads

$$\chi_{micro} = \beta\frac{1/\beta + I_2/I_0 - m^2}{1 - \beta(1/\beta + I_2/I_0 - m^2)(1 - 2m^2\beta)}. \tag{1.38}$$

We call it microcanonical susceptibility of the system.

### Continuum description of the HMF model

We discuss here the continuum limit of the HMF model. It consists in the evaluation of the dynamics in the infinite-$N$ limit, when the evolution of the system is fully described by the Vlasov equation [114].

In such a limit sums becomes integrals over the single particle phase space because the empirical density

$$f_{empirical}(q, p, t|\{q_i, p_i\}) = \frac{1}{N}\sum_{i=1}^{N}\langle\delta(q_i - q)\delta(p_i - p)\rangle \tag{1.39}$$

converges to the single particle distribution function $f(q, p, t)$, solution of the Vlasov equation (2.17). Here the brackets $\langle\cdots\rangle$ stand for the average over the $N$-particles phase space in the limit $N \to \infty$. As a consequence, magnetization components become

$$m_x[f] = \int dqdp\, f(q, p, t)\cos(q), \quad m_y[f] = \int dqdp\, f(q, p, t)\sin(q), \tag{1.40}$$

which now are functions of the distribution itself. The Hamiltonian of the system is

$$H[f](q, p, t) = \frac{p^2}{2} - m_x[f]\cos(q) - m_y[f]\sin(q), \tag{1.41}$$

while the single particle energy is

$$e[f](q,p,t) = \frac{p^2}{2} - \frac{1}{2}\left(m_x[f]\cos(q) + m_y[f]\sin(q)\right). \tag{1.42}$$

The mean value of the single particle energy is a constant of the motion, although the mean value of the Hamiltonian is not, because it represents the energy of a single particle which is not conserved.

# Chapter 2

# Kinetic Theory

*This Chapter gives a brief survey on Kinetic Theory. Kinetic theory is a useful tool to analyze collective behavior and relaxation to equilibrium in many-body systems. It relies on a rigorous construction but is nevertheless often based on several uncontrolled approximations. The first part of the Chapter is devoted to the derivation of the Bogoliubov-Born-Green-Kirkwood-Yvon (BBGKY) hierarchy of equations. In the second part we consider mean-field dynamics in which the system evolves without correlations. In the last part we consider the correlations as the source of the relaxation process to equilibrium.*

## 2.1 Introduction

Numerical simulations of isolated LRI systems [117] point out the existence of long living out of equilibrium states, called Quasi-Stationary States (QSSs). As discussed in Chapter 1, these states show a slow evolution towards equilibrium with a lifetime that grows algebraically with system size. Kinetic Theory offers a powerful tool to extract information on the relaxation problem and the equilibration process. It is a perturbation theory in which the small parameter for long-range interacting systems is $1/N$, where $N$ is the number of the particles of the system. Exact results [25,46] show that there is a time-scale that increases at least logarithmically with $N$. For shorter times the Vlasov equation [114] gives a reliable description of the dynamics of the system. Such equation is the leading order in the small parameter $1/N$ and it has an infinity of station-

ary solutions. Whenever these stationary solutions are stable, Vlasov dynamics governs the evolution on even longer time-scales, as shown numerically [117] and analytically [29, 30, 32]. The lifetime of QSS grows algebraically with $N$ and therefore these states can be observed in numerical experiments [64, 117]. On the contrary, when the initial state is not linearly stable the system goes towards a new stable state on a time-scale growing logarithmically with system size [62, 84], as predicted by the estimate of the kinetic theory.

The relaxation towards equilibrium is given by the next order term in the small parameter. For short range interactions this term is the collisional term of the celebrated Boltzmann equation [12], where relaxation is driven by two-body encounters. Every particle feels the interaction with the neighbouring ones and the exchange of energy occurs by collisions. On the contrary, for purely long-range interactions, encounters play a negligible role and the relaxation is described by the Lenard-Balescu equation [11, 73]. Here, relaxation is caused by the exchange of energy between a given particle and all the others, due to the long-range nature of the force. As a consequence, the typical time-scale of relaxation depends on system size.

In this Chapter we present the derivation of Kinetic equations from the Bogoliubov-Born-Green-Kirkwood-Yvon (BBGKY) hierarchy, briefly discussing some mathematical [75] and physical [12] problems. We consider only the Kinetic equations of long-range interactions, therefore, we will not mention at all the theory related to short-range interactions and the Boltzmann equation. More detailed references, but not exhaustive about Kinetic Theory in general, can be found in the bibliography.

For the sake of simplicity, we discuss only one-dimensional systems because the main analysis presented in this Chapter does not depend on the dimensionality and the generalization to higher dimensions is trivial. The dimensionality becomes important only in the last part of this Chapter for the Lenard-Balescu equation discussed in Section 2.6, where the integral that appears in the collisional term is zero for one-dimensional systems but in general not zero for higher dimensions. We will argue about the importance of dimension in that Section, in relation with the relaxation mechanism of long-range interacting systems. However, that equation is not important for the successive Chapters.

## 2.2 Liouville equation

Let us consider the following Hamiltonian system of $N$ particles

$$H_N = \sum_{i=1}^{N} \frac{p_i^2}{2m} + \sum_{i=1}^{N} U(q_i) + \frac{1}{2}\sum_{i,j}^{N} V(|q_i - q_j|) \ , \tag{2.1}$$

where $U(q)$ is an external potential acting on particle $i$ and $\mathrm{V}(|q_i - q_j|)$ is the two-body potential between particles $i$ and $j$. The coordinates $q_i \in \mathcal{D}$ are the positions of the particles in the one dimensional embedding space and $p_i \in \mathrm{R}$ are the conjugate momenta. The space $\mathcal{D}$ is assumed to be finite and with periodic boundary conditions, while momenta extend to infinity. The particles composing the system have the same mass and are identical.

It is usual to rescale time $t$ with the number of particle $N$ because the dynamics is governed by collective effects. Such rescaling introduces the Kac's prescription [66], which consists in putting a factor $1/N$ in front of the potential, making potential energy extensive. Let us define the new potential as

$$V(r) \to \frac{1}{N} V(r), \tag{2.2}$$

in order to apply the prescription.

Let us consider the distribution function of the system in the full phase space $f_N(q_1, p_1, \cdots, q_N, p_N, t)$. It gives the probability density that the particle $i$ is in the elementary volume with center in $(q_i, p_i)$ $\forall i$. Due to the identity of the particles, the distribution is symmetric under a permutation of labels and the initial state is a product state of single distribution functions

$$f_N(q_1, p_1, \cdots, q_N, p_N, t = 0) = \prod_{i=1}^{N} f_0(q_i, p_i). \tag{2.3}$$

Indeed, factorizability of the initial state introduces the statistical approach in Kinetic Theory [105]. The distribution evolves according to the Liouville equation [68]

$$\partial_t f_N + \mathcal{L}_N f_N = 0, \tag{2.4}$$

where

$$\mathcal{L}_N f_N = \sum_{i=1}^{N} p_i \partial_{q_i} f_N - \frac{1}{2N} \sum_{i,j} \partial_{q_i} V(|q_i - q_j|) \partial_{p_i} f_N, \tag{2.5}$$

is the Liouville operator which acts linearly on distributions. Equation (2.4) describes the conservation of phase space volume which holds for Hamiltonian systems. On one side, solving Liouville equation is a hard task, because it corresponds to the knowledge of the full dynamical evolution. On the other side, this information is too much for a macroscopic description of the system, thus we can manipulate it in order to eliminate some details.

In the following we use the notation

$$\text{"}1\text{"} = x_1 = (q_1, p_1), \tag{2.6}$$

that identifies the phase space coordinates of particle "1" in different ways. Whereas, we use a short hand notation for partial derivatives

$$\partial_t = \frac{\partial}{\partial t}, \quad \partial_q = \frac{\partial}{\partial q}, \quad \partial_p = \frac{\partial}{\partial p}. \tag{2.7}$$

## 2.3 BBGKY hierarchy

Kinetic theory is mainly interested in the evaluation of the time evolution of the single particle distribution function [105]. Therefore, we use a coarse-graining procedure in order to get such a distribution [75]. The single particle distribution function $f(x)$ is [34]

$$f(x) = \frac{1}{N}\sum_{i=1}^{N}\langle\delta(x - x_i)\rangle_N, \tag{2.8}$$

where the brackets $\langle\dots\rangle_N$ correspond to the average with respect to the solution of the Liouville equation (2.4) in the $N$-particle phase space. Starting from this definition, let us introduce the *$s$-distribution function* [12] as

$$f_s(x_1, \cdots, x_s, t) = \frac{N!}{(N-s)!N^s}\sum_{i_1,\cdots,i_s}\langle\delta(x_1 - x_{i_1})\cdots\delta(x_s - x_{i_s})\rangle_N, \tag{2.9}$$

where the factorial terms take into account the permutation symmetry of the $N$ particle distribution, while the $N^s$ factor is useful to get an intensive definition of $f_s$ [86].

The evolution of the reduced distributions is generated by the Liouville

equation and, using standard techniques, we get the BBGKY hierarchy

$$\partial_t f_s + \sum_{i=1}^{s} p_i \partial_{q_i} f_s - \frac{1}{N} \sum_{i,j=1\times 1}^{s\times s} \partial_{q_i} V(q_i - q_j) \partial_{p_i} f_s = \sum_{i=1}^{s} \int dq_{s+1} dp_{s+1} \partial_{q_i} V(q_i - q_{s+1}) \partial_{p_i} f_{s+1}. \tag{2.10}$$

In appendix A.1 we shortly derive this hierarchy of equations. Mathematically, this operator becomes exact in the $N \to \infty$ limit, which coincides with the Vlasov hierarchy [106].

The $s$-th equation of the hierarchy describes the evolution of the $s$-distribution function and its dynamics is related to that of the $(s+1)$-distribution. Therefore, the BBGKY hierarchy (2.10) provides an exact description of the dynamics, such as the Liouville equation, because we need the knowledge of $f_N$ in order to treat the evolution of the reduced distributions at a lower order. The information encoded in the BBGKY hierarchy is again too detailed and we have to use a truncation of the hierarchy in order to obtain a coarse grained description.

Let us divide the reduced distribution functions in connected and non-connected parts. We introduce the correlation functions $g_s$ [74] which derive from the relations

$$f_2(x_1, x_2, t) = f(x_1, t) f(x_2, t) + g_2(x_1, x_2, t), \tag{2.11}$$

$$\begin{aligned} f_3(x_1, x_2, x_3, t) &= \frac{1}{3} f(x_1, t) f_2(x_2, x_3, t) + \frac{1}{3} f(x_2, t) f_2(x_3, x_1, t) + \\ &\quad \frac{1}{3} f(x_2, t) f_2(x_3, x_1, t) + g_3(x_1, x_2, x_3, t), \end{aligned} \tag{2.12}$$

$$\begin{aligned} &= f(x_1, t) f(x_2, t) f(x_3, t) + \frac{1}{3} f(x_1, t) g_2(x_2, x_3, t) + \\ &\quad \frac{1}{3} f(x_2, t) g_2(x_3, x_1, t) + \frac{1}{3} f(x_3, t) g_2(x_1, x_2, t) + \\ &\quad g_3(x_1, x_2, x_3, t), \end{aligned} \tag{2.13}$$

$\dots$

and so on for the successive distributions. For practical reasons, we use here a $\frac{1}{3}$ factor which is not used in literature. Actually this constant does not modify the basic equations that we will use later.

Correlations, which are the connected parts of the $s$-distributions, take into account the conditional probability among different particles, thus they carry the information about energy exchanges among the particles. Invariance of the

correlations under permutations is directly inherited from the invariance of the solution of the Liouville equation under such permutations.

Using the decomposition of the distribution functions in connected and non-connected parts, the first equation of the hierarchy (2.10) becomes

$$\partial_t f + p_1 \partial_{q_1} f - \partial_{p_1} f \partial_{q_1} \phi[f](q_1, t) = \partial_{p_1} \int dx_2 \, g_2(x_1, x_2, t) \partial_{q_1} V(q_1 - q_2), \quad (2.14)$$

where

$$\phi[f](q_1, t) = \int dx_2 \, f(x_2, t) V(q_2 - q_1) \quad (2.15)$$

is the *mean-field potential* and we have set to zero the self-interaction of each particle. The initial value of the distribution function is given by a smooth function which describes the initial state $f_1(q, p, t = 0) = f_0(q, p)$. The connected correlation evolves with an equation derived from the equation for $f_2$, which reads

$$\begin{aligned} \partial_t g_2 \;=\; & -p_1 \partial_{q_1} g_2 + \partial_{q_1} \phi[f] \partial_{p_1} g_2 + \\ & \frac{1}{N} f(x_2) \partial_{q_1} V(q_1 - q_2) \partial_{p_1} f + \frac{1}{N} \partial_{q_1} V(q_1 - q_2) \partial_{p_1} g_2 + \\ & \partial_{p_1} f \int dx_3 \, g_2(x_2, x_3, t) \partial_{q_1} V(q_1 - q_3) + \\ & 3 \partial_{p_1} \int dx_3 \, g_3(x_1, x_2, x_3, t) \partial_{q_1} V(q_1 - q_3) + \{1 \longleftrightarrow 2\}, \end{aligned} \quad (2.16)$$

where $\{1 \longleftrightarrow 2\}$ means the same terms with the indices 1 and 2 exchanged.

## 2.4 The Vlasov equation

Discarding correlations in the first equation of the BBGKY hierarchy (2.14) one gets the Vlasov equation [50,114]

$$\partial_t f + p \partial_q f - \partial_p f \partial_q \phi[f] = 0, \qquad f(q, p, t = 0) = f_0(q, p), \quad (2.17)$$

where the potential is defined in Eq. (2.15) and it is a functional of the one-particle distribution itself. Therefore, this equation is a non linear equation [83]. It is exact in the limit in which the number of particle goes to infinity and correlations are negligible. This limit is called *mean-field limit* [25,69]. Although its solution should be simpler than the solution of the Liouville equation Eq. (2.4), the loss of linearity introduces some important features discussed below.

From the physical point of view, the Vlasov equation is used to describe the evolution of different systems, such as plasmas [88] or the dynamics of galaxies [17].

Rigorous results [25,46] state that the Vlasov equation gives a good description of large systems when the pair potential is long-range and it is not too pathological. For instance, a pathological potential is the $1/r$ one (electrostatic and Newtonian potential) because the divergence at the origin gives diverging integrals [1]. One can overcome such problem by introducing a cutoff at short distances and by evaluating the quantities of interest in the limit in which the cutoff goes to zero.

The Vlasov equation, Eq. (2.17), preserves the Lebesgue measure of the single particle phase space $dqdp$ (the Liouville measure). Therefore, the dynamical evolution described by this equation does not show standard relaxation phenomena. This feature is related to the time inversion invariance, a consequence of the Hamiltonian structure of the Vlasov equation. Although the Vlasov equation is endowed with an Hamiltonian structure, its analysis is more involved than the one of the finite $N$ equations, because it is an infinite dimensional system and the symplectic form is defined on an infinite dimensional space [81, 109]. Furthermore, one can define a mean-field Hamiltonian

$$H[f](q,p,t) = \frac{p^2}{2} + \phi[f](q,t), \tag{2.18}$$

which is a functional of the distribution which solves the Vlasov equation. The mean-field potential $\phi[f]$ is given in Eq. (2.15).

Vlasov equation possesses an infinite number of stationary solutions [41, 81, 110]. For instance, a class of such solutions is the Jeans' class [63], which includes every integrable function of a single argument, the Hamiltonian (2.18) of the system

$$f(q,p,t) = \mathrm{F}(H(q,p,t)). \tag{2.19}$$

Another important class of solution of the Vlasov equation is given by integrable and smooth functions which depend only on the velocities,

$$f(q,p,t) = h(p,t). \tag{2.20}$$

The Vlasov equation, which is defined in an infinite dimensional space, is endowed with an infinite number of conserved quantities, which are integrals

of motion. Indeed, for any smooth function $c$ of a single argument there is a related conserved quantity, called *Casimir*,

$$\mathcal{C}[f] = \int dqdp\, c(f(q,p,t)), \qquad \frac{d}{dt}\mathcal{C}[f] = 0. \tag{2.21}$$

We will discuss the constraints of the Vlasov equation in relation to the linearized dynamics in Chapter 4.4. Among all Casimirs, there is Boltzmann entropy (also called mean-field entropy)

$$\mathcal{S}[f] = -\int dqdp\, f \ln f. \tag{2.22}$$

Its conservation in time is related to the iso-entropic evolution of the Vlasov dynamics [81].

Others invariants are the mean-field Hamiltonian (2.18) and all the invariants deriving from the symmetries of the $N$ body system, such as momentum, angular momentum, etc.

In the following, we will study the stability of the stationary solutions of the Vlasov equation. Whenever a stationary solution is also stable there exists a time-scale in which this solution can approximate quite well the dynamics of the related finite system. This gives a theoretical foundation to QSSs.

## 2.5 Relaxation mechanism of the Vlasov dynamics

Vlasov dynamics is a time reversible dynamics and conserves Boltzmann entropy (2.22). This dynamics determines a continuous evolution of the state of the system, which is a priori incompatible with relaxation. Due to the incompressibility of the single particle phase space, each elementary volume evolves in finer and finer structures [83]. This filamentation is responsible for the difficulties in the numerical simulations of the Vlasov equation on long time-scales [26].

From a macroscopic point of view one is often interested in evaluating values of some observable. Here, a question naturally arises: Is it possible to find a stationary value of a generic observable for a system which evolves in such finer and finer structures? Macroscopic observables are averages over the phase space, and this introduces a weak form of convergence. The average smooths out the small scales in phase space and can induce a convergence of macroscopic observables to stationary values. Therefore, filamentation gives a formal relaxation of the state of the system and can determine a relaxation of

averaged quantities. Mathematically it is a weak convergence of the state that induces a relaxation of the macroscopic level.

In the context of Vlasov equation a second important question concerns the relaxation of macroscopic quantities when a stationary state is perturbed by different sources. A pioneering work of Landau [71] has shown that there exists a relaxation phenomenon in which small perturbations damp to zero. This implies that an initial stationary state could be stable and well represent the dynamics at the macroscopic level.

From the physical point of view, Landau damping is an effect in which the perturbation produces waves of the mean field and those waves can provide or remove energy from some part of the system [101, 104]. That energy exchange induces a relaxation effect which decreases the amplitude of the waves themselves whenever the state is stable. Therefore, a typical time-scale of Landau damping is the dynamical time-scale of the evolution of a single particle (here $\mathcal{O}(1)$) and not the relaxation time-scale of finite systems towards equilibrium (here, $\mathcal{O}(N^\delta)$).

In the first part of this Section we describe the filamentation process in the case of non-interacting particles in order to introduce some mathematical tools useful in the study of weak convergence to a steady state. In the following Subsection we introduce Landau damping as discussed by Landau itself [71] where an initial homogeneous state is perturbed by a small fluctuation.

### 2.5.1 Non interacting particles

The single particle distribution of a non interacting particle system evolves with the following equation

$$\partial_t f(q,p,t) = -p\partial_q f(q,p,t), \quad f(q,p,0) = h(q,p), \tag{2.23}$$

which is the equation of free transport and $h(q,p)$ is the initial state. Let us consider a system confined in a box in order to avoid technical problems. It is possible to demonstrate that, when the initial distribution has some regularities, the system relaxes to a given final state.

The solution of equation (2.23) is given by the formula

$$f(q,p,t) = h(q-pt,p). \tag{2.24}$$

The state at time $t$ is the initial state translated in space. Here, the only state that does not evolve in time is the homogeneous one, where the distribution is constant in $q$.

Let us consider a generic observable $a(q,p)$ of the single particle phase space. Weak convergence demands that the following limit

$$\lim_{t\to\infty}\int dqdpf(q,p,t)a(q,p) = A_\infty \tag{2.25}$$

exists and gives the asymptotic value $A_\infty$. Whenever the coordinates $(q,p)$ are not correlated, weak convergence is required at least in one variable. For example, we will show that weak convergence for homogeneous states is necessary in the velocity space in order to compare the theoretical density of the system with observations.

There are two ways of showing the decay of the time dependence of the observable.

### Fourier-Fourier transform

To obtain an estimate of the damping we perform the Fourier transform A.2 in both the coordinate and the related momentum. The solution (2.24) becomes

$$\tilde{f}(k,\eta,t) = \tilde{h}(k,\eta+kt), \tag{2.26}$$

therefore, the distribution is given by waves in mode space. We note that there is only one static mode $k=0$, which physically gives the normalization of the system.

The spatial distribution of the system is the integral on the momenta of the distribution function, and its modes are given by

$$\tilde{\rho}(k,t) = \int dp\int d\eta e^{-\imath\eta p}\tilde{f}(k,\eta+kt) = \tilde{h}(k,kt) \xrightarrow[k\neq 0]{t\to\infty} 0. \tag{2.27}$$

The Riemann-Lebesgue theorem states that when a function is smooth enough, every mode different from zero vanishes. Consequently, from the macroscopic point of view, the system experiences a relaxation and only the zero mode survives. This mode is not space dependent, therefore the system becomes uniform in the spatial region in which it is constrained. However, to get a time-scale of relaxation the modes of the initial distribution have to damp exponentially.

### Fourier-Laplace transform

The other way to show the relaxation is to perform the Laplace transform A.2 in time of the free transport equation (2.23), and the Fourier transform along the

space direction. We get

$$\imath\omega\tilde{f}(k,\omega) = \tilde{h}(k) + \imath kp\tilde{f}(k,\omega), \tag{2.28}$$

$$\tilde{f}(k,\omega) = -\imath\frac{\tilde{h}(k)}{\omega - kp}. \tag{2.29}$$

Its inverse Laplace transform A.3 is

$$\tilde{f}(k,t) = -\imath\tilde{h}(k)\int_{\imath\gamma-\infty}^{\imath\gamma+\infty}\frac{e^{-\imath\omega t}}{\omega - kp}d\omega. \tag{2.30}$$

where $\gamma$ is larger than all imaginary parts of the singularities of the integrand. In that case $\gamma$ has to be positive because there is a single pole at $kp$ on the real axis. However, a path with positive imaginary part does not gives a convergence of the integral but produces oscillations and a small divergence.

In order to study weak convergence, we look at the density, which is the integral over the momenta of the distribution function. It reads

$$\tilde{\rho}(k,t) = -\imath\int_{\imath\gamma-\infty}^{\imath\gamma+\infty} e^{-\imath\omega t}\int_{\mathbb{R}} dp\frac{\tilde{h}(k,p)}{\omega - kp}. \tag{2.31}$$

We perform an analytical continuation of the integral over momentum in order to get damping. Since the integrand has a single pole, we use the principal value integral (as explained in Appendix A.4) and we get

$$\begin{aligned}
\bar{\rho}(k,\omega) &= -\imath\int_{\mathbb{R}} dp\frac{\tilde{h}(k,p)}{\omega - kp} && \mathrm{Im}(\omega) > 0,\\
&= -\imath\fint_{\mathbb{R}} dp\frac{\tilde{h}(k,p)}{\omega - kp} - \pi\frac{\mathrm{sgn(k)}}{k}\tilde{h}\left(k,\frac{\omega}{k}\right) && \mathrm{Im}(\omega) = 0,\\
&= -\imath\int_{\mathbb{R}} dp\frac{\tilde{h}(k,p)}{\omega - kp} - 2\pi\frac{\mathrm{sgn(k)}}{k}\tilde{h}\left(k,\frac{\omega}{k}\right) && \mathrm{Im}(\omega) < 0,
\end{aligned} \tag{2.32}$$

where $\fint$ stays for the principal value integral and sgn is the sign function. Here, the density function is an analytic function and the integral over momentum (the imaginary part) has not poles. Therefore, its inverse Laplace transform gives a vanishing contribution. The integration contour of the inverse Laplace transform of the second term can be chosen in the lower half of the complex plane. Indeed, after a rescaling of the frequencies, we get

$$\tilde{\rho}(k,t) = \int_{\imath\gamma-\infty}^{\imath\gamma+\infty} e^{-\imath k\omega t}\tilde{h}\left(k,\omega\right)\theta(-\mathrm{Im}\{\omega\})d\omega = \tilde{\rho}(k,kt), \tag{2.33}$$

and we recover the same result of the Fourier-Fourier approach.

When the initial distribution is an analytic function the Fourier transform goes to zero exponentially fast. For instance, if the analytic function $h$ is defined in a strip of width $\lambda_h$, the amplitude of a mode $A_k$ goes to zero exponentially as $e^{-\lambda_h kt}$ (see Appendix A.3). Moreover, when the system is not confined in a box the wavelengths are not bounded from below, hence there are always modes that do not decay and the system does not relax even in a weak sense.

#### Example: The equilibrium distribution

The equilibrium distribution is defined as the exponential of $\beta H$, where $\beta$ is the Lagrange multiplier representing the inverse temperature of the system and $H(q,p)$ is the Hamiltonian. For homogeneous systems the Hamiltonian is kinetic energy only and the distribution becomes a Gaussian in velocities and uniform in space. It is called the Maxwellian distribution. When the system experiences a potential field $\phi(q)$ the Fourier transform of the equilibrium distribution must be performed in both coordinates and momenta, such that the density results into

$$\tilde{\rho}_{eq}(k,t) = \tilde{f}_{eq}(k,kt) = \frac{1}{Z(\beta)}\sqrt{\frac{2\pi}{\beta}}e^{-2(kt)^2/\beta}\mathcal{F}[e^{\beta\phi}]_k. \tag{2.34}$$

The Fourier transform of the potential part is supposed not to diverge faster than exponentially. Therefore, the Gaussian converges to zero even faster than exponential. This result is due to the fact that the Gaussian distribution cannot be analytically continued in the whole complex plane, therefore one has to consider a different path in the $\omega$ plane inside the analyticity strip . In that case, this choice of path induces a different scaling and a faster decay.

### 2.5.2 Landau damping

In order to show Landau damping, one has to consider an initial state of the system which is not stationary but close to a stationary state. When this stationary state is stable the dynamics converges weakly to it.

One represents the single-particle distribution function via a perturbative approach

$$f(q,p,t) = f_0(q,p) + \eta\delta f(q,p,t) + \mathcal{O}(\eta^2), \tag{2.35}$$

where $f_0(q,p)$ is the stationary distribution and $\eta$ measure the smallness of the distance to the stationary state. The function $\delta f(q,p,t)$ gives the variation at linear order in $\eta$ of the distribution function with respect to the stationary state.

The evolution in time is given by a perturbative expansion of the Vlasov equation. At order $\mathcal{O}(\eta^0)$ one finds the unperturbed Vlasov equation, which describes the evolution of the unperturbed state, here assumed stationary. For instance, one finds

$$\partial_t f_0 = -p\partial_q f_0 + \partial_q \phi[f_0](q)\partial_p f_0 = 0. \tag{2.36}$$

At the linear order in $\eta$ one gets the evolution equation of the perturbation $\delta f$, so-called *linear Vlasov equation*, which reads

$$\partial_t \delta f \;\; = \;\; -\Big(p\partial_q - \partial_q \phi[f_0](q)\partial_p\Big)\delta f + \partial_q \phi[\delta f](q,t)\partial_p f_0. \tag{2.37}$$

This is a linear integro-differential equation, where the time variation of $\delta f$ is driven by two terms: the first one is the unperturbed dynamics, while the second one takes care of the variation of the mean-field induced by the perturbation.

The solution of equation (2.37) is not a simple task when the initial state is inhomogeneous, i.e. the distribution depends on space. There are only few works about the solution of the linear Vlasov equation for such states [37, 93], where the authors consider integrable models in order to simplify mathematical and technical problems.

On the contrary, in the case of homogeneous states the solution can be obtained using Fourier-Laplace techniques. In the following we describe homogeneous Landau damping and we shortly discuss the inhomogeneous case.

### Homogeneous states

A homogeneous distribution is such that it does not depend explicitly on the spatial coordinates of the system, but only on momenta. It has the following properties:

- **Constant in space:** The distribution verifies

$$\partial_q f_0(q,p) = 0, \tag{2.38}$$

$$\rho_0(q) = \int dv\, f_0(q,v) = \textit{(const.)}. \tag{2.39}$$

- **Zero mean-field potential:** the mean field potential is constant and can be set to zero

$$\phi[f_0](q) = \int f_0(v)dv \int u(q-x)dx = 0, \tag{2.40}$$

because the integral is a constant and the energy is defined apart from constants.

- **Free dynamics:** At zero-th order in the perturbation the dynamics of the system is free transport. For instance, the unperturbed distribution function evolves as

$$f_{\eta=0}(q,p,t) = f_0(q-pt,p), \tag{2.41}$$

where $f_0(q,p)$ is the initial distribution. Hence, each stationary state does not depend on the coordinate $q$.

We consider that at time $t=0$ the system is close to a stationary stable state. Some fluctuations should indeed be present and the stability of the state requires that their size must become negligible at later times. For example, we could consider the role of thermal fluctuations.

The linear equation becomes

$$\begin{aligned} \partial_t \delta f &= -p\partial_q \delta f + \partial_p f_0 \partial_q \phi[\delta f](q,t), & (2.42)\\ \delta f(q,p,0) &= h(q,p), & (2.43) \end{aligned}$$

where $h(q,p)$ is the initial datum of the fluctuations. Let us use the Fourier transform in space and the Laplace transform in time. The modes are now decoupled, so that a given mode $k$ does not contribute to the dynamics of the mode $k' \neq k$. The Fourier transform gives

$$\partial_t \delta\tilde{f}(k) = -\imath kp\delta\tilde{f}(k) + \imath k\tilde{u}(k)\partial_p f_0 \int dv \delta\tilde{f}(k) \tag{2.44}$$

and in the equation only the single mode $k$ appears, because the Fourier transform of a convolution is the product of the Fourier transforms. Performing the Laplace transform, we obtain the following equation

$$(\imath\omega - \imath kp)\delta\tilde{f} = \tilde{h}(k,p) + \imath k\tilde{u}(k)\partial_p f_0 \int dv \delta\tilde{f}. \tag{2.45}$$

To solve it, we extract the variation of the density by integrating over the velocities. Therefore, we get

$$\delta\tilde{\rho}_k(\omega) = \int dv\, \delta\tilde{f} = \frac{1}{\epsilon(k,\omega)} \int_{\mathbb{R}} dv \frac{\tilde{h}_k}{\omega - kv} \tag{2.46}$$

which is the variation of the density in Fourier-Laplace space at linear order. It is important to stress that $\omega$ lies in the upper half complex plane, without ever reaching the real line. This is a consequence of having performed a Laplace transform, because the time integral with negative imaginary part of the frequency does not converge (A.2). The function $\epsilon$ is called the *dielectric function* [88], and it is defined as

$$\epsilon(k,\omega) = 1 - k\tilde{u}(k) \int_{\mathbb{R}} dv \frac{1}{\omega - kp} \partial_v f_0, \quad \mathrm{Im}\{\omega\} > 0. \tag{2.47}$$

This function has a discontinuity on the real axis, where it is not defined at all. Therefore, it is not an analytic function in $\mathbb{C}$ [42, 56].

To get the inverse Laplace transform we need to evaluate both the dielectric function and the variation of the density in the lower half complex plane, therefore we must analytically continue both of them. The analytic continuation means that we have to remove the discontinuity preserving all the singularities. We get the analytic continuation of the dielectric function as

$$\begin{aligned}
\epsilon(k,\omega) &= 1 - k\tilde{u} \int_{\mathbb{R}} \frac{dp}{kp - \omega} \partial_p f_0 && \mathrm{Im}(\omega) > 0, \\
&= 1 - k\tilde{u} \fint_{\mathbb{R}} \frac{dp}{kp - \omega} \partial_p f_0 - \imath\pi\tilde{u}\,\mathrm{sgn}(k) \partial_p f_0 \Big|_{\omega/k} && \mathrm{Im}(\omega) = 0, \\
&= 1 - k\tilde{u} \int_{\mathbb{R}} \frac{dp}{kp - \omega} \partial_p f_0 - 2\imath\pi\tilde{u}\,\mathrm{sgn}(k) \partial_p f_0 \Big|_{\omega/k} && \mathrm{Im}(\omega) < 0,
\end{aligned} \tag{2.48}$$

where $\fint$ is the principal value integral, shown in Appendix A.3. Using this trick, the dielectric function, Eq. (2.48), is no more discontinuous.

Also the integral in the momenta of the density has to be analytically continued with the same method, removing the discontinuity for real $\omega$

$$\begin{aligned}\int_{\mathbb{R}} dv \frac{\tilde{h}(k,v)}{\omega - kv} &= \int_{\mathbb{R}} dv \frac{\tilde{h}(k,v)}{\omega - kv} && \mathrm{Im}\{\omega\} > 0, \\ &= \fint_{\mathbb{R}} dv \frac{\tilde{h}(k,v)}{\omega - kv} - \imath\pi \tilde{h}(k,\omega/k) && \mathrm{Im}\{\omega\} = 0, \\ &= \int_{\mathbb{R}} dv \frac{\tilde{h}(k,v)}{\omega - kv} - 2\imath\pi \tilde{h}(k,\omega/k) && \mathrm{Im}\{\omega\} < 0.\end{aligned} \tag{2.49}$$

The inverse Laplace transform can now be performed, and we get the variation of the density as a function of time

$$\begin{aligned}\tilde{\delta\rho}_k(t) &= 2\pi \int \frac{1}{\epsilon(k,\omega)} \frac{e^{-\imath\omega t}}{kp - \omega} d\omega \theta(-\mathrm{Im}\{\omega\}) \tilde{h}(k,\omega/k) \\ &\quad - \int \frac{\imath}{\epsilon(k,\omega)} e^{-\imath\omega t} \int dp \frac{\tilde{h}(k,p)}{kp - \omega} d\omega,\end{aligned} \tag{2.50}$$

where the Laplace integral is computed on a contour which is closed on the lower half complex plane. Therefore, there are here two terms: the first term contains also singularities of the Fourier transform of the initial datum, while the second term has singularities arising only from the zeros of the dielectric function. These latter singularities determine Landau damping. The nearest zero to the real axis of the dielectric function gives the slower decay of the inverse Laplace transform, and we call $\lambda_\epsilon$ its imaginary part. On the other hand, we call $\lambda_h$ the radius of analyticity of the initial datum, therefore the system relaxes towards the stationary state with the law

$$e^{-\lambda t}, \qquad \lambda = \min\{\lambda_h, \lambda_\epsilon\}. \tag{2.51}$$

The solution of the linear Vlasov equation in the Laplace-Fourier space then reads

$$\delta\tilde{f} = \frac{1}{\imath\omega - \imath kp} \left[ \tilde{h}(k,p) - \frac{\imath k \tilde{u}(k) \partial_p f_0}{\epsilon(k,\omega)} \tilde{\delta\rho}(k,\omega) \right], \tag{2.52}$$

where the dielectric function and the density are defined in the whole complex plane.

An interesting feature is the stability of the initial state. For instance, one can obtain unstable distributions where, e.g., zeros of the dielectric functions lye

on the upper complex plane. Therefore, we can define some stability criteria which tell us when a state is stable [31,57,91]. Here we discuss Penrose stability criterion [98], which describes linear stability at all times.

#### Penrose stability criterion

Penrose criterion of linear stability of a state $f_0$ requires that the dielectric function cannot be zero for real frequencies $\omega$. Along the real axis of the $\omega$-plane, the imaginary part of the dielectric function could be zero only when the derivative with respect to the momentum is zero. Therefore, Penrose criterion reads

$$\forall \omega \in \mathbb{R} \quad s.t. \quad \partial_p f_0(\omega/k) = 0, \qquad \mathrm{Re}\{\epsilon(k,\omega)\} > 0. \tag{2.53}$$

Many distribution function have a zero derivative only in the origin, thus this statement corresponds to evaluate the dielectric function for $\omega \to 0$.

Another stability criterion is the one of Nyquist, which states that a stationary distribution is stable when its dielectric function has zeros only in the lower half complex plane.

Zeros on the real axis give marginally stable distributions (such as the Water-Bag one, discussed in Section 3.2.1) and therefore the state does not converge weakly towards the unperturbed one, but does not diverge either. The system oscillates on a long time-scale, compared to the dynamical scale.

#### Inhomogeneous states

Inhomogeneous states bring in a more complicated treatment, because the Fourier modes of the potential are coupled together and with the modes of the unperturbed state.

In Chapter 4 we will find an approximated solution under the hypothesis that there is a base of functions in which the modes can be decoupled. It is a spectral analysis [42,56]. For instance, in Ref. [93] the decoupling of the modes is obtained for integrable systems using action-angle variables [6].

## 2.6 Lenard-Balescu equation

Let us consider the equation that governs the time evolution of the correlation function, Eq. (2.16), and the order of magnitude of its terms. This equation

contains the three body correlation function $g_3$, the two body correlation $g_2$ and the products of single particle distribution function. First of all we set to unity the order of $f \approx 1$ as a reference scale. The derivative of the distribution function maintains the same order of magnitude because we assume that $f$ decays sufficiently fast at high momentum. Therefore the term that depends on the two body long-range potential reads

$$\lambda(N, q_1 - q_2)(\partial_{p_1} - \partial_{p_2}) f(x_1) f(x_2), \qquad \lambda(N, x) = -\frac{\partial_x V(x)}{N}. \tag{2.54}$$

Its order of magnitude is $\lambda$ which goes as $N^{-1}$ when the force is bounded in space. For instance, a central potential such as the gravitational one, has a singularity in the origin (or at infinity) which gives a different scaling [54]. For the sake of simplicity, we now focus on non-singular forces such that the order of magnitude of this term is $N^{-1}$.

Let us suppose that the order of the three body function is negligible when compared with the order of the two-body correlation function [74]. The time evolution of $g_2$ is then driven for early times by the stronger term between the initial condition $g_2(x_1, x_2, t = 0)$ and $\lambda(N, q_1 - q_2)$. The initial datum of correlations is of order $1/N$ or smaller; here we consider that it is negligible for the sake of simplicity. Therefore, one gets the order of magnitude of $g_2 \approx N^{-1}$ and a hierarchy of relations

$$g_s \approx \frac{1}{N^{s-1}}. \tag{2.55}$$

Therefore, the inverse of the size of the system $N$ is the small parameter on which one can build Kinetic Theory for long-range interacting systems.

It is quite common in the study of Kinetic Theory that a hypothesis cannot be checked a priori, but has to be self-consistent [12]. In our case, the hypothesis that there exists a hierarchy of order of magnitudes of correlations is self-consistent and allows a truncation and a closure of the BBGKY hierarchy at a chosen order. For instance, we consider only the next to leading order ($\mathcal{O}(N^{-1})$) and we can rescale the two body correlation function such as $g_2 \to N^{-1} g_2$. Then, the time evolution of the two body correlation function is

$$\begin{aligned} \partial_t g_2 \;=\; & -p_1 \partial_{q_1} g_2 + \partial_{q_1} \phi[f] \partial_{p_1} g_2 + f(x_2) \partial_{q_1} V(q_1 - q_2) \partial_{p_1} f + \\ & \partial_{p_1} f \int dx_3 \, g_2(x_2, x_3, t) \partial_{q_1} V(q_1 - q_3) + \{1 \longleftrightarrow 2\}, \end{aligned} \tag{2.56}$$

while the time evolution of the single particle distribution function reads

$$\partial_t f + p_1 \partial_{q_1} f - \partial_{p_1} f \partial_{q_1} \phi[f](q_1, t) = \frac{1}{N} \partial_{p_1} \int dx_2 \, g_2(x_1, x_2, t) \partial_{q_1} V(q_1 - q_2). \tag{2.57}$$

Thus, the two equations, (2.57) and (2.56), form a set of two closed equations coupled together [12]. A first important remark is that the evolution of the two body correlation function is driven by the linear Vlasov operator (2.37). Each solution of such equation for $g_2$ is therefore strongly related to the solution of the linear Vlasov equation. In the following Chapters we will show how it is possible to solve in general that equation and, moreover, which kind of questions one gets in the case of inhomogeneous states. See, for instance, Chapters 3 and 4.

Equations (2.57) and (2.56) are not simple to solve even numerically, and we need to assume more restrictions in order to get some useful equations.

Let us consider a stationary solution of the Vlasov equation, then it does not depend on spatial coordinates. The two-particle correlation $g_2$ evolves on time-scales of order one, whereas the one-particle distribution evolves on time-scales of order $N$. Indeed, for large systems, one can assume a time-scale separation where the distribution $f$ is stationary when $g_2$ reaches its stationary form: this is the Bogoliubov hypothesis [18], also called Markovianization assumption [105]. In order to verify this assumption the stationary solution of the Vlasov equation, which corresponds to the initial state of $f$, has to be linearly stable.

Applying the Markovianization hypothesis one gets the Lenard-Balescu (LB) equation [11, 12, 73]

$$\partial_t f = \frac{2\pi^2}{N} \int dk (k\partial_p) \int dp' \frac{\tilde{V}^2(k)}{|\epsilon(k, kp)|^2} \delta\left(k(p - p')\right) \left[k(\partial_p - \partial_{p'})\right] f(p) f(p'). \tag{2.58}$$

The right hand side of this equation is called the collisional integral, having in mind the right hand side of the Boltzmann equation. Actually, in the LB equation the right hand side is not related to *collisions*, which are rare in LRI, but rather to the energy transfer between each particle and the mean-field. A derivation of the Lenard-Balescu equation can be found in many textbooks, such as in Chapter 8 of [12] or in Appendix A of [88].

### 2.6.1 Properties of the Lenard-Balescu equation

The LB equation has some properties analogous to the Boltzmann equation [12], but it describes the relaxation of a QSS towards equilibrium of a long-range interacting systems instead of the relaxation to equilibrium of a short-range one. First of all, it conserves the mass, the kinetic energy and the total momentum of the system [12]. Moreover, for positive initial distribution $f_0(q,p) > 0$ (as required for a statistical and physical description [105]) the LB equation conserves its positivity at all times.

A second remark is about the dependence of the collisional term of Eq. (2.58) on dimensions of the physical space. For one dimensional systems the collisional integral is zero because the delta function gives $p = p'$ for each non zero mode, and the derivatives of the single particle distribution function are equal. Indeed, for one dimensional systems the homogeneous phase converges towards equilibrium with a time-scale longer than $N$ [117]. Typically, this time-scale is of order $N^2$, which ensures the correctness of Kinetic Theory at the next to leading order. On the contrary, for higher dimensional systems, the collisional integral selects the velocities such that $\vec{k} \cdot (\vec{p} - \vec{p}') = 0$, where $\vec{k}$, $\vec{p}$ and $\vec{p}'$ are vectors. Accordingly, the collisional term gives a damping that brings the system towards the equilibrium of Kinetic Theory one can prove that this is Boltzmann-Gibbs equilibrium.

Inside the collisional integral one finds the Fourier transform of the long-range potential divided by the modulus of the dielectric function. It describes the effective potential of the theory which takes into account collective effects. For instance, for plasmas, it describes Debye shielding [12, 88] and, therefore, the behavior at large distances of the effective interaction.

The LB equation satisfies an H-theorem, which states that the mean-field entropy

$$s(t) = \int dqdp\, f(q,p) \ln f(q,p) + const., \tag{2.59}$$

is a monotonously increasing function of time [12]. This feature is the same as for the solution of the Boltzmann equation and ensures that the equilibrium distribution exists from a physical point of view. Actually, the Maxwellian distribution gives the distribution which maximizes $s(t)$ when the system is homogeneous and conserves the mass.

One of the main problems of the LB equation is its non linear nature. This nature comes from both the $ff$ term in the collisional integral and from the

dielectric function, which depends itself on the single particle distribution function. This last term introduces a series of non linearities at any order $f^n$: one denotes this feature by "infinite" nonlinearity [88]. Whenever the dielectric function is close to one we can assume that the collisional integral is given by the long-range potential, instead of the effective one. This assumption brings to the Landau equation [72] which is quadratic instead of infinitely non linear, and it is simpler to solve. Moreover, the Landau equation can be translated into a Fokker-Planck equation in which the dynamical friction and diffusion coefficients depend on the single particle distribution function, therefore they depend on the state of the system [12,88]. This dependence corresponds to a non-linear Markov process [105].

A generalization of the Lenard-Balescu equation (2.58) to inhomogeneous systems is given in Ref. [55,85]. The authors derive a Lenard-Balescu-like equation when the system is integrable. In that case the action-angle coordinates allow for a separation of the contribution between the angle and the action in a similar way as for the homogeneous case.

Furthermore, a generalization of the LB equation to finite space-time domains is given in Ref. [7] in the case of electrostatic interactions. The authors here shows that unstable states can be described until the linear theory is a good approximation, thereby, in a first stage, unstable states evolve consistently with the linear theory.

# Chapter 3

# Linear response theory of homogeneous systems

*In this Chapter we describe the perturbation theory of a mean-field system, the central issue of our work. Homogeneous QSSs can be stable with respect to small fluctuations and in this Chapter we answer the question about their stability against external perturbations. In the first Sections we describe the linear theory of the Vlasov equation and its solution. In the central part we discuss the stability of the solutions and we compare the results with numerical simulations of a simple model. In the last Section we consider to what extent the theory at second order can be important.*

## 3.1 Introduction

Stationary solutions of the Vlasov equation (2.17) can be QSSs when they are stable. In Section 2.5.2 we have made a statement about the stability of an initial homogeneous stationary state $f_0$ under small fluctuations around it. The system evolves in time according to linear Vlasov theory and we have been able to describe it by using Fourier and Laplace techniques. Linearly stable states are attractive under such dynamics in a weak sense.

In this Chapter we perform the study of the stability and of the response to an external perturbation of a given stationary solution of the Vlasov equation [96]. Inspired by Kubo linear response theory [70], we analyse the response of a Vlasov-stable stationary state to the application of a small external perturba-

tion described by a time-dependent term in the Hamiltonian. The perturbation induces *forced* fluctuations around the stationary state that we treat to linear order in the strength of the perturbation, and study their evolution in time by using the linearized Vlasov equation. Such forced fluctuations are known to be generically finite for Boltzmann-Gibbs equilibrium states. We show here theoretically that they are finite and small, of the order of the perturbation, also for Vlasov-stable stationary states. Moreover, the system reaches a new QSS in the long-time regime, well described by the theory we develop. We support our analysis with $N$-particle numerical simulations of the HMF model.

The Chapter is organized as follows. In the second Section, Sec. 3.2, we present some remarks on the external perturbation and on some interesting stationary solutions of the Vlasov equation. In Sec. 3.3, we develop the linear response theory for a homogeneous QSS by using the Vlasov framework. In Sec. 3.4, we describe the solution of the linear theory and we apply it to get the response of different stationary states, as discussed above. Section 3.5 is devoted to compare the results of $N$-particle numerical simulations of the HMF dynamics with those of linear response theory. We also discuss the long-time relaxation of the water-bag QSS to Boltzmann-Gibbs equilibrium under the action of the perturbation. In the last Section, Sec. 3.6 of this Chapter we analyse the second order theory and we apply it to the HMF model. We draw our conclusions in Sec. 3.7.

## 3.2 Some introductory remarks

Let us consider an external perturbation of the form

$$H_{ext} = \sum_i \mathrm{b}(q_i, t), \qquad \mathrm{b}(q_i, t) = hg(t)b(q_i) \tag{3.1}$$

where $b(q)$ is a generic but smooth function while $g(t)$ is the time dependence of the external potential and has to be zero for times $t < t_0$ and positive definite. The constant $h$ is the size of the perturbation and in the following linear theory it is the small parameter. For instance, linear theory requires that $1 \gg h$ in order to ensure that the perturbation is small compared to the unperturbed state. Moreover, for finite systems the size of the perturbation has to be larger than the collisional terms, hence $h \gg N^{-1}$.

In order to get a perturbation theory we ask that the Vlasov equation of the modified dynamics does not change brutally. This implies that we can recover

the unperturbed state in the limit $h \to 0$ at every time, thus we don't get divergences. For instance, the external action breaks the conservation of energy doing some work on the system, but this work has to be smaller or comparable with the size of the perturbation. This corresponds to the requirement that the state of the system has to stable in order to obtain a qualitative and quantitative description valid for long times. On the contrary, for slightly unstable states linear theory looses validity on a short time-scale.

### 3.2.1 Initial homogeneous distribution

In the following we consider only some representative initial distributions in order to guess the picture on the phenomenon.

#### Boltzmann-Gibbs distribution

The Boltzmann-Gibbs (BG) distribution corresponds to the state of thermal equilibrium. In the homogeneous regime the state is uniform in the coordinate and the distribution is a Gaussian in momentum. Therefore, the momentum distribution is

$$f_{BG}(p) = \frac{1}{2\pi}\sqrt{\frac{\beta}{2\pi}}e^{-\beta\frac{p^2}{2}}; \quad p \in [-\infty, \infty]. \tag{3.2}$$

where $\beta > 0$ is the inverse temperature characterizing the state.

The analytical computation of the dielectric function (2.48) is not possible, but there are some numerical results tabulated, for instance, in [53]. In the long time limit we get

$$\epsilon(k, 0) = 1 - \frac{2}{\beta} \tag{3.3}$$

whenever the stability criterion (in Section 2.53) is satisfied. This implies that the homogeneous BG state is stable for $\beta < 2$.

#### Water-Bag distribution

The water-bag (WB) distribution is constant in a given domain of the single particle phase space, and zero outside. In the homogeneous state coordinates are uniformly distributed in $[0, 2\pi]$ and momenta are uniformly distributed in $[-p_0, p_0]$,

$$f_{WB}(p) = \frac{1}{2\pi}\frac{1}{2p_0}\Big[\Theta(p + p_0) - \Theta(p - p_0)\Big]; \quad p \in [-p_0, p_0]. \tag{3.4}$$

where $\Theta(x)$ denotes the unit step function or Heaviside function. The energy density of that state reads

$$\mathrm{e} = \frac{p_0^2}{6} + \frac{1}{2}. \tag{3.5}$$

The dielectric function may be obtained by using Eq. (2.48) to get

$$\epsilon(1,\omega) = 1 - \frac{1}{2(p_0^2 - \omega^2)}, \tag{3.6}$$

which is analytic in all the $\omega$-plane, except at the two points $\omega = \pm p_0$.

This is a peculiar result because, on one side, the WB distribution is one of the few distributions with a finite number of zeroes of the relative dielectric function, while on another side these zeros are on the real axis. Real zeros mean that the distribution shows oscillations which never damp in time. Therefore, formally, the WB distribution is not a stable QSS. It is only marginally stable. From kinetic theory, a marginally stable distribution could give some divergences, and the LB equation 2.6 cannot be used.

### Fermi-Dirac distribution

We now describe the Fermi-Dirac (FD) distribution. In the homogeneous state the coordinate is uniformly distributed in $[0, 2\pi]$, while the momentum distribution has the form:

$$f_{FD}(p) = A\frac{1}{2\pi}\frac{1}{1 + e^{\beta(p^2-\mu)}}; \quad p \in [-\infty, \infty]. \tag{3.7}$$

Here, $\beta \geq 0$ and $\mu \geq 0$ are parameters characterizing the distribution, while $A$ is the normalization constant. We consider the state (3.7) in the limit of large $\beta$ in which analytic computations of various physical quantities are easier. As $\beta \to \infty$ the Fermi-Dirac state converges to the water-bag state (3.4) with $p_0 = \sqrt{\mu}$. As shown in Appendix B.1, to leading order in $1/\beta^2$, the normalization is given by

$$A = \frac{1}{2\sqrt{\mu}}\Big(1 + \frac{\pi^2}{24\beta^2\mu^2}\Big), \tag{3.8}$$

while the energy density is

$$\mathrm{e} = \frac{\mu}{6}\Big(1 + \frac{\pi^2}{6\beta^2\mu^2}\Big) + \frac{1}{2}. \tag{3.9}$$

Let us now investigate the conditions for the stability of the state (3.7). As shown in the Appendix, to order $1/\beta^2$, we have

$$\epsilon(1,0) = 1 - \frac{1}{2\mu}\Big(1 + \frac{\pi^2}{6\beta^2\mu^2}\Big). \tag{3.10}$$

Therefore, the stability threshold is at a value of $\mu^*$ which corresponds to a zero of the dielectric function. To order $1/\beta^2$, we get

$$\mu^* = \frac{1}{2} + \frac{2\pi^2}{3\beta^2}, \tag{3.11}$$

which gives the corresponding energy density

$$e^* = \frac{7}{12} + \frac{\pi^2}{6\beta^2}, \tag{3.12}$$

such that at higher energies, the state (3.7) can be a QSS.

## 3.3 Linear Vlasov equation

The Vlasov equation describing the dynamics in presence of the external field is

$$\partial_t f - \mathcal{L}(q,p,t)[f]f = 0, \tag{3.13}$$

where the new Liouville operator is

$$\mathcal{L}[f](q,p,t) = -p\partial_q + \partial_q\Phi[f](q,t)\partial_p - hg(t)\partial_q b\partial_p, \tag{3.14}$$

and $\Phi[f](q,t)$ is the mean-field potential. It is defined as

$$\Phi[f](q,t) = \int dq'dp'\ v(q-q')f(q',p',t). \tag{3.15}$$

As a first step, we investigate the response of the system to the external field by monitoring the generic observable

$$\langle a(q,p)\rangle(t) \equiv \int dqdp\ a(q,p)f(q,p,t). \tag{3.16}$$

To obtain its time dependence, we need to solve Eq. (3.13) for $f(q,p,t)$, with the initial condition

$$f(q,p,0) = f_0(q,p). \tag{3.17}$$

Here, $f_0(q,p)$ is the initial state that characterizes a QSS, i.e., a stable and stationary solution of the Vlasov equation for the unperturbed dynamics (2.17). Thus, $f_0(q,p)$ satisfies

$$\mathcal{L}_0[f_0](q,p)f_0 = 0, \tag{3.18}$$

where

$$\mathcal{L}_0[f_0](q,p) = -p\partial_q + \partial_q\Phi[f_0](q)\partial_q, \tag{3.19}$$

is the unperturbed Liouville operator, for instance, the generator of the dynamics without the external field. $\Phi[f_0]$ is the mean field potential of the unperturbed state and does not depends on time.

To solve Eq. (3.13) for $h \ll 1$, we expand $f(q,p,t)$ to linear order in $h$. The distribution function is decomposed in the following form

$$f(q,p,t) = f_0(q,p) + h\delta f(q,p,t) + \mathcal{O}(h^2), \tag{3.20}$$

with the initial condition

$$\delta f(q,p,0) = 0. \tag{3.21}$$

The variation of the distribution function, $\delta f$, obeys a constraint because the mass of the system must stay constant. This statement is translated in the following equation

$$\int dqdp\, \delta f(q,p,t) = 0, \qquad \forall t. \tag{3.22}$$

Substituting Eq. (3.20) in Eq. (3.13), we get, at $\mathcal{O}(1)$

$$\partial_t f_0 - \mathcal{L}_0[f_0](q,p)f_0 = 0, \tag{3.23}$$

which corresponds to the unperturbed dynamics. At order $h$ one obtains

$$\partial_t \delta f - \mathcal{L}_0[f_0](q,p)\delta f = \mathcal{L}_{\text{ext}}[\delta f](q,p,t)f_0, \tag{3.24}$$

which is the linear Vlasov equation. The operator related with the external perturbation reads

$$\mathcal{L}_{\text{ext}}[\delta f](q,p,t) = \partial_q\Phi[\delta f](q,t)\partial_p - g(t)\partial_q b\partial_p. \tag{3.25}$$

It describes the effects of the external field, which are two-fold: (i) to generate a potential due to its direct coupling to the particles which is a source of the variation of the distribution, and (ii) to modify the mean-field potential (3.15) from its value $\Phi[f_0](q)$ in the absence of the field. Let us define the variation of the Hamiltonian at linear order due to the perturbation

$$\delta\mathcal{H}[\delta f](q,t) = \Phi[\delta f](q,t) - hg(t)b(q), \tag{3.26}$$

then the external operator becomes

$$\mathcal{L}_{ext} = \partial_q \delta\mathcal{H}\, \partial_p, \tag{3.27}$$

which shows a relation with the usual Kubo linear theory [70] of an $N$ body system.

Equation (3.23) is satisfied by virtue of the definition of $f_0$ that must be a stable and stationary solution of the unperturbed dynamics. We thus solve Eq. (3.27) for $\delta f$ in order to determine $f(q,p,t)$ at linear order from Eq. (3.20). With the condition (3.21), the formal solution is given by the Duhamel formula, and reads

$$\delta f(q,p,t) = \int_0^t d\tau\ e^{(t-\tau)\mathcal{L}_0} \partial_q \delta\mathcal{H}(q,p,\tau)\partial_p f_0(q,p). \tag{3.28}$$

Let us define the Poisson bracket between two dynamical variables $a(q,p)$ and $c(q,p)$ in the single-particle phase space as

$$\{a(q,p), c(q,p)\} = \partial_q a(q,p)\, \partial_p c(q,p) - \partial_q c(q,p)\, \partial_p a(q,p)\ , \tag{3.29}$$

thus, using Eq. (3.28) in Eqs. (3.16) and (3.20) one gets the change in the value of $\langle a(q,p)\rangle(t)$ due to the external field:

$$\begin{aligned} \langle \delta a\rangle(t) &\equiv \int dqdp\ a(q,p)\delta f(q,p,t) \\ &= \int_0^t d\tau \Big\langle \{a(t-\tau), \delta\mathcal{H}(\tau)\} \Big\rangle_0 . \end{aligned} \tag{3.30}$$

Here, angular brackets with 0 subscript denote averaging with respect to $f_0(q,p)$, e.g.,

$$\langle a(q,p)\rangle_0 \equiv \int dqdp\ a(q,p) f_0(q,p), \tag{3.31}$$

while

$$a(t-\tau) = e^{-(t-\tau)\mathcal{L}_0} a(q,p) \tag{3.32}$$

is the time-evolved $a(q,p)$ under the dynamics of the unperturbed system.

The above equation has a form similar to the Kubo formula for the response to an external perturbation of a dynamical quantity defined in the full $2N$-dimensional phase space [70]. The main difference between the two equations is that Kubo formula is a closed expression which defines self consistently the response of the system, while, the average of the Poisson bracket with respect to the initial distribution indicates that the response of the system depends on properties of the initial state. Whenever the system is initially at equilibrium, Kubo formula can be related to correlations and thus the response of the system starting from equilibrium is driven by correlations. Moreover, correlations can be related with other thermodynamics quantities, such as transport coefficients and susceptibilities.

On the contrary, in the first formula (3.30) one sees that the response of the system is a more involved expression because the potential that drives the response, here, namely the variation of the Hamiltonian $\delta\mathcal{H}$, depends itself on the variation of the distribution function. It is a first hint that the full response of the system has to be weighted with a resistance of the system itself. A perturbation on the system determines a variation of the mean-field and, consequently, a variation of the state. That variation absorbs a part of the energy injected into the system, thus the response is dragged by the mean-field.

In the following Section, we show the consequences of this approach for homogeneous QSS, i.e., when the distribution $f_0(q,p) = f_0(p)$ is a function solely of momentum, and we will be able to obtain an explicit form of the formal solution (3.28).

### 3.3.1 Solution of the homogeneous state in the Fourier-Laplace space

For homogeneous states the mean-field potential is a constant that we can put equal to zero. In this peculiar regime the modes of the system are decoupled, thus one can write down an equation for every mode. In order to obtain such an equation we perform the Fourier transform.

The unperturbed operator Eq. (3.19) reduces to

$$\mathcal{L}_0(q,p)[f_0] = -p\partial_q, \tag{3.33}$$

so that the Duhamel formula, Eq. (3.28), becomes

$$\delta f(q,p,t) = \int_0^t d\tau \; e^{-(t-\tau)p\partial_q} \partial_q \delta\mathcal{H}(\tau)\partial_p f_0(p). \tag{3.34}$$

The spatial Fourier and temporal Laplace transform of $\delta f(q,p,t)$ satisfies A.2

$$\begin{aligned}\widehat{\delta f}(k,p,\omega) &= \partial_p f_0(p)\imath k \mathrm{L}[e^{-\imath tpk}] \\ &\times \Big[2\pi\widetilde{v}(k)\int dp' \; \widehat{\delta f}(k,p',\omega) - \widehat{g}(\omega)\widetilde{b}(k)\Big].\end{aligned} \tag{3.35}$$

Here, L denotes the Laplace transform:

$$\mathrm{L}[e^{-\imath tpk}] = \int_0^\infty dt \; e^{\imath\omega t - \imath tpk} = \frac{1}{\imath(kp-\omega)}, \qquad \mathrm{Im}\{\omega\} > 0 \tag{3.36}$$

and the imaginary part of $\omega$ has to be positive in order to obtain a good convergence of the time integral of the Laplace transform. Following the same procedure in Chapter 2 one finds the solution, which is given by

$$\widehat{\delta f}(k,p,\omega) = \widehat{g}(\omega)\frac{\widetilde{b}(k)}{\epsilon(k,\omega)}\frac{k}{\omega - kp}\partial_p f_0(p). \tag{3.37}$$

Here, $\epsilon(k,\omega)$ is the dielectric function (2.48), analytically continued to the lower half of the complex plane.

The variation of the Hamiltonian reads

$$\delta\mathcal{H}(k,\omega) = \widehat{g}(\omega)\frac{\tilde{b}(k)}{\epsilon(k,\omega)}. \tag{3.38}$$

This result states that the variation of the field felt by every single particle is equal to the external field, but with a modulated amplitude. This modulation is given by the dielectric function, which acts, in the Fourier space, as a resistance of the system to the perturbation. Indeed, part of the energy injected into the system serves to modify the mean-field and does not contribute to the dynamics of the particles.

## 3.4 Solution for real times and the time asymptotic regime

The solution in real space-time involves the inverse Laplace transform. It requires the knowledge of all the zeros of the dielectric function and the poles of

the Laplace transform of $\widehat{g}(\omega)$. Formally, the solution becomes

$$\delta f(q,p,t) = \partial_p f_0(p) \int dk e^{-\imath kq} \widetilde{b}(k) \int_{\mathrm{C}} d\omega e^{-\imath\omega t} \frac{\widehat{g}(\omega)}{\epsilon(k,\omega)} \frac{k}{\omega - kp}. \tag{3.39}$$

While the inverse Fourier transform is often doable analytically or numerically, performing the inverse Laplace transform can be quite complicated. In general this is a too complicated task but one can overcome that problem by focusing on the asymptotic behavior of the response. We here use a theorem which states that whenever the two following limits exist they are equal[1]

$$\lim_{t\to\infty} F(t) = \lim_{\omega\to 0^-} \omega \widehat{F}(\omega) \tag{3.40}$$

where $F(t)$ is a generic but integrable function. Hence, we can obtain the time asymptotic response by evaluating its Laplace transform in the limit of vanishing frequency $\omega$.

In the remaining part of this Section we will focus on the HMF model (see Chapter 1.4). Here, we study the response of a QSS to an external perturbation of the form

$$H_{\mathrm{ext}} = -hg(t) \sum_{i=1}^{N} \cos q_i, \tag{3.41}$$

which corresponds to the choice

$$b(q) = \cos q, \tag{3.42}$$

in Eq. (3.26). The specific $g(t)$ we choose is a step function:

$$g(t) = \begin{cases} 0 & \text{for } t < t_0, \\ 1 & \text{for } t \geq t_0. \end{cases} \tag{3.43}$$

and, for the sake of simplicity, we can consider the initial time $t_0 = 0$ thanks to the time translation invariance of the unperturbed Vlasov equation.

We focus on a simple observable of the HMF model, its order parameter, the magnetization. The change of the $x$-component of the magnetization due to the field is

$$\begin{aligned} \delta m_x(t) &= \int dq dp \delta f(q,p,t) \cos q \\ &= \frac{1}{2} \int_C d\omega \; e^{-\imath\omega t} \int dp \left( \widehat{\delta f}(1,p,\omega) + \widehat{\delta f}(-1,p,\omega) \right), \end{aligned} \tag{3.44}$$

[1] see Appendix A.2

and for the $y$-component

$$\begin{aligned}\delta m_y(t) &= \int dqdp\ \delta f(q,p,t)\sin q \\ &= \frac{1}{2\imath}\int_C d\omega\ e^{-\imath\omega t}\int dp\ \left(\widehat{\delta f}(-1,p,\omega)-\widehat{\delta f}(1,p,\omega)\right). \end{aligned} \tag{3.45}$$

These quantities correspond to the susceptibilities along the $x$ and $y$ directions, since we extract the linear dependence of $\delta m_{x,y}$ on the size of the perturbation $h$.

The Laplace and Fourier transforms of the long-range potential, the external potential and the time dependence of the external perturbation are:

$$\widetilde{v}(k) = \left[\delta_{k,0}-\frac{\delta_{k,-1}+\delta_{k,1}}{2}\right], \tag{3.46}$$

$$\widetilde{b}(k) = \frac{\delta_{k,-1}+\delta_{k,1}}{2}, \tag{3.47}$$

$$\widehat{g}(\omega) = -\frac{1}{\imath\omega}, \tag{3.48}$$

hence, Eqs. (3.44) and (3.45) give

$$\delta m_x(t) = \frac{1}{2\pi}\int_C d\omega\ e^{-\imath\omega t}\frac{1}{\imath\omega}\frac{\epsilon(1,\omega)-1}{\epsilon(1,\omega)}, \tag{3.49}$$

and

$$\delta m_y(t) = 0. \tag{3.50}$$

Here, we have used the fact that, for the HMF model, there is the following symmetry of the dielectric function

$$\epsilon(1,\omega) = \epsilon(-1,\omega), \tag{3.51}$$

as may be easily checked by using Eq. (3.46) in Eq. (2.48). It may also be seen that

$$\epsilon(k,\omega) = 1 \text{ for } k \neq \pm 1. \tag{3.52}$$

because the long-range potential is a cosine, so it has only the two symmetric modes $k = \pm 1$.

Now, using the knowledge that the initial state is homogeneous, the initial magnetization is zero $m_x = m_y = 0$. Equations (3.49) and (3.50) imply that, at linear order we get

$$m_x(t) = \frac{h}{2\pi}\int_C d\omega\ e^{-\imath\omega t}\frac{1}{\imath\omega}\frac{\epsilon(1,\omega)-1}{\epsilon(1,\omega)}, \tag{3.53}$$

and

$$m_y(t) = 0. \tag{3.54}$$

This result that the magnetization along the $y$ direction is zero holds at every order in perturbation theory when the momentum distribution is even, because the $y$-magnetization observable is an odd function while the rest is even.

We are now led to evaluate these results for the different QSSs introduced in Section 3.2.

### 3.4.1 The water-bag case

As discussed in Sec. 2, zeros of the dielectric function determine the temporal behavior of the variation of the distribution function, $\int dp\ \delta f(q,p,t)$. The zeros of (3.6) occur at $\omega_{\rm p} = \pm\sqrt{p_0^2 - 1/2}$. For $p_0 < p_0^* = 1/2$, (correspondingly, $e < e^* = 7/12$), the pair of zeros lies on the imaginary-$\omega$ axis, one in the upper half-plane and one in the lower half. The one in the upper half-plane makes the water-bag state linearly unstable for $e < e^*$. As $e$ approaches $e^*$ from below, the zeros move along the imaginary-$\omega$ axis and hit the origin when $e = e^*$. At higher energies, the zeros start moving on the real-$\omega$ axis away from the origin in opposite directions. The fact that the zeros of the dielectric function are strictly real for $e \geq e^*$ implies that the water-bag state is marginally stable. However, one can check that it is a QSS, since no observable diverges in time.

From the discussions in Sec. 3.3 and those following Eq. (3.53), one derives that the result of linear Vlasov theory, Eq. (3.53), is valid and physically meaningful only when $p_0^2 > 1/2$. Using Eq. (3.6) in Eq. (3.53) and performing the integral by the residue theorem gives

$$m_x(t) = \frac{2h}{2p_0^2 - 1} \sin^2\Big(\frac{t}{2}\sqrt{p_0^2 - \frac{1}{2}}\Big); \qquad p_0^2 > \frac{1}{2}, \tag{3.55}$$

while $m_y = 0$. Thus, linear Vlasov theory predicts that, in the presence of an external field along $x$, the corresponding magnetization exhibits undamped oscillations and does not approach any time-asymptotic constant value. This prediction is verified in numerical simulations discussed in Sec. 3.5. The average of $m_x(t)$ over a period of oscillation $T$ is

$$\langle m_x \rangle_{\text{Time average}} \equiv \frac{1}{T}\int_0^T dt\ m_x(t) = \frac{h}{2p_0^2 - 1} \quad p_0^2 > \frac{1}{2}. \tag{3.56}$$

In Section 3.5, we will compare this average with numerical results.

We can consider an external perturbation acting on the system only for a finite time. For instance, we consider the following time dependence of $g$

$$g(t) = \theta(t) - \theta(T_0 - t), \tag{3.57}$$

thus when the time becomes larger than a given value $T_0 > 0$, the perturbation vanishes. We can argue that the final state predicted by linear theory is the initial state whenever $f_0$ is stable, but the WB distribution is only marginally linear stable. If the parameter $T_0$ is such that the perturbation switched off when the magnetization is at the maximum of an oscillation, the conservation law of the unperturbed Vlasov equation, in the WB state, implies that the oscillation is preserved. On the contrary we can destroy the oscillations by choosing $T_0$ such that $m_x$ is at his minimum. Therefore, we define the destructive and constructive times:

$$T_0^d = \frac{2\pi n}{\sqrt{p_0^2 - 1/2}}, \tag{3.58}$$

$$T_0^c = \frac{2\pi(n+1)}{\sqrt{p_0^2 - 1/2}}, \tag{3.59}$$

for $n \in \mathbb{N}$.

In Section 3.5 we will show numerical simulations in which a WB distribution persists with an oscillating magnetization or not.

### 3.4.2 The long time regime

When the zeros of $\epsilon(1, \omega)$ lie only in the lower-half complex-$\omega$ plane, we get the time asymptotic limit of equation (3.53), which reads

$$\overline{m}_x \equiv \lim_{t\to\infty} m_x(t) = h\Big(\frac{1 - \epsilon(1,0)}{\epsilon(1,0)}\Big). \tag{3.60}$$

This equation implies a diverging magnetization at $\epsilon(1, 0) = 0$, which is clearly not possible as the magnetization is bounded from above by unity. Therefore, in such a case, linear response theory makes incorrect prediction. Thus, we rely on formula (3.60) only when the result is much smaller than unity.

An interesting property of the dielectric function is its behavior in such a long time regime. Let us consider $\sigma$ as an inverse energy scale, hence the dielectric function reads as

$$\epsilon(k, 0) = 1 - \frac{\sigma_c(k)}{\sigma}, \tag{3.61}$$

where

$$\sigma_c(k) = 2\pi\tilde{v}(k)\int \frac{\partial_p f_0(p)}{p}dp, \tag{3.62}$$

is the critical parameter below which the homogeneous distribution becomes unstable. The variable $p$ now is scale independent, because we consider $p \to \sqrt{\sigma}p$. The response of the magnetization, namely the susceptibility, diverges as a power law as a function of that parameter $\sigma$. At equilibrium, the inverse energy scale corresponds to the inverse temperature and therefore the divergence near criticality follows a power law behavior as in the classical theory of second order phase transitions.

Note that $\widehat{g}(\omega)$, given in Eq. (3.48), has a pole only at $\omega = 0$. Following the discussions in Sec. 3.4, we thus conclude that condition (3.6) only determines the parameters characterizing the distribution $f_0(p)$ such that it is marginal stable. For the HMF model, we need to consider only $k = \pm 1$. Since $\epsilon(1,\omega) = \epsilon(-1,\omega)$, we can restrict ourselves to consider real frequencies $\omega_{\rm re}$, so that these conditions become

$$1 + \pi\!\!\!\!\!\!\int_{-\infty}^{\infty} \frac{dp}{p \mp \omega_{\rm re}}\partial_p f_0(p) = 0, \tag{3.63}$$

$$\partial_p f_0(p)|_{\omega_{\rm re}} = 0. \tag{3.64}$$

They define a stability criterion for the HMF model perturbed by an external field.

The WB distribution is only marginally stable, hence the limit value of the response becomes ill defined. For instance, for the WB the oscillations survive forever for the linear theory.

The BG distribution shows a good time asymptotic limit and its dielectric function is tabulated in [53]. The magnetization value at infinite times reads

$$\overline{m}_x = \frac{2h}{\beta - 2}; \quad \beta < 2. \tag{3.65}$$

For the FD distribution, following the discussions on the regime of validity of the linear Vlasov theory, and using Eq. (3.10) in Eq. (3.60), we get

$$\overline{m}_x = \frac{h\left(1 + \frac{\pi^2}{6\beta^2\mu^2}\right)}{2\mu - 1 - \frac{\pi^2}{6\beta^2\mu^2}}; \qquad \mu > \mu^*. \tag{3.66}$$

## 3.5 Numerical results

In order to verify the analysis presented in Sec. 3.4, we have performed extensive numerical simulations of the $N$-particle dynamics for the HMF model, (1.4), for large $N$. The equations of motion were integrated using a fourth-order symplectic scheme [78], with a time step varying from $0.01$ to $0.1$. In simulations, we prepare the HMF system at time $t = 0$ in an initial state by sampling independently the coordinate $q$ of every particle uniformly in $[0, 2\pi]$ and the momentum $p$ according to either the water-bag, the Fermi-Dirac, or the Gaussian distribution. Thus, the probability distribution of the initial state is

$$F_N(q_1, p_1, q_2, p_2, \ldots, q_N, p_N) = \prod_{i=1}^{N} f_0(p_i) \tag{3.67}$$

where $f_0(p)$ is given by either of (3.4), (3.7), or (3.2). The energy of the initial state is chosen to be such that the system is in a QSS. Then, at time $t_0$, we switch on the external perturbation, Eqs. (3.41) and (3.43), and follow the time evolution of the magnetization along $x$, $m_x$.

In obtaining numerical results, two different approaches were adopted. On the one hand, we have followed in time the evolution of a *single realization* of the initial state. These simulations are intended to check if our predictions based on the Vlasov equation for the smooth distribution $f(q, p, t)$ for infinite $N$ are also valid for a *typical* trajectory. Rigorous results due to Braun and Hepp and further analysis by Jain *et al.* show that these typical trajectories stay close to the trajectory of $f(q, p, t)$ for times that increase at least logarithmically with $N$ [25,62]. When $f_0(p)$ is a stable stationary solution of the Vlasov equation, it is known numerically [117] and analytically [30] that these times diverge as a power of $N$, and are therefore sufficiently long to allow us to check even for moderate values of $N$ the predictions of our linear Vlasov theory for perturbations about Vlasov-stable stationary solution $f_0(p)$.

On the other hand, we have obtained numerical results by averaging over an *ensemble of realizations* of the initial state. The time evolution that we get using this second method is different from the first one. This approach allows us to reach the average and/or asymptotic value of an observable, here $\langle m_x \rangle(t)$, on a faster time-scale because of a mechanism of convergence in time, as we describe below.

### 3.5.1 Simulations for single realizations

#### Water-Bag distribution

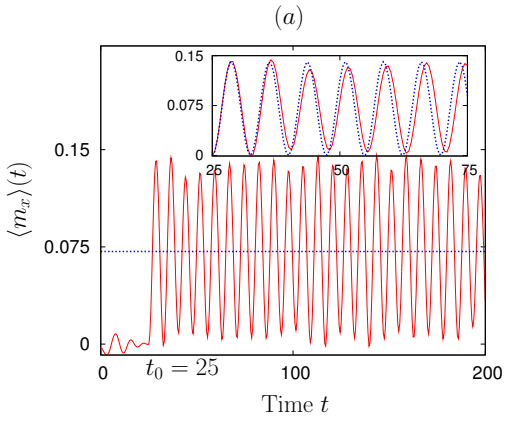


Figure 3.1: $m_x(t)$ vs. time $t$ for the water-bag QSS in the HMF model under the action of the perturbation, Eqs. (3.41).

The oscillatory behavior of $m_x(t)$ predicted for the water-bag state, see formula (3.55), is checked in Fig. 3.1. Oscillations around a well-defined average persist indefinitely with no damping, as predicted by the theory. In the inset of the same panel, the theoretical prediction is compared with the numerical result for a few oscillations. While the agreement is quite good for the first two periods of the oscillations, numerical data display a small frequency shift with respect to the theoretical prediction. Moreover, an amplitude modulation may also be observed. We have checked in our $N$-particle simulations that different initial realizations produce different frequency shifts, which has a consequence when averaging over an ensemble of initial realizations.

The numerical simulations are performed with the perturbation (3.43), with $h = 0.1$ switched on at time $t_0 = 25$. The full line in the main plot shows the result of an $N$-particle simulation, while the dashed horizontal line is the theoretical time-averaged value of $m_x(t)$ given in Eq. (3.56). The system size is $N = 10^5$, while the parameter $p_0$, corresponding to energy $e = 0.7$, is approximately $1.095$. In the inset, the numerical result (full line) is compared with the theoretical prediction (3.55) (dashed line).

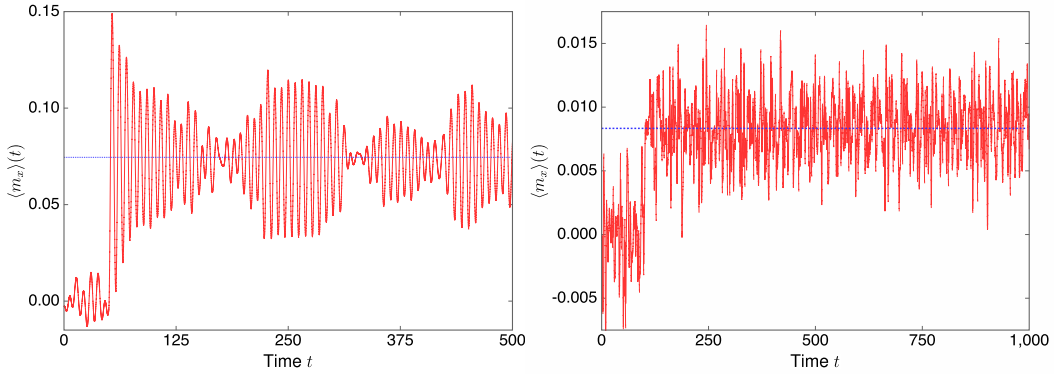


Figure 3.2: $m_x(t)$ vs. time $t$ for the Fermi-Dirac QSS the HMF model. The left panel shows the evolution of the magnetization of the Fermi-Dirac state with $\beta = 10$, while the right panel shows the time evolution of the magnetization with $\beta = 0.5$.

### Fermi-Dirac distribution

In Fig. 3.2, we show $m_x(t)$ for two numerical simulations of the Fermi-Dirac QSS. The left panel of figure 3.2, shows a numerical simulation of a Fermi-Dirac distribution with $\beta = 10$. For this high value of $\beta$, the Fermi-Dirac distribution is very close to the WB one. In this case, we can calculate the theoretical prediction only for the asymptotic value $\overline{m}_x$ given in Eq. (3.66) in series of $\beta^{-2}$. The time evolution of $m_x(t)$ displays beatings and revivals of oscillations around this theoretical value, shown by the dashed horizontal line in the figure. Indeed, we cannot conclude that there will be damping in time, such as in the case of single realization of the WB distribution. However, the mean of the oscillations fits well to the linear theory predictions.

The right panel of figure 3.2 shows a numerical simulation of a Fermi-Dirac distribution with $\beta = 0.5$. In this case the Fermi-Dirac distribution is very close to the Gaussian one, and we have no prediction for the asymptotic response. However, the blue dotted horizontal line shows the theoretical prediction of the Gaussian distribution, which represents well the average value.

The numerical simulations in Fig. 3.2 were done with the system size $N = 10^5$ and $\mu = 1.2$. In the left panel we have used $\beta = 10$, giving an energy $e \approx 0.7$. The external perturbation of the HMF model is (3.43), $h = 0.1$ and switched on at time $t_0 = 25$. The full line represents simulation results, while the horizontal dashed line is the theoretical asymptotic value given in (3.66). In the right panel of Fig. 3.2 we have used $\beta = 0.5$, giving an energy $e \approx 1.2$.

### Boltzmann-Gibbs distribution

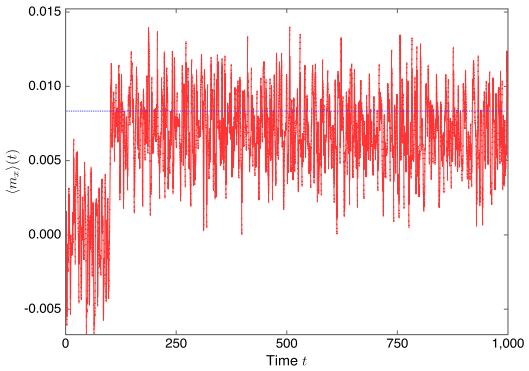


Figure 3.3: $m_x(t)$ vs. time $t$ for the BG state in the HMF model.

In Fig. 3.3, we show $\langle m_x \rangle(t)$ for the Gaussian QSS. After the application of the external field, the magnetization sharply increases and then fluctuates around a value which is slightly below the theoretical prediction, Eq. (3.65). The discrepancy between the asymptotic value of the response obtained analytically and the one found in the numerical simulation of Fig. 3.3 is mainly due to finite-size effects.

The numerical simulations were done using the perturbation in Eqs. (3.41) and (3.43), with $h = 0.025$ switched on at time $t_0 = 25$. The red line represents the result of the $N$-particle simulation, while the dotted horizontal line is the theoretical asymptotic value given in Eq. (3.65). The system size is $N = 10^5$, while $\beta = 0.5$, so that the energy $e = 1.5$.

## 3.5.2 Ensemble average over different realizations

In this Section, we present numerical results for the three initial QSSs (water-bag, Fermi-Dirac, Gaussian), obtained after averaging the time evolution of $m_x(t)$ over a set of realizations[2] of the initial state. We define the average as

$$\langle m_x \rangle_{\text{ Ensemble average}}(t) = \frac{1}{N_s} \sum_{n=1}^{N_s} m_x \Big|_n (t), \tag{3.68}$$

where $\cdots \Big|_n$ labels the sample and $N_s$ is the total number of different realizations.

[2] typically a thousand

In all cases, we observe a relaxation to an asymptotic value. For the water-bag distribution, this value compares quite well with the time-averaged magnetization given in formula (3.56), see Fig. 3.7 panels 1(a) and 1(b) found at the end of this Chapter. The mechanism by which the relaxation to the asymptotic value occurs in the water-bag case, in the absence of a true relaxation of a single initial realization, is the frequency shift present in the different initial realizations. This leads at a given time to an incoherent superposition of the oscillations of the magnetization. For other distributions, the numerically determined asymptotic value is compared with the theoretical value for the single realization $\overline{m}_x$, given in formulas (3.66), and Fig. 3.7 panels 2(a) and 2(b), and formula (3.65) and Fig. 3.7 panels 3(a) and 3(b). The agreement is quite good.

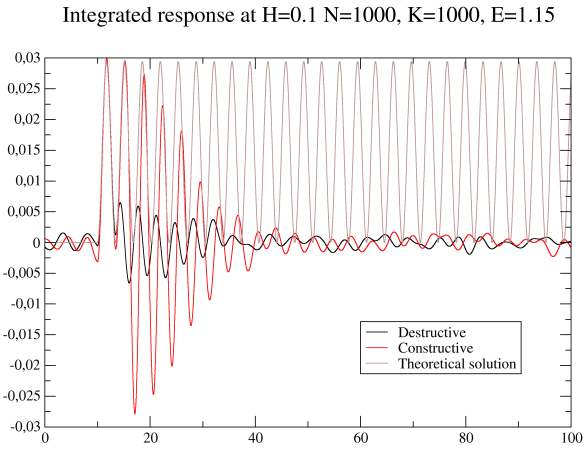


Figure 3.4: Oscillations of the magnetization for a WB distribution with a finite time perturbation. The figure shows the constructive (red line) and the destructive (black line) cases.

In this setting we focus our analysis on perturbations for finite times of the WB distribution, as discussed in 3.3. The ensemble average allows a fast convergence towards the unperturbed state destroying the incoherent oscillations. Moreover, in a finite system we have a source of incoherence due the finite $N$ correction, thus we argue that whenever we remove the external field at $T_0^d$ the state converges quickly towards the initial state. On the contrary, when we consider $T_0^c$ the oscillation persists for longer times. After that the system relaxes towards the finite $N$ QSS without oscillations, as shown in Fig. 3.4.

### 3.5.3 Relaxation towards equilibrium

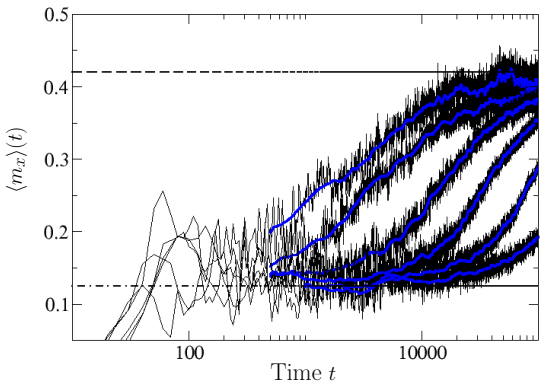


Figure 3.5: Two-step relaxation of the WB QSS towards the BG equilibrium: $m_x(t)$ vs. time $t$ for increasing system size from $N = 2000$ to $N = 64000$ (left to right).

For finite values of $N$, the perturbed HMF system finally relaxes to the BG equilibrium state. The presence of a two-step relaxation of the initial water-bag QSS with energy $e = 0.65$, first to the perturbed Vlasov state and then to equilibrium, is shown in Fig. 3.5 for increasing system sizes, Eqs. (3.41) and (3.43), with $h = 0.01$. The relaxation to the first magnetization plateau with value $m \approx 0.125$ predicted by the linear response theory takes place on a time of $O(1)$. The final relaxation to the equilibrium value of the magnetization $m^{eq} \approx 0.42$ occurs on a timescale that increases algebraically with system size, presumably with an exponent between one and two.

## 3.6 Perturbative theory at second order

Let us now consider the perturbation theory at second order in the size of the perturbation $h$. We define the variation of the distribution function at second order as follows

$$f(q,p,t) = f_0(q,p) + h\delta f(q,p,t) + h^2 \Delta f(q,p,t) + \mathcal{O}(h^3). \tag{3.69}$$

We call it the second variation. The initial condition of the second variation is zero, $\Delta f(t=0) = 0$, such as for the first variation.

The equation that describes the time evolution of the second variation reads

$$\partial_t \Delta f + p\partial_q \Delta f = \partial_q \Phi[\Delta f]\,\partial_p f_0 + \partial_q \delta\mathcal{H}[\delta f]\,\partial_p \delta f, \tag{3.70}$$

where $\delta f$ is the solution of the first order equation (3.24). The solution at first order appears on the right hand side of Eq. (3.70) and plays the role of a source term.

Let us apply a Fourier-Laplace transform to equation (3.70)

$$(\imath\omega - \imath pk)\widehat{\Delta f} = \imath k\tilde{v}(k)\partial_p f_0(p) \int dp'\, \widehat{\Delta f} + \widehat{S}[\delta f], \tag{3.71}$$

where $S$ is the source term which depends on $\delta f$. Using the same procedure discussed in Section 3.3, we write the variation of the density at second order

$$\widehat{\Delta\rho}(k,\omega) = -\frac{\imath}{\epsilon(k,\omega)} \int dp \frac{\widehat{S}[\delta f](k,p,\omega)}{\omega - kp}. \tag{3.72}$$

Thereby, the variation of the distribution reads

$$\widehat{\Delta f}(k,p,\omega) = \frac{\imath}{\omega - kp}\left[\frac{\imath k\tilde{v}(k)\partial_p f_0(p)}{\epsilon(k,\omega)} \int dp' \frac{\widehat{S}(k,p',\omega)}{\omega - kp'} - \widehat{S}(k,p,\omega)\right], \tag{3.73}$$

and its Fourier and Laplace inverse transform gives the formal solution of the Vlasov equation at second order.

Let us discuss how to implement the inverse analytic continuation on the lower half of the complex plane of the frequencies $\omega$, in order to get the inverse Laplace transform. First of all, we see that the source term couples different modes. Using the definition of the variation of the Hamiltonian, Eq. (3.37), and the definition of the variation of the distribution at first order, Eq. (3.38), we get

$$\begin{aligned}\widehat{S}(k,p,\omega) \;=\; & -\frac{\imath}{(2\pi)^{2d}} \int dl \int dm \int_{\mathrm{C}_1} d\omega_1 \int_{\mathrm{C}_2} d\omega_2 \frac{\tilde{b}(l)}{\epsilon(l,\omega_1)} \frac{\tilde{b}(m)}{\epsilon(m,\omega_2)} \times \\ & \hat{g}(\omega_1)\hat{g}(\omega_2)(l\cdot\partial_p)\frac{m\cdot\partial_p}{\omega_2 - pm} f_0(p) \times \\ & \int dq e^{\imath q(k-l-m)} \frac{1}{(2\pi\imath)^2} \int_0^\infty dt\, e^{\imath t(\omega-\omega_1-\omega_2)}.\end{aligned} \tag{3.74}$$

The two contours $\mathrm{C}_1$ and $\mathrm{C}_2$ are such that the inverse Laplace transform is well defined. In the last line of Eq. (3.74) we have an integral over the coordinate $q$,

which gives a Dirac delta function, $\delta(k-l-m)$. Furthermore, the integral over time $t$ gives $1/(\omega-\omega_1-\omega_2)$ with the constraint that the imaginary part of the denominator has to be positive.

We have to evaluate the following integral

$$\mathcal{I}(\omega)=\int_{\mathrm{C}_2}\frac{\hat{g}(\omega_2)}{\epsilon(m,\omega_2)}\frac{1}{\omega_2-mp}\frac{1}{\omega-\omega_1-\omega_2}d\omega_2, \qquad \mathrm{Im}\{\omega-\omega_1-\omega_2\}>0. \tag{3.75}$$

The first ratio, $\hat{g}/\epsilon$, has poles only in the lower half of the complex plane, whenever the unperturbed state $f_0$ is linearly stable. The ratio $1/(\omega_2-mp)$, gives a pole that lies on the real axis, while the last ratio of (3.75) gives a pole in the upper half of the complex plane. Therefore, we take a contour $\mathrm{C}_2$ that passes in the upper half complex plane in order to get only the residue of the pole at $\omega_2=\omega-\omega_1$, as shown in Figure 3.6. As a drawback, this path induces

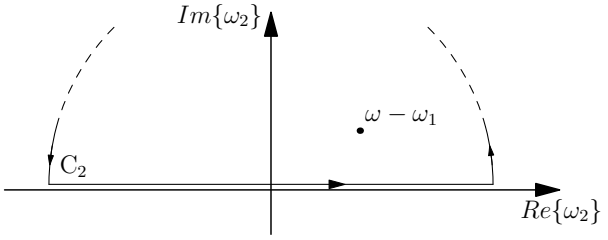


Figure 3.6: The integration path $\mathrm{C}_2$ of $\omega_2$ in formula (3.75).

the constraint on the imaginary part of the other frequency $\mathrm{Im}\{\omega-\omega_1\}>0$, since $\mathrm{Im}\{\omega_2\}>0$.

After the integration along $\mathrm{C}_2$, the source term, $\hat{S}$, reads

$$\begin{aligned}\widehat{S}(k,p,\omega) &= -\frac{1}{(2\pi)^{d+1}}\int dl\int_{\mathrm{C}_1}d\omega_1\frac{\tilde{b}(l)}{\epsilon(l,\omega_1)}\frac{\tilde{b}(k-l)}{\epsilon(k-l,\omega-\omega_1)}\times\\ &\quad \hat{g}(\omega_1)\hat{g}(\omega-\omega_1)(l\cdot\partial_p)\frac{(k-l)\cdot\partial_p}{\omega-\omega_1-(k-l)p}f_0(p).\end{aligned} \tag{3.76}$$

It is a double convolution in the frequencies and in the Fourier modes, with the constraint on the frequencies $\mathrm{Im}\{\omega\}>0$.

We introduce the analytical continuation of the source term following the discussion in Chapter 2. The variation of the density reads

$$\widehat{\Delta\rho}(k,\omega)=-\frac{\imath}{\epsilon(k,\omega)}\int_{\mathrm{C}}dp\frac{\widehat{S}[\delta f](k,p,\omega)}{\omega-kp}, \tag{3.77}$$

where C is the Landau contour, which continues analytically the solution in the region of the complex plane with negative imaginary part.

We remark that the structure of the solution of the equations at any successive order $h^s$, with $s > 2$, is the same as (3.70) because the external field, $b$, couples only at linear order. The difference between solutions at different orders lies in the source term because it depends on all the solutions at lower orders. However, the functional form of the solution is the one shown in equation (3.77).

### 3.6.1 The HMF case

Let us restrict the study to the HMF model (discussed in Section 1.4) in order to get the second order solution for such a model. The solution at the first order is shown in Section 3.3 in equation (3.37).

The external potential is a cosine and its Fourier modes are $\tilde{b}(k) = 1/2(\delta_{k,1} + \delta_{k,-1})$. The zero mode, $k = 0$, is zero because the perturbation does not change the normalization of the system. Thereby, the source term reads

$$\begin{aligned}\widehat{S}(k,p,\omega) &= -\frac{\delta_{k,2}}{4(2\pi)^2}\int_{\mathrm{C}_1} d\omega_1 \frac{1}{\epsilon(1,\omega_1)}\frac{1}{\epsilon(1,\omega-\omega_1)} \times \\ &\quad \hat{g}(\omega_1)\hat{g}(\omega-\omega_1)(\partial_p)\frac{\partial_p}{\omega-\omega_1-p} f_0(p) \\ &\quad -\frac{\delta_{k,-2}}{4(2\pi)^2}\int_{\mathrm{C}_1} d\omega_1 \frac{1}{\epsilon(-1,\omega_1)}\frac{1}{\epsilon(-1,\omega-\omega_1)} \times \\ &\quad \hat{g}(\omega_1)\hat{g}(\omega-\omega_1)(\partial_p)\frac{\partial_p}{\omega-\omega_1+p} f_0(p), \end{aligned} \tag{3.78}$$

where only the two modes $k = \pm 2$ give a non vanishing contribution. The mean-field potential at second order is

$$\Phi[\Delta f](q,t) = \int dk\, e^{ikq}\tilde{v}(k)\widetilde{\Delta\rho}(k,t) = 0, \tag{3.79}$$

and it vanishes because $\tilde{v}$ has only two modes $k = \pm 1$, while the variation of the distribution at second order has the modes $k = \pm 2$. Therefore, the second variation of the order parameter $m$, namely the magnetization, is zero. Indeed, only odd orders of the perturbative expansion give a contribution to the variation of the magnetization. As a consequence, linear response theory turns out to be quite robust because the first correction is of order $h^3$, which is below the finite $N$ noise in many molecular dynamics simulations.

## 3.7 Conclusions

In this Chapter, we have studied the response of a Hamiltonian long-range system in a quasistationary state (QSS) to an external perturbation. The perturbation is characterized by an external field that couples to the canonical coordinates of the particles. We pursued our study by analyzing the Vlasov equation for the time evolution of the single-particle phase space distribution. The initial QSSs are related to stable stationary states of the Vlasov equation in the absence of the external perturbation. We have developed in a series expansion the perturbed Vlasov equation around the QSS for a small size of the external perturbation. At linear order, we have obtained a formal expression for the response observed in a single-particle dynamical quantity. The perturbation induces two different effects: the first one is directly related to the action of the external field on each particle of the system. This kind of process is comparable to Kubo response of Hamiltonian systems. The second effect is the variation of the mean-field potential induced by the perturbation itself. Therefore, each particle feels an effective interaction modulated by both the effects. This introduces a non-linear behavior in the response mechanism. This non linearity gives a different response compared to the Kubo one although both of them show the same formal definition.

For an initial homogeneous QSS, which is uniform in the coordinates, we have derived a closed form expression for the response function. We have applied this formalism to the Hamiltonian mean-field model and we have studied the analytical prediction for three representative QSSs: the water-bag QSS, the Fermi-Dirac QSS and the Gaussian QSS. For the Gaussian and Fermi-Dirac distributions we have derived the time asymptotic value of the response and, indeed, we have fully characterized the new QSS in which the system settled down. On the other hand, in the case of the Water-Bag distribution we were able to derive the finite time response and the time asymptotic one for the ensemble in which we average different realizations. Moreover, we have derived the variation at second order in the size of the perturbation of the response of the system for which a coupling between different modes of the long-range interaction appears.

We have compared the theoretical values of the response for the three different QSSs with numerical $N$-body simulations for different sizes $N$ of the system. The theoretical prediction is in good agreement with numerical experiments on the time-scale in which the Vlasov dynamics describes well the evolution of the

system, as shown by kinetic theory (Chapter 2). We have also analysed the long-time relaxation of the water-bag QSS to the Boltzmann-Gibbs equilibrium state.

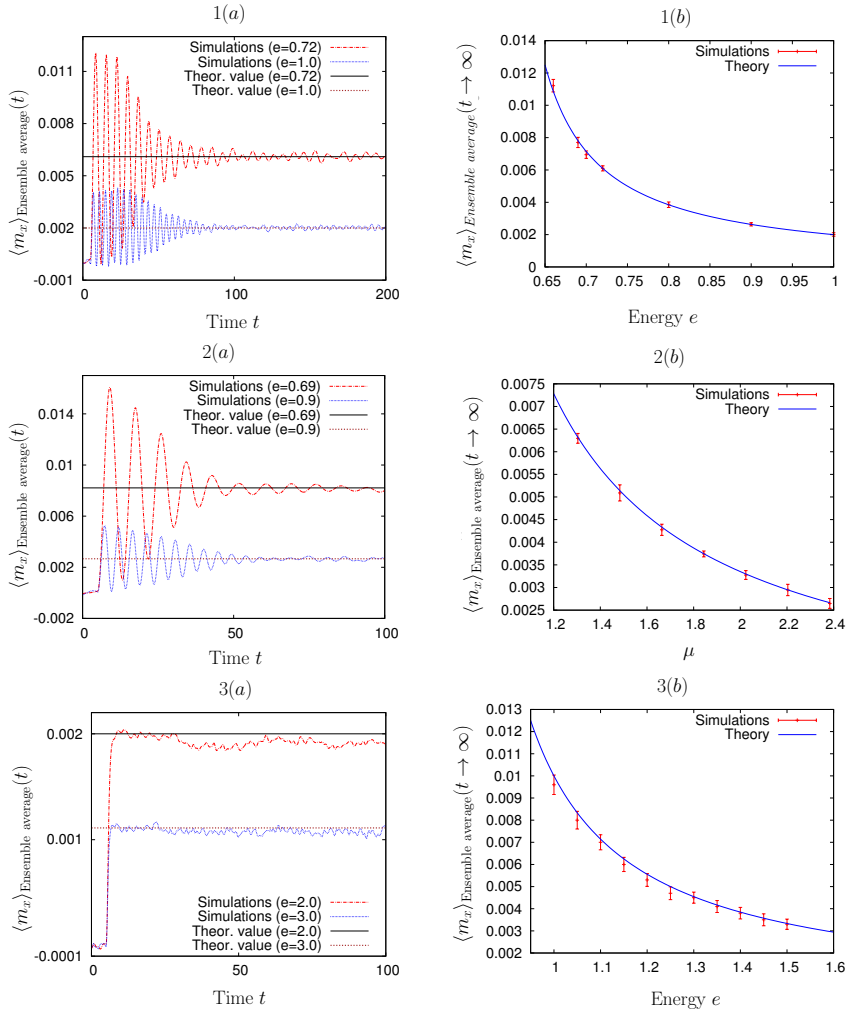


Figure 3.7: Linear response of a water-bag QSS (panels 1(a), 1(b)), a Fermi-Dirac QSS with $\beta = 10$ (panels 2(a), 2(b)), and the homogeneous equilibrium state (panels 3(a),3(b)) for the HMF model under the perturbation, Eqs. (3.41) and (3.43), with $h = 0.01$. All simulation data have been averaged over several realizations of the initial state. In each case, panel (a) shows the time evolution of the averaged magnetization $\langle m_x \rangle_{\text{Ensemble average}}(t)$ as obtained from $N$-particle simulations, and its asymptotic approach either to the time average in Eq. (3.56) for the water-bag initial state or to $\overline{m}_x$ given in Eq. (3.66) for the Fermi-Dirac QSS, or to $\overline{m}_x$ given in Eq. (3.65) for the Gaussian QSS. In panel (b), we show the $N$-particle simulation results for the asymptotic magnetization as a function of energy (the parameter $\mu$ in the Fermi-Dirac case). The error bars denote the standard deviation of fluctuations around the asymptotic value. The system size $N$ is $16,000$ for panels 1(a), 1(b) , 2(a), 2(b), and $10,000$ for panels 3(a), 3(b).

# Chapter 4

# Linear response theory of inhomogeneous systems

*In this Chapter we discuss the linearized Vlasov equation around inhomogeneous QSSs. In the first Section we consider the equation for the variation of the mean-field potential felt by every particle instead of the evolution equation for the variation of the distribution function, as it is usually done. The formal solution is given in the second Section and in the central part of the Chapter we show the difficulties behind the studies of inhomogeneous systems. In the following part we compare the theoretical prediction with numerical simulations. In the last Section, we discuss the behavior of the solution close to the points in which the distribution looses its stability. In some regime one can define critical exponents similarly to equilibrium phase transitions.*

## 4.1 Introduction

In this Chapter, we consider perturbations of the dynamics obtained by the addition of a conservative external field. As in previous Chapter 3, we restrict ourselves to the study of small perturbations within linear response theory. However, we do not use integrability as a requirement to derive the linear response formula as done in Refs. [14, 15, 93]. This has a drawback, because integrals of motion have to be imposed by hand in order to obtain the correct result. The Vlasov equation has an infinity of conserved quantities besides

those related to symmetries, the so-called Casimirs [82]. Since we are unable to impose this infinity of constraints, we consider a finite number of them (e.g. normalization of the single-particle distribution) and therefore derive an approximate response formula. The advantage with respect to previous approaches is that our response formula can be obtained in general also for non integrable systems. Moreover, our method allows us to consider many different unperturbed states, both homogeneous and inhomogeneous.

In order to illustrate the validity of our approach we explicitly derive the response to an externally applied field for the Hamiltonian Mean-Field (HMF) model (Section 1.4). This allows us to compare our approximate formula with the exact one derived in Ref. [93]. We obtain a good agreement excluding a region of energy close to the second-order phase transition of the model, where the response diverges.

The stability threshold shows a critical behavior in analogy with second order phase transitions with universal exponents independent of the chosen distribution. We derive and analyse numerically the behavior close to those critical points using the exact linear response theory in Ref. [93]. However, the approximate linear response theory is not precise enough to describe the divergence around the inhomogeneous side of the critical point because Casimirs play an important role in this regime. Indeed, the approximate linear response theory will get classical critical exponents and not the Vlasov one.

The Chapter is organized as follows. In Section 4.2 we derive our linear response formula for generic inhomogeneous states. its time asymptotics is studied in Section 4.3. Section 4.4 is devoted to the discussion of the constraints of the dynamics. We apply our response formula in Section 4.5 to the HMF model and, in Section 4.6, we demonstrate the agreement of our predictions with numerical simulations realized for different unperturbed states of the HMF model. The last Section 4.7 is devoted to the study of the critical behavior ruled by the exact solution of the inhomogeneous distribution.

## 4.2 Derivation of the response formula

In the previous Chapter 3 we have obtained the linear Vlasov equation (3.24) for a general initial distribution and, using Duhamel formula, we have derived closed equations for both the variation of the distribution function $\delta f$ and the variation of the Hamiltonian $\delta\mathcal{H}$. Since the variation of the Hamiltonian does

not depend on velocity, it is convenient to develop a method based on it. The corresponding equation, Eq. (3.26), is an inhomogeneous integro-differential equation. Moreover, obtaining a solution of this equations allows one to derive $\delta f$ using the same Duhamel formula (3.28).

Laplace transforming (Appendix A.2) both sides of (3.26) yields

$$\delta\hat{\mathcal{H}}(q,\omega) = \hat{b}(q,\omega) + \int dxdv\, u(q-x)\mathrm{R}(\omega)\{\delta\hat{\mathcal{H}}(x,\omega), f_0\}, \tag{4.1}$$

$$\mathrm{R} = \mathrm{L}[\mathcal{U}](\mathrm{s}) = \int_0^\infty e^{-\imath\omega t} e^{t\mathcal{L}_0} dt = \frac{1}{\imath\omega - \mathcal{L}_0}, \tag{4.2}$$

where the hat identifies Laplace transformed functions and the operator $\mathrm{R}$ is the Laplace transform of the evolution operator $e^{t\mathcal{L}_0}$. We consider Jeans' distributions (2.19) as initial states, which appear as the most natural ones.

The Hille-Yosida theorem [100] states that the Laplace transform of an operator, defining a semi-group by the generator $\mathcal{L}_0$, is the resolvent of the generator itself. A general property of resolvents, such as (4.2), is that they satisfy the identity

$$\mathrm{R}\mathcal{L}_0 = \imath\omega\mathrm{R} - \mathrm{I} - [\mathrm{R}, \mathcal{L}_0]\ . \tag{4.3}$$

In the following, we will consider that the commutator between the Liouville operator and its resolvent is zero in order to avoid technical problems. The dependence of the initial distribution on the unperturbed Hamiltonian transforms the Poisson bracket in Eq. (4.1) into the Liouville operator

$$\{\delta\mathcal{H}, f_0\} = \sigma_0 f_0' \mathcal{L}_0 \delta\mathcal{H}, \tag{4.4}$$

where

$$f_0'(q,p) = \frac{d\mathsf{F}}{d\mathsf{x}}\Big|_{\mathrm{x}=\sigma\mathcal{H}_0(q,p)}\ . \tag{4.5}$$

With $\mathrm{x}$ we identify the argument of the Jeans' distribution, which corresponds to an adimensional quantity, $\mathrm{x} = \sigma\mathcal{H}$, where $\sigma$ is an inverse energy scale that can depend on some macroscopic parameter. For instance, at equilibrium the inverse energy is equal to the inverse temperature, times some constants. The equation for the variation of the Hamiltonian in the complex Laplace space can be written in the following compact form

$$\delta\hat{\mathcal{H}}(q,\omega) = \hat{b}(q,\omega) + \chi[\delta\hat{H}](q,\omega), \tag{4.6}$$

where the operator $\chi$ is defined as

$$\chi[\varphi](q,\omega) = \int dxdv\, \sigma_0 u(q-x) f_0' \mathrm{K}(\omega)\varphi(x), \tag{4.7}$$

$$\mathrm{K}(\omega) = -1 + \imath\omega \mathrm{R}(\omega), \tag{4.8}$$

and $\varphi(x)$ is a generic function (test function).

A feature of homogeneous initial states is that Fourier modes are decoupled and equation (4.6) can be solved using the Fourier transform A.2. In this framework, the modes of the variation of the Hamiltonian are

$$\delta\tilde{\mathcal{H}}(k,\omega) = \frac{\tilde{b}(k,\omega)}{\epsilon(k,\omega)}\ , \tag{4.9}$$

where $\epsilon(k,\omega)$ is the dielectric function (2.48).

On the contrary, inhomogeneous initial states have a coupling among all the modes and equation (4.6) cannot be simplified using the Fourier transform. Therefore, we are led to assume that there exists a *base of eigenfunctions* $\varphi_i(q), i \in \mathrm{N}$, which solves the eigenvalue equation on $\chi$

$$\chi[\varphi_i](q,\omega) = \lambda_i(\omega)\varphi_i(q)\ , \qquad i = 1, \cdots, N \tag{4.10}$$

where $\lambda_i$ is the associated eigenvalue. This base plays the role of the Fourier base in the inhomogeneous regime. Thereby, we consider external potentials that belong to the subspace of functions spanned by these eigenfunctions

$$\hat{b}(q,\omega) = \sum_i a_i(\omega)\varphi_i(q), \quad q_i(\omega) \in \mathbb{C} \tag{4.11}$$

A basic tool to solve integral equations is to use the *Liouville-Neumann series* [67] which is a recursive formula. This allows us to obtain $\delta\hat{\mathcal{H}}$ and, in turn, the response (3.30). The Liouville-Neumann series reads

$$\delta\tilde{\mathcal{H}}(q,\omega) = \hat{b}(q,\omega) + \sum_{n=1}^{\infty} \chi^n[\hat{b}](q,\omega)\ , \tag{4.12}$$

where $\chi^n$ is the $n$th iterate of $\chi$. Substituting the definition of the external potential in terms of the eigenfunctions into Eq. (4.12) and resumming the geometric series one gets

$$\delta\hat{\mathcal{H}} = \sum_{i\in\mathrm{N}} a_i(\omega)\frac{\varphi_i(q)}{1-\lambda_i(\omega)}, \quad |\lambda_i| < 1\ . \tag{4.13}$$

The variation of the Hamiltonian which solves Eq. (4.6) shows the same eigenfunctions of the external potential but with a different amplitude. That solution has some properties related to the ones of the homogeneous regime. For instance, by analogy, we can denote the denominator of (4.13) as

$$\varepsilon_i(\omega) = 1 - \lambda_i(\omega), \tag{4.14}$$

the dielectric-like function in the real space in the case of inhomogeneous systems. Indeed, it plays the role of the dielectric function (2.48) of the homogeneous case, because whenever it is zero in the complex-$\omega$ Laplace space, $\delta\hat{\mathcal{H}}$ gets a pole. Therefore, zeros of (4.14) characterize the inverse Laplace transform A.2, which gives the solution in real time. Moreover, when the system is homogeneous, formula (4.14) converges to formula (2.48) and the eigenfunctions $\varphi_i$ become the Fourier modes with the indices $i$ that map to the modes $k$.

Furthermore, we obtain a stability criterion because the geometric series can be computed only when $|\lambda_i| < 1$. On the contrary, when the eigenvalue is larger than one in modulus the state is unstable and linear theory cannot be used.

We remark that integral equations can also be solved using Fredholm determinants [116], but in this case the solution is more involved and more complicated when the kernel of the integral is itself a non-trivial operator.

## 4.3 Time asymptotic behaviour

The Limit theorem relates the asymptotic value of a function $g(t)$ at $t \to \infty$ with the limit of its Laplace transform $\hat{g}(\omega)$ for $\omega \to 0$, see Appendix A.2.

Let us denote every quantity evaluated in this regime with the index $\infty$, e.g., the external potential

$$\hat{b}_\infty(q) = \lim_{\omega\to 0^-} \imath\omega\hat{b}(q,\omega) = \lim_{t\to\infty} \hat{b}(q,t). \tag{4.15}$$

The Liouville-Neumann series for asymptotic times reads

$$\delta\hat{\mathcal{H}}_\infty(q) = b_\infty(q) + \sum_{i=1}^{\infty} \chi_\infty[b_\infty](q), \tag{4.16}$$

and the limit of the eigenvalue equation (4.10) is

$$\begin{aligned} \lambda_i\varphi(q) &= -\sigma_0 \int dxdv f_0'(x,v)u(q-x)\varphi(x), \\ &\quad +\imath\sigma_0 \int dxdv f_0' u(q-x) \lim_{\omega\to 0} \omega\mathcal{R}(\omega)\varphi(x). \end{aligned} \tag{4.17}$$

The first integral does not depend on the Laplace variable $\omega$ while the second one depends on $\omega$ through the kernel operator $\omega\mathcal{R}(\omega)$. This latter integral converges to zero when the initial state is homogeneous, because its Fourier transform is $\omega(\epsilon(k,\omega)-1)$ and in the limit $\omega \to 0$ it results in a vanishing contribution. On the contrary, when the initial state is inhomogeneous the integral could converge to a finite value in the same limit.

Let us consider a function $g(x,v)$: when it is in the kernel of the Liouville operator (2.5) the action of the resolvent becomes trivial and the limit $\omega \to 0$ gives the identity

$$\lim_{\omega\to 0} \omega\mathcal{R}(\omega)g(x,v) = g(x,v). \tag{4.18}$$

Consequently, the operator $\mathrm{K}(0)$ in the time asymptotics gives zero when evaluated on these functions.

The operator $\mathcal{L}_0$ has an empty continuum spectrum also on some manifolds in the phase space and these manifolds could give a finite contribution to the response. The Fourier transform of the second integral of Eq. (4.17) is

$$\mathcal{J}_\omega = \int dxdv f_0'(\mathcal{H}_0) e^{\imath kx} \frac{\omega}{\omega - \imath\mathcal{L}_0}\varphi(x), \tag{4.19}$$

and in the asymptotic time limit it gives a non zero integrand whenever the larger (in modulo) eigenvalue of $\mathcal{L}_0$ goes as $\omega$. We call $\mathcal{M}$ the manifold in which the Liouville operator is identically zero, thus the manifold where the integrand could get a contribution in our limit. Unfortunately we don't know how to obtain this manifold in general and even if it really exists. We will discuss in more detail formula (4.19) in Appendix C.1 and hereafter we assume that its contribution can be negligible, since in the homogeneous phase it is indeed zero.

Discarding the second integral in Eq. (4.17), the operator $\mathrm{K}$ becomes proportional to the identity and the other quantities become

$$\mathrm{K}(0) = -1 \tag{4.20a}$$

$$\lambda_i\varphi_i(q) = \sigma_0 \int u(q-x) f_0'\varphi_i(x) \tag{4.20b}$$

$$\delta\hat{f}_\infty(q,p) = \sigma_0 \delta\hat{\mathcal{H}}_\infty(q) f_0'(q,p) \tag{4.20c}$$

Let us make two short remarks:

The first remark is that the response (3.30) at every time becomes ill defined. Let us introduce the integrated response for asymptotic times, defined by

$$\delta\bar{a} = \lim_{t\to\infty} \frac{\partial}{\partial h}\Big(\langle a\rangle_t - \langle a\rangle_0\Big)\Big|_{h=0}, \tag{4.21a}$$

$$= \int dpdq\, \delta f_\infty(q,p)a(q,p). \tag{4.21b}$$

This formula describes the finite variation of a single-particle observable $a(x,v)$ at the linear order in the perturbation parameter $h$.

The second remark is about a *stability criterion* of the initial state. From the geometric series, we get a criterion to perform the resummation of the series: it reads $|\lambda_i| < 1$ for each $i$. In the asymptotic time regime this inequality can be seen as a criterion for which the initial state is stable because otherwise the series diverges. It can be compared with other stability criteria [91,98].

## 4.4 Constraints

Vlasov dynamics is characterized by the existence of constraints of different nature [57]. We will here restrict to discuss those constraints that play a relevant role in the derivation of our response theory. The first constraint derives from mass conservation, which is a consequence of considering a *closed system*. However, our system can exchange energy with the environment, hence we can evaluate the work done on the system by the external perturbation. The entailed generalized energy conservation relation imposes, as we will see, a constraint on the dynamics. Isolated systems also conserve total momentum. However, one can choose perturbations of the dynamics which determine variations $\delta f(q,p,t)$ that are even functions of $p$. This in turn implies that momentum is necessarily conserved and can for convenience be set to zero. The effect of the conservation of other global invariants associated to symmetries, like angular momentum, will not be discussed in this paper, since the systems we will consider are one-dimensional.

On top of that, the Vlasov equation is endowed with an infinity of conserved quantities, the so-called Casimirs [57,82]. They all take the form $\int c(f(x,v))dxdv$, with $c$ a smooth function. For instance, mass is one of such Casimirs. We will assume that the effects induced by all these conservations, besides mass, are negligible. However, in Section 4.7 we will show that Casimirs are not always negligible and they will play an important role in some region of the phase diagram.

### 4.4.1 Mass constraint

The mass of the system is given by

$$M(t) = \int f(x,v,t)\, dxdv \ . \tag{4.22}$$

At first order in the size of the perturbation $h$ we get

$$M(t) = M(0) + h \int \delta f \, dxdv + \mathcal{O}(h^2). \tag{4.23}$$

For a closed system mass is conserved $M(t) = M(0)$, hence

$$\int \delta f(x,v,t)\, dxdv = 0 \ . \tag{4.24}$$

In the following we will set the total mass to one, $M = 1$.

### 4.4.2 Energy constraint

The system is perturbed by an external field, hence the total energy

$$E(t) = \int \mathrm{E}[f](x,v,t) f(x,v,t) dxdv \tag{4.25}$$

$$\mathrm{E}[f](q,p,t) = \frac{p^2}{2} + \frac{1}{2}\phi[f](q,t) + hb(q,t) \ . \tag{4.26}$$

is not a conserved quantity. However, since the time evolution of the distribution function is determined by the full perturbed Hamiltonian (the external forces are conservative), the variation of the total energy is equal to the work $W(t)$ done by the external forces on the system

$$E(t) - E_0 = W(t) \ , \tag{4.27}$$

where

$$W(t) = h \int f(x,v,t) b(x,t) dxdv \ . \tag{4.28}$$

This is a generalized energy conservation law, in analogy with mechanics.

Let us remark that the functional $\mathrm{E}[f]$ is the phase-space observable associated with the total energy and differs from the Hamiltonian $\mathcal{H}[f]$ by the factor $1/2$ in front of the mean-field potential. This avoids the double counting of the interaction energy between two separated regions in phase-space.

At linear order in $h$ one gets the following constraint on the variation of the distribution function

$$\int \mathcal{H}_0[f_0](x,v)\delta f(x,v,t)dxdv = 0, \quad \forall t > 0, \tag{4.29}$$

where we have used the identity $\int f\phi[\delta f]dqdp = \int \delta f \phi[f]dqdp$.

### 4.4.3 Implementation of the constraints

The final stationary state is described by the stationary linear Vlasov equation

$$\left(p\frac{\partial}{\partial q} - \frac{\partial \phi_0}{\partial q}\frac{\partial}{\partial p}\right)\delta f_\infty + \frac{\partial \delta\mathcal{H}}{\partial q}\frac{\partial}{\partial p}f_0 = 0. \tag{4.30}$$

The formal solution of this equation is

$$\delta f(q,p) = f_0'(q,p)\delta\mathsf{x}(q,p), \tag{4.31}$$

and it corresponds to the Duhamel formula (3.28) for large times. The variation $\delta\mathsf{x}$ cannot a priori be defined because the kernel of the Liouville operator (2.5) is not null. For example, the function

$$\delta\mathsf{x} = \sigma_0\delta\mathcal{H} + \mathcal{H}_0\delta\sigma + \delta M, \tag{4.32}$$

with $\delta M, \delta\sigma \in \mathbb{R}$ two arbitrary constants, gives a solution of the linear stationary Vlasov equation. These new terms are useful to implement the constraints of the system. For instance, the two equations (4.24) and (4.29) become

$$\int f_0'(\sigma_0\delta\mathcal{H} + \mathcal{H}_0\delta\sigma + \delta M)\mathcal{H}_0\, dqdp = 0, \tag{4.33}$$

$$\int f_0'(\sigma_0\delta\mathcal{H} + \mathcal{H}_0\delta\sigma + \delta M)\, dqdp = 0, \tag{4.34}$$

where the phase space dependencies are dropped out to derive more concise equations. In order to solve this linear problem we define

$$J_{\mathcal{H}_0^2} = \int f_0'\mathcal{H}_0^2\, dqdp, \tag{4.35a}$$

$$J_{\mathcal{H}_0} = \int f_0'\mathcal{H}_0\, dqdp, \tag{4.35b}$$

$$J_1 = \int f_0'\, dqdp, \tag{4.35c}$$

$$J = J_{\mathcal{H}_0^2}J_1 - J_{\mathcal{H}_0}^2, \tag{4.35d}$$

then equations (4.33) and (4.34) give the following functional relations

$$\delta M[\delta\mathcal{H}_\infty] = -\sigma_0 \frac{J_{\mathcal{H}_0^2}\int f'\delta\mathcal{H}dqdp - J_{\mathcal{H}_0}\int f'\mathcal{H}_0\delta\mathcal{H}dqdp}{J}, \tag{4.36}$$

$$\delta\sigma[\delta\mathcal{H}_\infty] = -\sigma_0 \frac{J_1\int f'\mathcal{H}_0\delta\mathcal{H}dqdp - J_{\mathcal{H}_0}\int f'\delta\mathcal{H}dqdp}{J}. \tag{4.37}$$

These parameters, $\delta M$ and $\delta\sigma$, take into account the variation of the mass of the system and the variation of the inverse energy scale, due to the perturbation. They are linear functionals with respect to their arguments, here the variation of the Hamiltonian, and add more terms to equation (4.1). Therefore,at infinite times the equation for the variation of the Hamiltonian with two constraints becomes

$$\begin{aligned}\delta\mathcal{H}_\infty(q) &= b + \sigma_0\int u(q-x)f_0'\delta\mathcal{H}_\infty + \\ &\quad \delta\sigma[\delta\mathcal{H}_\infty]\int f_0'u(q-x)\mathcal{H}_0 + \\ &\quad \delta M[\delta\mathcal{H}_\infty]\int f_0'u(q-x).\end{aligned} \tag{4.38}$$

The linearity property of these new terms preserves the Liouville-Neumann form of the solution, but with a modified eigenvalue equation, which reads

$$\begin{aligned}\lambda_i\varphi_i(q) &= \sigma_0\int u(q-x)f_0'\varphi_i + \\ &\quad \delta\sigma[\varphi_i]\int u(q-x)f_0'\mathcal{H}_0 + \\ &\quad \delta M[\varphi_i]\int u(q-x)f_0'\end{aligned} \tag{4.39}$$

Although the form of the solution (4.13) is the same, the eigenvalues change their value by imposing the constraints (4.33) and (4.34). We show in the next Section 4.5 this property for the HMF model.

The case in which the system has only the mass constraint can be computed with $\delta\sigma = 0$. The linear functional $\delta M$ related to the variation of the mass is

$$\delta M[\delta\mathcal{H}] = -\sigma_0\frac{\int f'\delta\mathcal{H}}{J_1} \tag{4.40}$$

and the eigenvalue equation reads

$$\lambda_i\varphi_i = \sigma_0\int u(q-x)f_0'\varphi_i + \delta M[\varphi_i]\int u(q-x)f_0' \tag{4.41}$$

On top of that, for homogeneous initial states, the mean field $\phi_0$ is zero and both the unperturbed Hamiltonian $\mathcal{H}_0$ and the initial distribution function $f_0$ do not depend on space. In equations (4.33) and (4.34) only the variation of the Hamiltonian $\delta\mathcal{H}$ depends on the space variable $q$ and usually its integral over space is zero. Thus, the two equations of the constraints can be satisfied only with $\delta\sigma = 0$ and $\delta M = 0$, independently of the initial distribution $f_0$. Therefore, both the constraints are automatically fulfilled in homogeneous systems.

## 4.5 Application of the response formula

Let us consider the eigenvalue equation (4.10) of a system that is initially at equilibrium or in a Fermi-Dirac QSS. The long-range potential is a cosine, then, using the addition formula of trigonometries functions, we obtain that the eigenfunctions $\varphi_i$ must be sums of sines and cosines. We consider the base composed by the two parallel and perpendicular directions with respect to the spontaneous unperturbed magnetization $\vec{m}$

$$\varphi_1(q) = \alpha_1 \left( \cos(q) + \frac{m_y}{m_x} \sin(q) \right), \tag{4.42}$$

$$\varphi_2(q) = \alpha_2 \left( \frac{m_y}{m_x} \cos(q) + \sin(q) \right), \tag{4.43}$$

where $\alpha_1, \alpha_2 \in \mathbb{R}$ are two constants defined by the orthogonality relations

$$\int dxdv\, \varphi_i(x)\varphi_j(x) f_0'(x,v) = \delta_{i,j}, \quad i,j = 1,2. \tag{4.44}$$

Invariance under angle translations of the HMF model in the unperturbed state allows us to define arbitrary $x$ and $y$ directions. We identify with $x$ the direction of the spontaneous magnetization; the magnetization components then become $m_y = 0$ and $m_x = |\vec{m}| = m$ and the two eigenfunctions are

$$\varphi_1(q) = \alpha_1 \cos(q), \quad \varphi_2 = \alpha_2 \sin(q). \tag{4.45}$$

Without loss of generality, we put the external field in the direction of the spontaneous magnetization $x$, because we are not interested in the Goldstone modes. For instance, an external field applied perpendicularly to the spontaneous magnetization direction excites modes that persist for indefinite time, due

to the rotational symmetry of the unperturbed Hamiltonian. With $\alpha_1 = 1$ the eigenvalue equation is transformed into the following integrals

$$\lambda_1 = \beta\Phi[f_0'\varphi_1], \tag{4.46}$$

$$\Phi[r] = -\int dxdv\,\varphi(x)r(x,v). \tag{4.47}$$

In the next Subsections we will consider the solution of the eigenvalue equation for the equilibrium state in three cases: zero constraints, the mass constraint and both the energy and mass constraints. Later, we will discuss the eigenvalue equations for the Fermi-Dirac distribution with the same constraints.

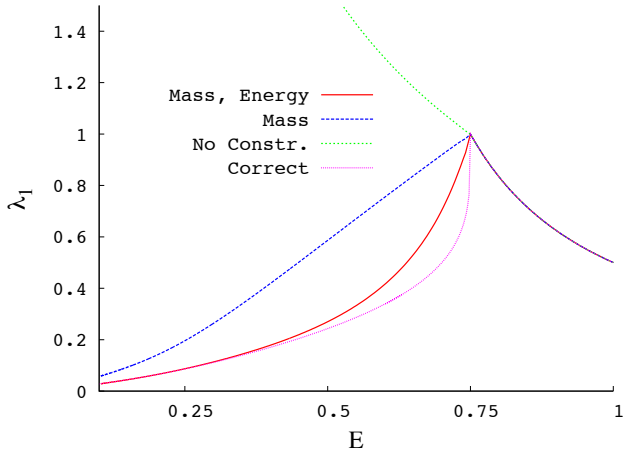


Figure 4.1: Different eigenvalues $\lambda_1$ versus the energy $E$ of an unperturbed system at equilibrium with different constraints. The full red line is the eigenvalue when both the energy and the mass constraints are imposed, given by the formula (4.55). The dash-dotted blue line is the eigenvalue when the system verifies only the mass constraint given by the formula (4.51), and the dotted green line is the unconstrained case, given by (4.48). From high energies the eigenvalue $\lambda_1$ converges to the one of the critical energy $E_c = 0.75$, which is the phase transition point.

### 4.5.1 Equilibrium without constraints

The eigenvalue of the sine function is zero, $\lambda_2 = 0$, because the distribution is even in $q$. On the contrary, along the $x$ direction we get

$$\lambda_1 = \beta\frac{I_1(\beta m) + \beta m I_2(\beta m)}{\beta m I_0(\beta m)}, \tag{4.48}$$

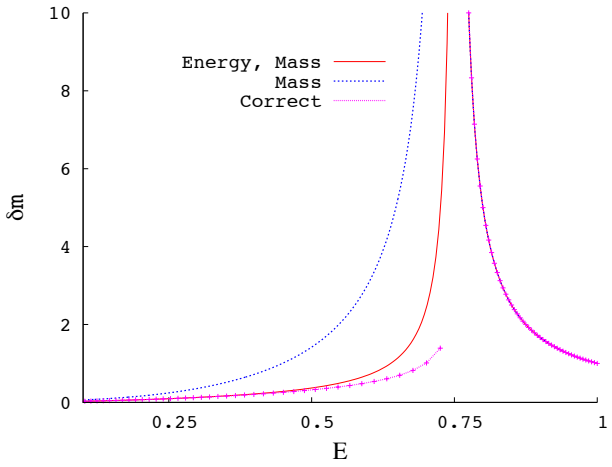


Figure 4.2: Different responses $\delta m$ vs. energy $E$ of an unperturbed system at equilibrium with different constraints. The full red line corresponds to the system with the energy and mass constraint given using the formulas (4.49) and (4.55). The dash-dotted blue line corresponds to the system with the mass constraint given by (4.52). The unconstrained case is not shown because it is equal to the others in the homogeneous regime and it diverges in the inhomogeneous one because $\lambda_1 < 1$.

where $I_0, I_1, I_2$ are the modified Bessel's functions of order $0, 1, 2$, respectively. In the homogeneous region the r.h.s. is equal to $\beta/2$, because the magnetization is zero, and it is consistent with the result obtained in Ref. [96]. Using formula (4.21) we find the integrated response of the magnetization

$$\delta m = \varphi_1(0)\frac{\lambda_1}{1-\lambda_1}, \tag{4.49}$$

where $\varphi_1(0) = 1$. The Liouville-Nemuann series converges when the eigenvalue is, in modulo, less than one. Formula (4.48) gives an eigenvalue larger than one for every $E < E_c$, in the inhomogeneous phase. As a consequence, equilibrium without constraints is unstable in linear theory. This result can be consistent because the system could evaporate or concentrate in a point and the response of the system then becomes undefined here. This result was previously obtained in Ref. [31].

The green dotted line in figure 4.1 shows the eigenvalue as a function of $E$. In the inhomogeneous region ($E < E_c$) it becomes undefined.

### 4.5.2 Equilibrium with the mass constraint

The mass constraint imposes a different kernel of the integral (4.41). The eigenvalue has the same eigenfunctions (sine and cosine), but it is described by

$$\lambda_i = \beta\Phi[\varphi_i f'_{eq}] - \phi_0(q)\Phi[f'_{eq}]. \tag{4.50}$$

where $\phi_0(q) = m\cos(q)$. The two eigenvalues $\lambda_{1,2}$ are

$$\lambda_1 = \beta\frac{I_1(\beta m) + \beta m I_2(\beta m)}{\beta m I_0(\beta m)} - \beta m^2, \quad \lambda_2 = 0. \tag{4.51}$$

The dotted blue line of figure 4.1 shows the eigenvalue in both the homogeneous and inhomogeneous regions. Inserting it in formula (4.49), the response magnetization becomes

$$\delta m = \frac{1 + \beta I_2/I_1 - \beta m^2}{\beta m^2 - \beta I_2/I_1}, \tag{4.52}$$

which is equal to the canonical susceptibility (1.33).

In this case the eigenvalue $\lambda_1$ is equal to one only at the critical energy $E_c$. Below this point it is smaller than one, which ensures an asymptotic linear stability in the canonical ensemble.

### 4.5.3 Equilibrium with both energy and mass constraints

The equilibrium case with both the energy and the mass constraints is described by the following eigenvalue equation

$$\lambda_1 = \beta\Phi[f'\varphi] + \delta\beta[\varphi]\Phi[f'\mathcal{H}_0] + \delta M[\varphi]\Phi[f'] \ . \tag{4.53}$$

Denoting the term

$$c_2 = \frac{I_1(\beta m) + \beta m I_2(\beta m)}{\beta m I_0(\beta m)}, \tag{4.54}$$

and performing some algebraic manipulations, we obtain the formula for the eigenvalues

$$\lambda_1 = \beta\left(c_2 - m^2\frac{1 + 2\beta^2 c_2(c_2 - m^2)}{1 + 2\beta^2 m^2(c_2 - m^2)}\right), \quad \lambda_2 = 0. \tag{4.55}$$

The red line of figure 4.1 shows the value of $\lambda_1$ for different energies. That eigenvalue is again equal to one only at the critical energy $E_c$. Moreover, the integrated response of the magnetization (4.49) gives the same expression as the microcanonical response (1.38).

The full red line of figure 4.2 shows the response of magnetization in both the homogeneous and inhomogeneous regions for the two cases corresponding to different constraints. The response of the system with more constraints is smaller, consistently with the result known for the equilibrium response [31,32].

The purple line in figures 4.1 and 4.2 reproduces the exact eigenvalue and the exact susceptibility of Ref. [93], where action-angle variables are used. As expected, the response of the system with all the Casimir constraints gives a smaller response when compared to equilibrium.

### 4.5.4 The Fermi-Dirac initial distribution

The Fermi-Dirac (FD) distribution is defined as (see Section 3.2.1)

$$f_{fd}(\mathsf{x}) = \frac{1}{Z}\frac{1}{1+e^{\mathsf{x}}}, \tag{4.56}$$

where $Z$ is the normalization. This distribution is useful because it gives a mapping between different QSSs often studied in the framework of the long-range interacting systems: the BG equilibrium and the Water-Bag states. The eigenvalue equation uses the first derivative of the distribution with respect to its argument, which is

$$f'_{fd} = -\frac{1}{4Z}\frac{1}{\cosh^2(\frac{\mathsf{x}}{2})} \ . \tag{4.57}$$

At variance with equilibrium, the eigenvalue equation for the FD distribution does not show simple physical terms like the unperturbed magnetization. Therefore, we have to solve numerically the equation for $\lambda_1$.

Figure 4.3.$a$ shows the dependence of the eigenvalue $\lambda_1$ on energy $E$. It grows to 1 at the critical energy $E_c \simeq 0.7$, which corresponds to the critical energy where the system changes its phase: below $E_c$ the state is clustered, while above it is homogeneous. Although it is an out-of-equilibrium distribution, it shows a continuum transition between the two regions, mimicking equilibrium phase transitions. The eigenvalue at the critical energy in figure 4.3 is smaller than one, because the algorithm used to get that value is an iterative algorithm.

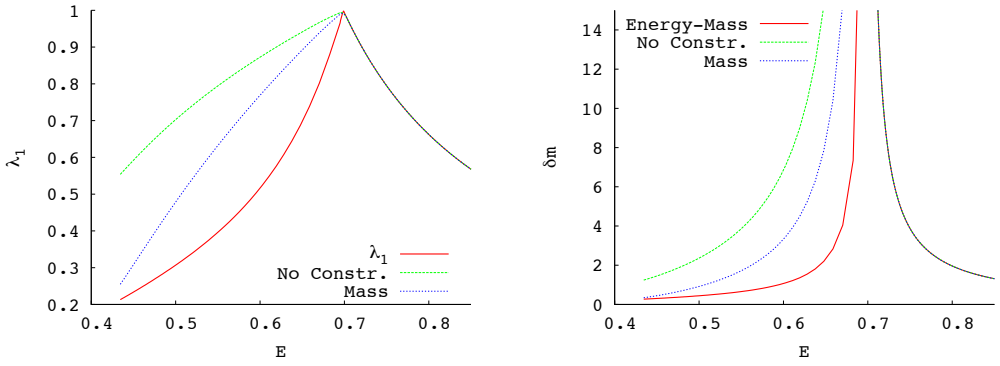


(a) (b)

Figure 4.3: Eigenvalue $\lambda_1$ (panel $a$) and response $\delta m$ (panel $b$) for the Fermi-Dirac initial distribution with both energy and mass constraints. The value of $E$ where $\lambda_1$ is equal to one corresponds to the critical energy $E_c \simeq 0.7$.

It does not converge at $E_c$ but it gives a closer and closer value by increasing the number of iterations. It is intriguing that the zero constraint case gives an eigenvalue smaller than one in the inhomogeneous phase. For instance, the FD state is more compact if compared to equilibrium and therefore it is probably more stable under evaporation. Panel $(b)$ shows the response of magnetization $\delta m$ versus the energy $E$.

## 4.6 Numerical comparison

In order to verify our theoretical analysis we have implemented numerical simulations with the distributions described above. In this Section we briefly discuss the method used to implement the numerical simulations. Afterwards, we discuss some results in a range of energies in which linear theory works approximately well.

### 4.6.1 Methods

We use the weighted particles algorithm, described in Ref. [15], to simulate the HMF model. We prepare $N$ particles on a regular lattice in $q$ and $p$ and we associate a weight to each site with the chosen initial distribution. Vlasov dynamics conserves the support of every distribution at constant weight [82]. The time evolution is realized using a symplectic integrator and every observable is

evaluated with the weighted average.

The phase-space is compact in the $q$ direction, then errors depend on the lattice parameter. On the contrary, in the $p$ direction we have another source of errors: for every distribution with a non compact support we have to use a cutoff on the weightless part of the momentum space. We choose a $p_{max}$, as a maximum value of the velocity spanned by the lattice, which must be large enough in order to avoid important errors. This procedure and the scale of $p_{max}$ depend on the particular distribution considered.

The initial state is prepared at a given inverse energy scale $\sigma$. Solving an implicit equation we get the magnetization and the energy values associated with the chosen energy scale. The perturbation starts at time $t_0 > 0$, after a relaxation of the system to the stationary state. We perturb along the direction of the spontaneous magnetization, $x$, thanks to the invariance under rotations of the unperturbed system. Therefore, $m_x = m$, $m_y = 0$.

Linear theory does not show a well precise limit where it can be used as a good approximation. Whenever a solution exists there will be a sufficiently small $h$ which gives a reasonably good result. In general we know empirically that in the homogeneous regime the amplitude of the perturbation must verify the relation

$$\sigma h \ll 1. \tag{4.58}$$

In the inhomogeneous phase we have another scale, which is related to the magnetization. It is quite reasonable to assume that

$$\frac{h}{m} \ll 1, \tag{4.59}$$

in order to avoid that the external field gives dominant contributions to the energy as compared with the magnetization.

A first numerical check of the validity of the linear regime is that the variation of the magnetization must be smaller than the magnetization itself

$$\frac{h\delta m}{m} \ll 1, \tag{4.60}$$

for every time in which the Vlasov picture is a good approximation of the finite $N$ dynamics.

### 4.6.2 Equilibrium

The panels of figure 4.4 show two plots with the comparison between numerical simulations and the asymptotic values of the equilibrium magnetization (3.2.1).

Figure 4.4.$a$ shows a simulation of a system initially at an inverse energy scale $\beta = 7$, which corresponds to an energy $E \simeq 0.14$ and a modulus of the magnetization $m \simeq 0.92$. At $t_0 = 50$ the perturbation is applied and the system begins to oscillate with a damping, a behavior that can be described within the theory of Landau damping [71]. After some time, which depends principally on the initial energy and on the distance between the energy of the state and the critical one, the system relaxes to a stationary state whose magnetization is in agreement with theoretical predictions.

Figure 4.4.$b$ shows a simulation at an inverse energy scale $\beta = 5$, which corresponds to an energy $E \simeq 0.22$ and a magnetization $m \simeq 0.88$. As in the previous case, after damping, the system relaxes to a state with a magnetization close to the value predicted by linear response theory.

### 4.6.3 Fermi-Dirac distribution

The panels of figure 4.5 show the comparison between the numerical simulations and theoretical predictions for the magnetization of the Fermi-Dirac distribution (4.56). In this case eigenvalues cannot be related in a simple way to physical parameters, and are evaluated numerically by integrating equation (4.53).

Figure 4.5.$a$ shows the time evolution of the magnetization at an inverse energy scale $\sigma = 8$, which corresponds to an energy $E \simeq 0.45$ and the magnetization $m \simeq 0.69$, while figure 4.5.$b$ shows what happens for an initial state at the inverse energy scale $\sigma = 9$. This latter value corresponds to an energy $E \simeq 0.44$ and a magnetization $m \simeq 0.70$. The system relaxes to an unperturbed stable state and, after $t_0 = 10$, the magnetization begins to oscillate and damps to a final stationary state which coincides with the prediction of linear response theory.

## 4.7 Critical exponents of a mean-field system

Linear response theory of integrable systems is derived in Ref. [93], and the authors obtain the correct response function for the HMF model. We can use that solution to study the behaviour of different initial configurations in different

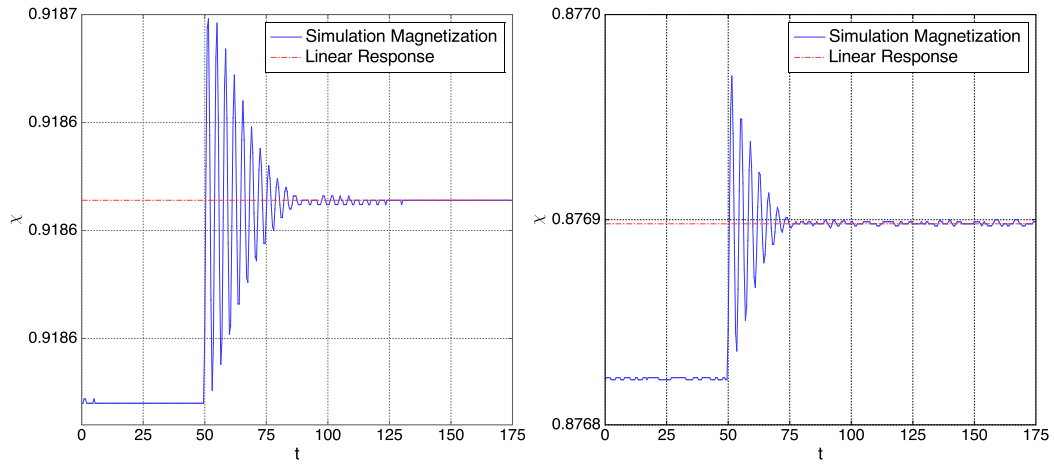


(a) (b)

Figure 4.4: Variation of the magnetization $\delta m$ in time $t$ obtained in numericals simulations of a system starting in inhomogeneous equilibrium. Panel $(a)$ shows the simulation of the system at an energy $E = 0.14955$ and magnetization $m = 0.91856$, which corresponds to the inverse energy scale $\beta = 7$. The full red line is the numerical evolution of the magnetization along the $x$ axis and the blue dashed line is the theoretical prediction for asymptotic time. Panel $(b)$ shows the simulation of the system at an energy $E = 0.21559$ and magnetization $m = 0.87682$, which corresponds to an inverse energy scale $\beta = 5$. The full red line is the numerical evolution of the magnetization along the $x$ axis and the blue dashed line is the theoretical prediction for asymptotic time.

regimes. An interesting regime is the one where a given distribution looses its stability. Having in mind the equilibrium distribution as a reference state, we will show here that there is an instability in the Vlasov regime which corresponds to a second order phase transition in statistical equilibrium. Close to the second order phase transition point the response of the system to the action of an external field, namely susceptibility, diverges with a power-law. In the case of mean-field systems, one gets the celebrated Curie-Weiss law, discussed in many textbooks on phase transitions.

These results pose the following question: is it possible to find some common features in the behavior of the Vlasov dynamics when a given state reaches a stationary regime?

For instance, we know that in the homogeneous phase, the time asymptotic response (3.60), ruled by the dielectric function (3.61), shows a power-law dependence on the inverse energy scale $\sigma$, independently of the particular dis-

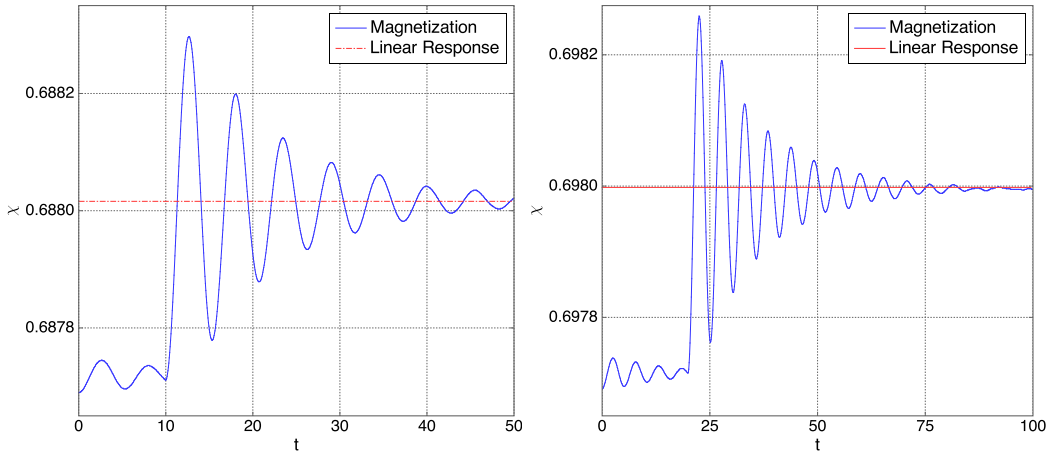


(a) (b)

Figure 4.5: Susceptibility $\delta m$ as a function of time $t$ in numerical simulations of a system starting in the inhomogeneous Fermi-Dirac state. Panel $(a)$ shows the simulation of the system at an energy $E = 0.44812$ and a magnetization $m = 0.6877$ , which corresponds to an inverse energy scale $\sigma_0 = 8$. The full red line is the numerical evolution of the magnetization $\delta\langle m_x\rangle_t$ along the $x$ axis and the blue dashed line is the theoretical prediction for asymptotic time. Panel $(b)$ shows the simulation of the system at an energy $E = 0.44016$ and a magnetization $m = 0.6977$ , which corresponds to the inverse energy scale $\sigma_0 = 9$. The full red line is the numerical evolution of the magnetization $\delta\langle m_x\rangle_t$ along the $x$ axis and the blue dashed line is the theoretical prediction for asymptotic time.

tribution function. Each distribution gives a different critical threshold $\sigma_c[f_0]$, but the power-law behavior is the same.

A study of critical exponents in the Vlasov context was first proposed in Ref. [40]. Here, the authors consider a homogeneous unstable Maxwellian plasma slightly below the stability threshold and obtain critical exponents that differ from the ones of classical theory. Moreover, numerical simulations [60,61] display such exponents in the general setting of the Vlasov equation for singular potentials around unstable homogeneous states. Contrary to these studies, we are here interested in stable states.

We analyse Vlasov response and the associated critical exponent of susceptibility using the solutions found in Refs. [93,96]. We focus on the HMF model, due to its simplicity, but we remark that this result is generalizable to uniform configurations of generalized HMF models, such as the $\alpha$-HMF model [2,8]. The results contained in this Section are reported in Ref. [92].

The approximated linear theory of the first part of this Chapter, cannot be used because the presence of infinite conserved quantities plays a crucial role when evaluating the behavior of the system close to the transition point. Moreover, in Section 4.3 we obtain that magnetic susceptibility is equal to microcanonical and canonical ones, hence their critical exponents are given by classical theory.

### 4.7.1 Dielectric function for inhomogeneous states

The dielectric function (DF) for asymptotic times of Ref. [93] (formula 102) is

$$D_x = 1 - C_2[f_0](\sigma) - A[f_0](\sigma), \tag{4.61}$$

where $\sigma$ is the inverse energy scale, that parametrizes the distribution, while the functionals are

$$\begin{aligned} C_2[f_0](\sigma) &= -\int dqdp \frac{1}{p}\frac{\partial}{\partial p} f_0 \cos^2(q), & (4.62)\\ A[f_0](\sigma) &= \frac{4}{\sqrt{m_0}}\int_0^1 K(x)\left(2\frac{E(x)}{K(x)}-1\right)^2 \frac{df_0}{dx}dx & (4.63)\\ &\quad + \frac{4}{\sqrt{m_0}}\int_1^\infty \frac{K(1/x)}{x}\left(2x^2\frac{E(1/x)}{K(1/x)}+1-2x^2\right)^2\frac{df_0}{dx}dx. \end{aligned}$$

The variable $x$ depends on the unperturbed single particle Hamiltonian $\mathcal{H}_0$ through the relation

$$x = \sqrt{\frac{m_0 + \mathcal{H}_0}{m_0}}. \tag{4.64}$$

As before, $\sigma$ is an inverse energy scale and $m_0$ is the spontaneous magnetization assumed to be parallel to the $x$ axis. The two functions

$$\begin{aligned} K(x) &= \int_0^1 \frac{dt}{\sqrt{(1-t^2)(1-xt^2)}}, & (4.65)\\ E(x) &= \int_0^1 \sqrt{\frac{1-xt^2}{1-t^2}}dt, & (4.66) \end{aligned}$$

are the complete elliptic functions of first and second kind.

Vlasov susceptibility in the stationary state does not depend on time and reads

$$\chi(\sigma) = \frac{1 - D_x(\sigma)}{D_x(\sigma)}. \tag{4.67}$$

Therefore, the DF contains all the information about the divergence when the unperturbed state $f_0$ approaches critical stability. We restrict our analysis to initial states that belong to the Jeans' class (2.19).

Let us define $\gamma_\pm$ the two critical exponent with which susceptibility diverges, hence

$$\chi \sim |\sigma - \sigma_c|^{\gamma_\pm^{\mathrm{V}}}, \qquad D \sim |\sigma - \sigma_c|^{-\gamma_\pm^{\mathrm{V}}}. \tag{4.68}$$

The critical exponent of the homogeneous phase is given by the relations (3.61) of Chapter 3

$$\gamma_+^{\mathrm{V}} = -1. \tag{4.69}$$

This exponent does not depend on the choice of the distribution.

As a consequence of the use of Jeans' distributions, the derivative that appears in the evolution of $A$ takes the form

$$\frac{df_0}{dx} = [4m_0 x]\frac{df_0}{d\mathcal{H}}. \tag{4.70}$$

Hence, we get an extra magnetization factor which influences the critical behavior.

The dielectric function (4.61) and the relative response (4.67) derive their peculiarities from the properties of $A$. Actually, this is due to the presence of an infinity of Casimirs, which are invariants of the Vlasov dynamics, as discussed in Chapter 2. Any Casimir introduces a conservation law and the last term of the dielectric functional takes care of all of them. Let us discuss this feature using action-angle, $(J, \theta)$, variables.

The variation of the distribution $\delta f = f_h - f_0$ satisfies

$$0 = \int [c(f_0 + \delta f) - c(f_0)]dqdp = \int c'(f_0(J))\widetilde{\delta f}_0(J)dJ, \tag{4.71}$$

up to linear order, where $\widetilde{\delta f}_0(J)$ is the zero Fourier mode of $\delta f$ with respect to the angle $\theta$. This constraint must hold for any smooth function $c$, and hence $\widetilde{\delta f}_0(J) = 0$ [91]. Let us derive $f_h$ from the trial function

$$g_h(q, p; \sigma) = \frac{F(\sigma\mathcal{H}_h(q,p))}{\int F(\sigma\mathcal{H}_h(q,p))\, dpdq}, \tag{4.72}$$

which corresponds to the Jeans' distribution with the perturbed Hamiltonian instead of the unperturbed one. We guess that it describes the final QSS in

which the system settles down after the perturbation is switched on, since the Casimirs do not evolve on a short time-scale.

By the definition of susceptibility $\chi^{\mathrm{V}}$, the magnetization $\langle m\rangle_h$ is written as $\langle m\rangle_h = \langle m\rangle_0 + h\chi^{\mathrm{V}} + O(h^2)$. Subtracting the zero Fourier mode from $g_h - f_0$, the variation must satisfy $\delta f = g_h - f_0 - \langle g_h - f_0\rangle_J = g_h - \langle g_h\rangle_J$ and

$$f_h = f_0 - \frac{h(\chi^{\mathrm{V}}+1)}{\int F\ dqdp} F'(\sigma\mathcal{H}_0)\left(\cos q - \langle\cos q\rangle_J\right). \tag{4.73}$$

Multiplying by $m(q)$ and integrating in the $\mu$ space, we get Vlasov susceptibility (4.67) and the dielectric functional (4.61).

### 4.7.2 Jeans initial distribution functions

We study the behavior of the dielectric function for Jeans' distributions. When the energy is conserved or the external perturbation is switched on adiabatically the inverse energy scale $\sigma$ depends on the initial energy, $\sigma = \sigma(E)$. In the HMF model there is a one to one correspondence between $\sigma$ and $E$ when the critical point corresponds to a second order phase transition for which magnetization is a continuous function of energy. Otherwise, we get two critical points, one for the homogeneous state and the other for the inhomogeneous state.

Magnetization is given by the self-consistency equation

$$m(\sigma) = \frac{\int f_0\cos(q)dqdp}{\int f_0 dqdp}. \tag{4.74}$$

We want to evaluate this relation close to the critical point, then for $\sigma \searrow \sigma_c$. Let us denote $f_c$ as the unperturbed distribution at the critical energy, which corresponds to a homogeneous distribution ($m(\sigma_c) = 0$). Above the critical energy magnetization is zero, therefore, we expand in Taylor series in the small parameter $\sigma m(\sigma)$ and around the critical state

$$m \simeq \frac{\int f_c\cos(q) + \sigma m\int f_c^1\cos^2(q) + \sigma^2 m^2\int f_c^2\cos^3(q) + \cdots}{\int f_c + \sigma m\int f_c^1\cos(q) + \cdots}. \tag{4.75}$$

Here, $f_c^{(n)}$ is the $n$-th order derivative of the distribution at the critical point. That distribution is homogeneous and all the integrals with an odd number of cosines are zero by parity, and we get only even terms. For instance, the leading terms in the numerator are the powers 1 and 3 of $\sigma m$. Thereby, Jeans' distributions have the magnetization which grows with the exponent $\beta = 1/2$.

This exponent does not depend on the particular distribution, since this latter changes only the critical value of the inverse energy scale $\sigma_c[f_0]$. In formulas, we get

$$m \simeq \sigma m G_1 + \sigma^3 m^3 G_3 + \mathcal{O}(m^5), \tag{4.76}$$

$$m \sim \frac{1}{\sigma\sqrt{\sigma G_1 G_3}}\sqrt{\sigma - \frac{1}{G_1}}, \qquad \sigma \searrow \sigma_c \tag{4.77}$$

$$G_1 = \frac{1}{2}\frac{\int f_c^1(p)dp}{\int f_c(p)dp} = \frac{1}{\sigma_c}, \tag{4.78}$$

$$G_3 = \frac{3}{48}\left[\frac{\int f_c^3(p)dp}{\int f_c(p)dp} - \frac{\int f_c^1(p)dp}{\int f_c(p)dp}\frac{\int f_c^2(p)dp}{\int f_c(p)dp}\right], \tag{4.79}$$

$$f_c^n(p) = \frac{d^n}{d(\sigma_c H)^n}F(\sigma_c H). \tag{4.80}$$

The distributions and their derivatives become functions of the velocities $p$, with no dependence on $q$. We integrate in $q$ to get the coefficients in front of these formulas.

Whenever the third moment is zero ($G_3 = 0$) the exponent goes to the successive order and, e.g., we get $\beta = 1/4$ when $G_5$ is not vanishing.

Let us compute the dielectric function (4.61) term by term. We find that the exponent of $C_2$ is twice the exponent of the magnetization

$$1 - C_2 \sim \frac{\sigma^2}{4}m^2\int f^3\cos^4(q) \sim (\sigma - \sigma_c)^{2\beta}, \tag{4.81}$$

close to criticality. The successive terms of the DF read

$$A[f](\sigma) = \frac{\sqrt{m}}{Z(\sigma)}\,\alpha[f](\sigma), \tag{4.82}$$

$$\begin{aligned}\alpha = {} & 16\int_0^1 K(x)\left(2\frac{E(x)}{K(x)} - 1\right)^2\frac{dF}{d\mathcal{H}}x dx \\ & +16\int_1^\infty \frac{K(1/x)}{x}\left(2x^2\frac{E(1/x)}{K(1/x)} + 1 - 2x^2\right)^2\frac{dF}{d\mathcal{H}}x dx.\end{aligned} \tag{4.83}$$

We obtain the exponent $\gamma_-^{\mathrm{V}} = -1/4$ because the first ratio goes as the square root of the magnetization and the functional $\alpha[f_c]$ is a continuous function of $\sigma$ and does not diverge. In formula, it behaves as

$$A[f] \xrightarrow{\sigma\to\sigma_c} \frac{(\sigma - \sigma_c)^{\beta/2}}{Z(\sigma_c)}\alpha[f_c]. \tag{4.84}$$

Any term which diverges with a smaller exponent determines the behavior, because there always exists a region near the critical point in which it dominates over the others.

On top of that, all Jeans' distributions have the same critical exponent equal to

$$\gamma_-^{\mathrm{V}} = -\frac{\beta}{2} = -\frac{1}{4}, \tag{4.85}$$

unless the coefficient $G_3$ becomes zero, in which case one would get $\gamma_-^{\mathrm{V}} = -1/8$ if $G_5 \neq 0$.

Although different initial conditions, hence different initial states, bring to different critical stability points $\sigma_c[f_0]$, the behavior of Jeans' states close to the transition does not depend on $f_0$. Actually, Vlasov critical exponents don't depend on the initial condition.

We remark here that the existence of further invariants may affect these equilibrium properties. Indeed, local temperature in isolated crystalline clusters is not uniform because of the conservation of momentum and angular momentum [89]. Moreover, it is known that conservation laws change the behavior near phase transitions also at equilibrium [108].

It is not surprising that in the Vlasov regime the existence of an infinity of conserved quantities changes critical exponents. The surprise it the existence, at least for particular systems, of well defined and quite general exponents in a theory that, to the best of our knowledge, does not possess any thermodynamic functional, such as entropy and free-energy. For instance, scaling arguments fail in standard formulations built on the free-energy.

### 4.7.3 Numerical comparison for the equilibrium distribution

Let us now consider the case of the equilibrium Boltzmann-Gibbs distribution

$$f_{eq} = \frac{e^{-\sigma(p^2/2 - m_0\cos(q))}}{Z(\sigma)}, \qquad Z(\sigma) = 2\pi\sqrt{\frac{2\pi}{\beta}} I_0(\sigma m_0), \quad m_0 = \frac{I_1}{I_0}(\sigma m_0). \tag{4.86}$$

Its critical point corresponds to the second order phase transition, which allows us to obtain a comparison between the classical theory of the mean-field universality class and Vlasov prediction.

Following our analysis, we propose a scenario of relaxation as follows: the system starts from a QSS, here the equilibrium at a given temperature. When

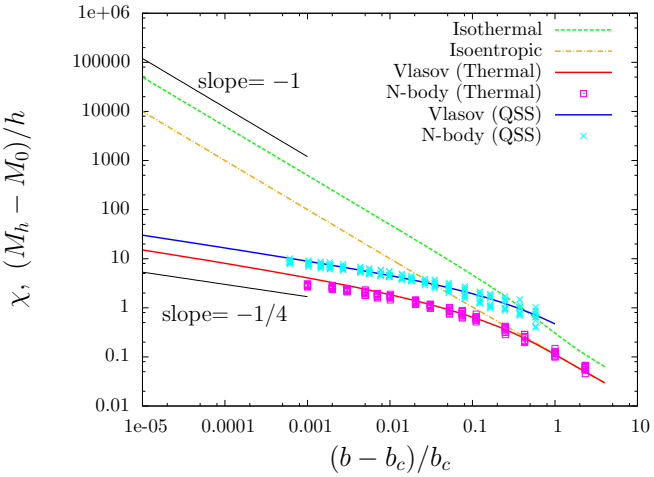


Figure 4.6: Vlasov susceptibility $\chi^{\mathrm{V}}$ for the equilibrium initial distribution (red solid line) and for the Fermi-Dirac initial distribution (Blue solid line). The parameter $b$ of the $x$-axis corresponds to the inverse energy scale; at equilibrium it is the inverse temperature. The canonical susceptibility $\chi^T$ (green broken upper line) and the micro-canonical susceptibility $\chi^S$ (blue dashed middle line) are reported for comparison. The black straight lines are guides to the eyes for the slopes $-1/4$ and $-1$. Purple square and cyan cross points are computed by time averages over the period $0 \leq t \leq 500$ in $N$-body simulations with $N = 10^6$ and a time step $0.1$. For each $T$, $10$ points are plotted corresponding to $10$ realizations.

an external field is switched on, the system gets trapped into a new QSS on a time-scale of the order of the dynamical time-scale. This happens whenever the initial state is stable. To keep Casimir's invariants constant in time, the system responds with the *anomalous* critical exponent $\gamma_-^{\mathrm{V}} = -\beta/2$. This result is summarized in figure 4.6. The red full line is the numerical solution of Vlasov equation for equilibrium and purple points are numerical simulation of a finite system in the Vlasov regime. Blue full line and cyan points show the Vlasov critical exponent for the Fermi-Dirac distribution, which is taken as a prototype of an out-of-equilibrium state. The green dotted and yellow dashed lines show the canonical and microcanonical susceptibilities at equilibrium, while the black straight lines are guides to the eyes for the classical and the Vlasov slopes. Such numerical result shows that for early times the response of the system for inhomogeneous Jeans' states is in a good accordance with the theoretical predictions of Vlasov dynamics.

However, Vlasov dynamics is not the true dynamics for the finite system,

thus Casimirs are not exactly conserved but evolve on a time-scale which diverges with $N$. Consequently, the system goes towards Boltzmann equilibrium recovering the classical exponent when relaxation to equilibrium is completed. Actually, such a scenario can be examined by direct $N$-body simulations, shown in figure 4.7. For $t < 0$, the system is at equilibrium with a temperature $T = 0.499 < 1/2 = T_c$. An external field with a small size $h = 0.01$ is switched on at $t = 0$, and the system jumps to the QSS predicted by linear response theory. In the long time regime Casimirs are no more conserved due to the presence of "collisions" [12], and the system goes towards the new equilibrium with the external field. Simulations indicate that the time-scale of relaxation from the QSS to equilibrium grows linearly with $N$, as found for isolated inhomogeneous QSSs [28].

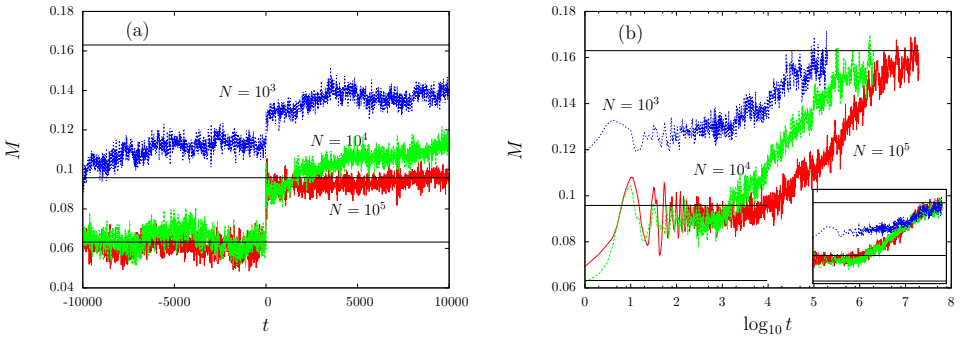


Figure 4.7: $N$-body simulations of the HMF model with external field. $N = 10^3$ (100), $10^4$ (10) and $10^5$ (1), where the numbers within brackets are the numbers of realizations over which the orbits are averaged. The system is initially at equilibrium with a temperature $T = 0.499$ and the external field is turned on with $h = 0.01$ at $t = 0$. In each panel, the three horizontal lines represent equilibrium levels with the microcanonical susceptibility (upper), the QSS level predicted by Vlasov linear response theory (middle) and the initial equilibrium (lower). (a) Short time evolution of the magnetization. (b) Long time evolution. The $x$-axis is in logarithmic scale, which is scaled as $\log_{10}(t/N)$ in the inset.

## 4.8 Conclusions

In this Chapter we have discussed linear response theory of the Vlasov equation for inhomogeneous initial states. The linear response theory in such a regime has been obtained for integrable systems in Ref. [93]. Here, we discuss an

approximative method which is applicable to non-integrable systems. We face problems arising when the initial state is inhomogeneous, hence the Fourier modes of the distribution function are coupled with the modes of the mean-field potential. In order to get a solution we assume the existence of a base of functions which decouples the system, such as the Fourier base does for homogeneous states.

Moreover, we discuss the presence of infinite integrals of the motion for Vlasov dynamics. The linear theory that we derive does not conserve any constraint and we must take care of them by hand. To impose an infinity of constraints is an hard task and in general it is not possible. Thereby, we consider the case of few of them and we apply the derived formulas to an integrable system: the HMF model. To get the solution of the problem for all times we need to know the analyticity properties determined by the initial state. Therefore, we are led to evaluates the response of the system at long times when the state of the system reaches a new stationary state.

The comparison between the correct solution and the approximate one gets better as the number of constraints is increased and, for instance, at low energies they are not distinguishable by using just a few constraints. A numerical comparison in a range of energies in which the two theories agree is discussed in order to analyse the correctness of both of them. It shows an accuracy of the value of the response similar to the one found in the homogeneous phase (see Chapter 3).

Afterwards, we study the behavior of the HMF model close to the stability thresholds. Each stationary solution of the Vlasov equation has a different threshold point but for a wide class of solutions, the Jeans' distributions, the behavior approaching such critical point is universal. We obtain analytically from the correct solution the value of the critical exponent of magnetic susceptibility and we discuss the nature of the anomalous behavior arising in comparison with the statistical mechanics of mean-field systems. For instance, even equilibrium states go to a QSS with a non-classical exponent when they are perturbed by an external field. The presence of infinite conserved quantities modifies the classical behavior for the time-scale in which the Vlasov equation is a good approximation of the dynamics. Finally, we perform numerical $N$-body simulations around the critical point at equilibrium, which illustrates our results for the HMF model.

# Chapter 5

# Small systems interacting with bigger systems

*Perturbation theory can be used to discuss the interaction between a big and a small mean-field long-range interacting systems. It is known in the literature that the classical definition of thermal bath fails for long-range interacting systems because the nature of the force does not allow the distinction between bulk and surface interactions. In the first part of this Chapter we analyse a linear theory where the small parameter is the relative size of two subsystems of an isolated mean-field system. The evolution equation of the small subsystem is driven by the evolution of the bigger one.*

## 5.1 Introduction

Until today, the large majority of studies aimed at elucidating the fundamental properties of LRI's have been carried out for isolated systems, *i.e.* under the assumption that the system properties are not influenced by the external environment. However, recognizing whether a non-equilibrium QSS is stable to an external perturbation is of great importance [86], both from a theoretical and an experimental point of view. A related fundamental problem concerns the mechanism through which a LRI system exchanges energy with the surroundings.

The out-of-equilibrium dynamical properties of LRI systems in contact with a thermal bath have been studied for the first time only recently [9, 10, 38]. As a possible realization of thermal bath, these authors considered a large

Hamiltonian system with nearest-neighbour interactions, coupled to a fraction of the spins in the system. They concluded that the coupling with the bath introduces a new time scale in the evolution of the system: the weaker the coupling strength, the longer the system remains trapped in a QSS before relaxing to equilibrium.

At variance with the above studies, we investigate here the dynamics of a LRI in long-range contact with an additional large system trapped in a QSS [27]. This defines an interaction scheme that can be regarded as more realistic, opening the way to applications in several fields, from cosmology to plasma physics. For example, one may think of the collisionless mixing between plasmas, or the operation of magnetic fusion devices for energy production or the merging of globular clusters to a self-gravitating galaxy.

We construct a perturbation theory around the Vlasov equation where the small parameter is the relative mass of two subsystems of an isolated system. Isolated short-range systems can be described by a statistical mechanics approach in which one obtains the thermodynamic laws. A statistical mechanics approach, inspired by the seminal work of Lynden-Bell [76], can be done also for long-range interacting systems. This theory can be used to characterize analytically some QSS features but it is not known if it can capture statistical laws, such as in the short-range case. Lynden-Bell's approach is based on the definition of a locally-averaged ("coarse-grained") distribution, yielding an entropy functional defined from first-principle statistical-mechanics prescriptions. By constrained maximization of such an entropy, one obtains closed analytical expressions for the single-particle distribution in the QSS regime [4, 5]. As a natural consequence, the QSSs can be equally interpreted as equilibrium configurations of the corresponding continuous description. In this setting the study of a coupling between big and small systems is a parallel with the study of the canonical ensemble in statistical mechanics.

In Section 5.2 we describe the model and the perturbation procedure and we make some preliminary remarks. In Section 5.3 we develop the theory at the leading-order for a generic model and we focus on the particular case of the HMF model (see Section 1.4). In Section 5.4 we discuss the successive orders, while in the last Section 5.5, we compare numerical simulations with the theoretical analysis.

## 5.2 The model

Let us consider a long-range isolated system divided in two parts, one bigger than the other. We label $B$ the bigger subsystem and $S$ the smaller one. We restrict the analysis to periodic systems and in particular we perform both the numerical simulations and the analytical evaluation on the HMF model, in order to simplify the calculations.

Let $f_B(\theta, p)$ be the normalized single-particle distribution that characterizes the larger subsystem. The QSS of the big subsystem that we consider here corresponds to the stationary and stable solution of the underlying Vlasov equation (2.17). In the simulations presented, we obtain such a function corresponding to an inhomogeneous Water-Bag initial distribution (the homogeneous one is defined in Chapter 3),

$$f_0(p,\theta) = 1/[4\Delta\theta_B \Delta p_B], \quad \theta \in [-\Delta\theta_B, \Delta\theta_B], \quad p \in [-\Delta p_B, \Delta p_B], \tag{5.1}$$

and zero elsewhere. The QSS in which the big system gets trapped is very well described by the Lynden-Bell theory. We stress anyway that small discrepancies are present, and we address the reader to [16, 64] for a careful discussion on the accuracy of the Lynden-Bell theory.

At a given time, $t = 0$ in our discussion, another HMF system with water-bag profile is coupled and let evolve consistently with the big subsystem. This system, $S$ in the following, is described in terms of its associated single-particle distribution $f_S(\theta, p)$. Clearly $B$ should be significantly larger than the system to which it is coupled. This can be accomplished through the following normalization condition

$$\int f_S(\theta, p, t)\, d\theta\, dp = 1 - \int f_B(\theta, p, t)\, d\theta\, dp = \epsilon \tag{5.2}$$

where $\epsilon \ll 1$ sets the relative size of the two mutually interacting $S$ and $B$ HMF systems. We are interested in tracking the time evolution of the distribution $f(\theta, p, t) \equiv f_B(\theta, p, t) + f_S(\theta, p, t)$ under the constraints (5.2). From the physical point of view, we are reproducing the microcanonical dynamics of one isolated HMF system ($S+B$), composed of two subsystems supposed as distinguishable: the larger subsystem $B$ has already relaxed to its QSS. The subsystem $S$ is initially confined in a generic water-bag type configuration.

To monitor the evolution of both subsystems, we follow the kinetic temperatures $T_\alpha(t) \equiv \Gamma_\alpha \int p^2 f_\alpha(p, \theta, t)\, d\theta\, dp$, with $\alpha = B, S$ and the corresponding

magnetizations $M_\alpha$. Here, $\Gamma_S = 1/\epsilon$ and $\Gamma_B = 1/(1-\epsilon)$. A typical time evolution of these observables, obtained by numerical integration of the Vlasov equation (2.17), is illustrated in figure 5.1. After a short transient, the subsystem $S$ reaches a quasi-stationary state where the mean value of the kinetic temperature is *different* from the one of $B$. In other words, the big subsystem and the small one do not reach the same kinetic energy; the two subsystems do not thermalize in the usual sense. Similarly, the two magnetizations converge to different values. Importantly, we note that the specific values of temperature and magnetization attained by the system spotlight a non-trivial interaction with the two subsystems. $T_S$ and $M_S$ are indeed substantially different from the values that the system would reach when evolved microcanonically from the same initial condition. We obtain equivalent results upon simulating the discrete $N$-body dynamics (5.3). In this case, after a time scale that gets progressively longer as the system size $N = N_S + N_B$ is increased, $\Delta T = T_B - T_S$ and $\Delta M = M_B - M_S$ tend to zero. Thus, granularity causes thermalization, which is instead prevented in the continuum ($N \to \infty$) limit, as shown in Chapter 2. We call *canonical QSS* the quasi-stationary configurations that the system $S$ explores when it is in a long-range contact with a QSS. This peculiar regime is attained when the observables of both the subsystems do not evolve in time.

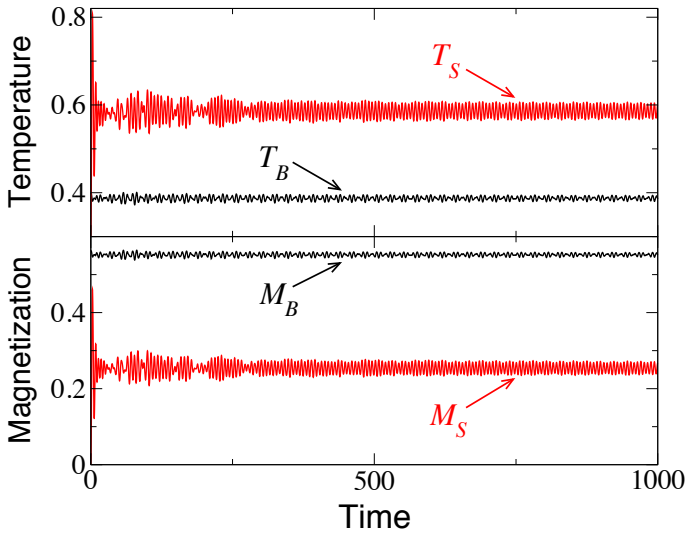


Figure 5.1: Time evolution of temperature and magnetization for both the large, $B$, and small, $S$, QSSs. The large QSS originates from a water-bag with energy $0.54$ and initial magnetization $0.6$. The system is initially homogeneous in space (zero magnetization) and its energy is set to $0.65$. The coupling constant $\epsilon = 0.024$.

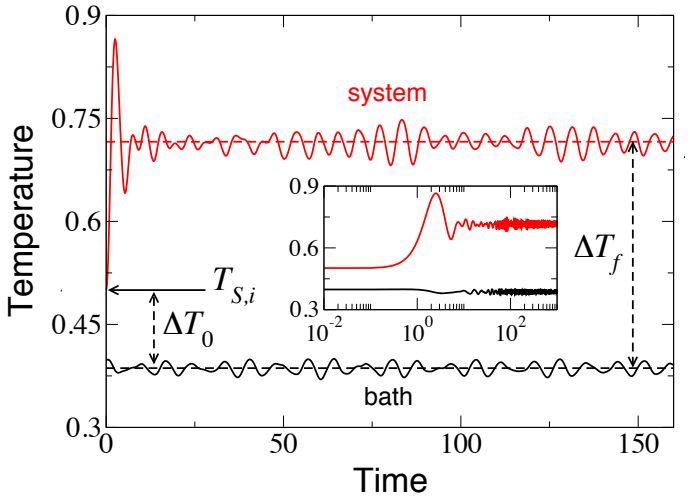


Figure 5.2: $B$ (here "bath") and $S$ (here "system") kinetic temperatures versus time. The subsystem $S$ is initially spatially homogeneous (zero magnetization) and has energy $0.75$. Inset: same plot with logarithmic time scale. Other parameters are as in fig. 5.1.

In the $N \to \infty$ limit, when $S$ is trapped in a canonical QSS, we find that the average energy flux between the big and small subsystems indeed vanishes, making the two subsystems by all means decoupled and thus preventing thermalization. It is remarkable that a zero-flux state is reached for $T_B \neq T_S$ in the non-collisional regime, at variance with what is normally found in most collisional systems.

Even more surprising is the behaviour of the system during the "violent relaxation" stage towards the canonical QSS, which is characterized by a net energy flux from the (cold) subsystem $B$ to the (hot) one $S$. We stress that this behaviour is not related to the negative specific heat, a feature present in some LRI at microcanonical equilibrium [32]. To better illustrate the scenario, we plot $T_B$ and $T_S$ versus time in fig. 5.2. Note that $T_S$ is larger than $T_B$ at $t = 0$, the time of injection which is when the two subsystems become coupled. As time progresses, the difference $\Delta T$ increases even further, resulting in a counter-intuitive energy transfer from $B$ to $S$. In short, the *hot* system gets *hotter* when placed in contact with a large long-range QSS reservoir. This observation, although fighting intuition, does not violate any laws of physics, as the second law of thermodynamics is only expected to hold at thermal equilibrium.

Once the system has settled down in its canonical QSS at zero average energy flux, $\Delta T$ and $\Delta M$ are found to be different from zero. In order to pinpoint

the relation between $\Delta T$ and $\Delta M$, we performed a series of simulations for the big subsystem conditions as specified in the caption of fig. 5.1, and varying the initial energy of the system $S$. Different initial energies of $S$ lead to distinct canonical QSS's, as it happens to isolated systems trapped in microcanonical QSS's. At first glance, it is tempting to speculate that canonical QSS might originate from a net balance of two opposing thermodynamic forces, presumably related to $\Delta T$ and $\Delta M$. However, we find that the dynamical evolution of $S$ is *not* influenced by the temperature of the big subsystem $T_B$, at least for $\epsilon \ll 1$, but only responds to its magnetization $M_B$. Therefore, provided $M_B$ is kept fixed, $T_B$ can be set to an arbitrary value, without significantly altering the system dynamics. This is illustrated by the data collapse reported in fig. 5.4.

## 5.3 Leading-order dynamics

Let us consider an Hamiltonian long-range system, made of two subsystems $S$ and $B$, which is described by the Hamiltonian:

$$H_T = \sum_{i=1}^{N_S} \frac{p_i^2}{2} + \sum_{i=1}^{N_B} \frac{P_i^2}{2} + \frac{1}{2N} \sum_{i,j=1}^{N_S} v(q_i - q_j) + \frac{1}{2N} \sum_{i,j=1}^{N_B} v(Q_i - Q_j) + \frac{1}{N} \sum_{i=1}^{N_S} \sum_{j=1}^{N_B} v(q_i - Q_j)\,, \tag{5.3}$$

where the variables for $S$ are in lower case where those for $B$ in upper case. The energy of the $i$-th particle of $S$ with position $q_i$ and momentum $p_i$ is hence given by

$$E_i = \frac{p_i^2}{2} + \frac{1}{2N} \sum_{j=1}^{N_S} v(q_i - q_j) + \frac{1}{N} \sum_{j=1}^{N_B} v(q_i - Q_j)\,. \tag{5.4}$$

In the Vlasov limit we obtain that $B$ is described by some distribution function $f_B(q, p, t)$ which is normalized to unity and obeys

$$\partial_t f_B(q, p, t) + p \partial_q f_B - \partial_p f_B \partial_q \Phi[f_B + f_S] = 0, \tag{5.5}$$

where $\Phi$ is the usual mean field potential, defined as

$$\Phi[f](q) = \int dq' dp'\, f(q', p', t) v(q - q')\,, \tag{5.6}$$

and $f_S(q, p, t)$ is the distribution function of the subsystem $S$, and it is normalized to $\epsilon$. This can be obtained thinking that a particle of the system with

position $q$ and momentum $p$ has, considering the whole system $S+B$ in the Vlasov limit, an energy given by:

$$H_S(q,p,t) = \frac{p^2}{2} + \Phi[f_S](q) + \Phi[f_B](q)\,, \tag{5.7}$$

which is nothing else but the single-particle Hamiltonian.

We will suppose $\epsilon \ll 1$, which is the analogous to $N_B \gg N_S \gg 1$ in the Vlasov approach. The evolution of $f_B$ is coupled to the evolution of $f_S$

$$\partial_t f_S(q,p,t) + p\partial_q f_S - \partial_p f_S \partial_q \Phi[f_B + f_S] = 0\,. \tag{5.8}$$

The kinetic temperature of $B$, of $S$ and of $B+S=T$, as well as other observables like magnetization etc.., are defined in the Vlasov picture as

$$T_B = \frac{1}{1-\epsilon}\int dpdq\, p^2 f_B(q,p,t), \tag{5.9}$$

$$T_S = \frac{1}{\epsilon}\int dpdq\, p^2 f_S(q,p,t), \tag{5.10}$$

$$T_T = \int dpdq\, p^2 [f_B + f_S], \tag{5.11}$$

where one should observe that the factors in front of the integrals come from the normalization of the distribution functions. This is important for the following approximations.

The coupled evolution of $f_S$ and $f_B$ is very hard to handle analytically. However, as far as we are interested only in observables of the system $S$ we can use a very simple approximation which should bring us to solve the problem analytically.

First of all, let us observe that the term $\partial_p f_S \partial_q \Phi[f_B]$ in Eq. (5.8) gives a modification of order $\epsilon$ to $f_S$ and hence a modification of order one of the observables, such as kinetic temperature. This is the most important term. On the other hand, remembering that $f_S \sim \epsilon$, we obtain that $\partial_p f_S \partial_q \Phi[f_S]$ in Eq. (5.8) is of order $\epsilon^2$, hence negligible.

Let us now consider the term $\partial_p f_B \partial_q \Phi[f_S]$ in Eq. (5.5), which gives a modification of order $\epsilon$ to the evolution of $f_B$. In turn this implies, from Eq. (5.8), a modification of order $\epsilon^2$ to the evolution of $f_S$. This term implies a modification to order $\epsilon$ of kinetic temperature (or of any other observable) of the big subsystem. Neglecting this effect corresponds to say that the leading subsystem $B$ does not change kinetic temperature when coupled to the subsystem $S$.

Let us also observe that observables of the total system, such as $T_T$, evolve following a value driven by the reservoir. Therefore, neglecting $\partial_p f_S \partial_q \Phi[f_S]$ is still a valid approximation (plus terms of order $\epsilon^2$). On the other hand, in this case, the two terms $\partial_p f_B \partial_q \Phi[f_S]$ and $\partial_p f_S \partial_q \Phi[f_B]$ both give a contribution of order $\epsilon$ and hence none of them is negligible.

The above reasoning leads us to the two following coupled equations:

$$\partial_t f_B(q,p,t) + p\partial_q f_B - \partial_p f_B \partial_q \Phi[f_B] = 0, \tag{5.12}$$

$$\partial_t f_S(q,p,t) + p\partial_q f_S - \partial_p f_S \partial_q \Phi[f_B] = 0\,. \tag{5.13}$$

Solving the first one means only that the bath is in a QSS, hence in the Vlasov picture:

$$f_B(q,p,t) = f_B(q,p,t=0), \tag{5.14}$$

for all times $t$. The equation for $f_S$ is now extremely simple, because it corresponds only to the Liouville equation for a single particle moving in an external potential ($f_B$ is fixed in time).

## 5.4 Next-to leading order dynamics

Let us briefly discuss the next-to leading order dynamics in the perturbation parameter. The evolution equation of both distributions in the $N \to \infty$ limit is described jointly by the pair of Eqs. (5.12) and (5.13). Here, we have to consider the collisional integral of size $1/N$. The perturbative parameter is the same of Kinetic Theory and, indeed, we must consider both the equations for the single distributions and the equations for the correlation, because there should be a mixing between the two terms. Following the discussion of Chapter 2, we get

$$\partial_t f_B - p\partial_q f_B - \partial_q \phi[f_B]\partial_p f_B = \partial_q \phi[f_S]\partial_p f_B + \frac{1}{N}\sum_{\alpha=S,B}\int dx' V'(q-q') g_{B\alpha}, \tag{5.15}$$

$$\partial_t f_S - p\partial_q f_S - \partial_q \phi[f_B]\partial_p f_S = \partial_q \phi[f_S]\partial_p f_S + \frac{1}{N}\sum_{\alpha=S,B}\int dx' V'(q-q') g_{S\alpha}, \tag{5.16}$$

where we use standard notations, as discussed in Chapter 2. The r.h.s. of Eq. (5.15) shows two terms: the first term is of order $\epsilon$, while the second term

is a sum on the label $\alpha = S, B$ with size $1/N$. Actually, the part with label $\alpha = B$ is of order $\frac{\epsilon}{N}$ while the part with label $\alpha = S$ is of order $\frac{\epsilon^2}{N}$, following the assumptions of Section 2.6 and the size of the relative distributions $f_{B,S}$ . Our hypotheses are that both systems can be described by a continuum theory, therefore the number of particles of both the systems go to infinity. There are two possibilities: the first case is that $\epsilon$ is vanishing in the $N \to \infty$ limit, and we obtain the description of a single particle in a QSS reservoir. This case is well discussed in [22,23,101] where the authors show the presence of anomalous diffusion with algebraic time behavior of autocorrelations.

We are here interested in the second case, namely, when there is a separation between the two perturbative constants. We get $\epsilon \gg \frac{1}{N}$, actually, we consider $\epsilon$ small but finite. We solve formally Eq. (5.15) using linear theory around the solution of (5.13), described in Chapter 3 and 4. Thereby, we put such solution in Eq. (5.16) and we solve it using again the same linear theory.

Although linear theory is known, at least for integrable systems, the solution above is mathematically quite complicated. It is not within the scope of this work to give that analytical solution, but it is still an interesting question. For instance, we can argue which is the relaxation process of both the systems. On a short time-scale, system $S$ relaxes to the stationary solution of Eq. (5.13) and $B$ does not evolve from its QSS. On a time-scale of order $\epsilon^{-1}$, both the systems slightly evolve, as described by linear theory, but this evolution is iso-entropic and does not converge to some preferred state. On a time-scale of order $N$ there are two different cases: when $B$ is homogeneous then $S$ relaxes to the state of $B$ and both take a time-scale of order $N^2$ to equilibrate. When $B$ is inhomogeneous the whole state $B + S$ relaxes to equilibrium on a time-scale of order $N$, forgetting the initial states.

## 5.5 Application to the HMF model and corresponding numerical experiments

In the case of the HMF model, supposing the magnetization $M_B$ of the bath to be along the $x$ axis, we have

$$\partial_t f_S(q,p,t) + p\partial_q f_S - M_B \sin(q)\partial_p f_S = 0\,, \tag{5.17}$$

where one can already see the remarkable prediction that the evolution of $f_S$ depends only on $M_B$. Observe that the solution of the equation for $f_s$ strongly

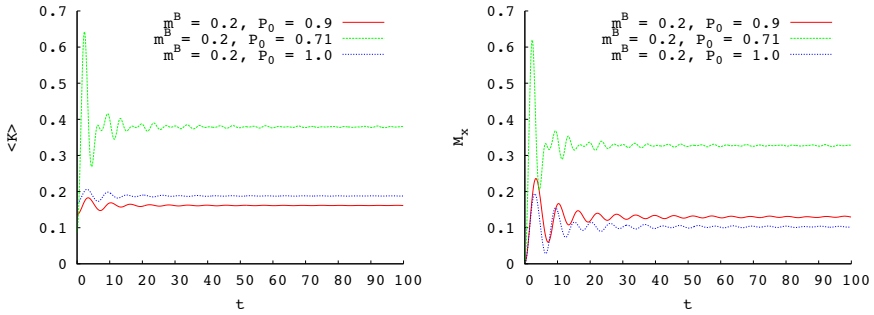


Figure 5.3: Kinetic energy (left panel) and magnetization along $x$ (right panel) of the initial WB distribution.

depends on the initial condition (QSS in which the system is prepared). It is an evolution of the initial conditions where each phase space point evolves independently with respect to the other points.

First of all, we consider the relaxation of the small subsystem towards a stationary state, as shown in the non interacting gas of particles in Chapter 2. The big subsystem is in a generic distribution which produces a magnetization along the $x$ axis equal to $M_B = 0.2$. At the coupling time, here $t = 0$, the subsystem $S$ is in a homogeneous Water-Bag state (see Section 3.2) with three different initial widths $p_0 = \{0.71, 0.9, 1.0\}$. Moreover, the initial distribution is built on a regular lattice to avoid finite $N$ fluctuations. The system is evolved using a symplectic algorithm of fourth order [78]. Figure 5.3 shows the time dependence of kinetic energy and magnetization along the $x$ axis. They relax to a stationary value which depends only on the external field produced by the big subsystem.

As discussed above, the leading-order evolution of $f_S$ depends only on $M_B$ and not on $T_B$. The phase space of the pendulum is foliated in trajectories with constant energy

$$e = \frac{p^2}{2} - M_B \cos\theta \,, \tag{5.18}$$

hence, $p(\theta) = \sqrt{2}\,[e + M_B \cos\theta]^{1/2}$. We want to discuss an analytic estimate of the difference between the kinetic temperature of the small subsystem $(T_{S,f} - T_{S,i})/M_B$ for $\Delta p_S = 0$ and for an initial homogeneous system, $M_S(t = 0) = 0$. This analysis can be extended to cover the case $\Delta p_S \neq 0$, and also $M_S(t = 0) \neq 0$. We note that $T_{S,i} = 0$ for $\Delta p_S = 0$. To evaluate $T_{S,f}$, we first consider the average kinetic temperature of the particles which are assigned a given

energy $e$. In formulae

$$\langle p^2 \rangle_e = \frac{1}{T(e)} \int_0^{T(e)} \dot{\theta}^2 \, dt, \tag{5.19}$$

where $\langle \cdot \rangle_e$ indicates a time average over one period

$$T(e) = \frac{4}{\sqrt{M_B}} K\left(\frac{e + M_B}{2M_B}\right), \tag{5.20}$$

and $K(\cdot)$ being the complete elliptic integral of the first kind. Expression (5.19) takes the equivalent form

$$\langle p^2 \rangle_e = \frac{2}{T(e)} \int_{-\bar{\theta}(e)}^{\bar{\theta}(e)} p(\theta) \, d\theta, \tag{5.21}$$

where $\bar{\theta}(e) = \cos^{-1}(-e/M_B)$ is the angle of inversion of the selected (closed) trajectory. By performing the integral, one eventually gets

$$\frac{\langle p^2 \rangle_e}{M_B} = \frac{2\sqrt{2(M_B + e)}}{\sqrt{M_B} K\left(\frac{e+M_B}{2M_B}\right)} E\left(\frac{\bar{\theta}(e)}{2}, \frac{2M_B}{e + M_B}\right), \tag{5.22}$$

where $E(\cdot, \cdot)$ is the incomplete elliptic integral of the second kind. The final temperature of the system can now be evaluated as

$$T_{S,f} \equiv \langle p^2 \rangle = \int_{-M_B}^{M_B} \langle p^2 \rangle_e \rho(e) \, de, \tag{5.23}$$

where $\rho(e)$ is the density of states of the system, which is univocally fixed by the initial condition. The integral in eq. (5.23) extends from $-M_B$ to $M_B$, *i.e.* the energies that identify the separatrix of the pendulum. In fact, the system is trapped inside the separatrix $|e| = M_B$, given the specific condition selected here ($\Delta p_S = 0$, hence no particle lies outside the resonance at $t = 0$). Recalling eq. (5.18), the distribution $\rho(e)$ can be calculated easily, as

$$\rho(e) = \frac{1}{\pi} \left| \frac{de}{d\theta} \right|^{-1} = \frac{1}{\pi} \frac{1}{\sqrt{M_B^2 - e^2}}. \tag{5.24}$$

Plugging eq. (5.24) into eq.(5.23) and recalling eq. (5.22), one eventually obtains

$$\frac{T_{S,f}}{M_B} = \sqrt{\pi} \int_{-1}^{1} \frac{E\left(\cos^{-1}(-y)/2, \frac{2}{1+y}\right)}{K\left(\frac{1+y}{2}\right)} \frac{dy}{\sqrt{1 - y^2}}. \tag{5.25}$$

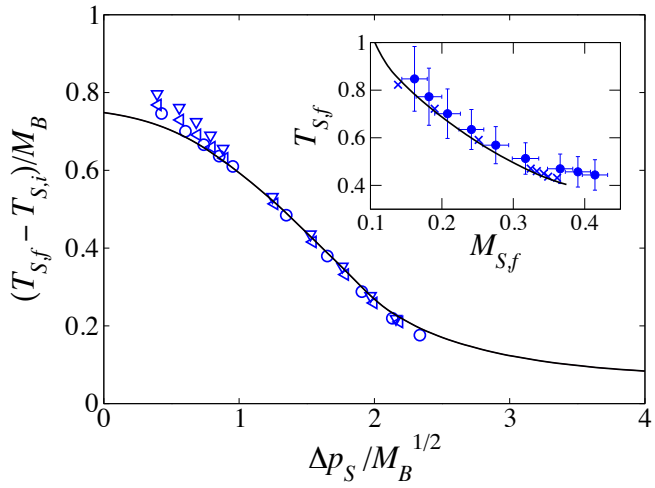


Figure 5.4: Difference between final and initial temperature of the subsystem $S$ versus width of its initial water-bag, in reduced units. Data refer to different choices of the reservoir parameters and to different initial energies of the (initially homogeneous) system $S$. Symbols: direct integration of eqs. (5.8) for $M_B \in [0.1, 0.55]$, $T_B \in [0.3, 0.4]$. Solid line: numerical solution of eq. (5.17). Inset: $T_{S,f}$ vs. $M_{S,f}$ for the same choice of parameters for $B$ as in fig. 5.1. Circles: $N$-body simulations (average over 100 independent realizations), $N_B = 4 \times 10^3$, $N_S = 10^2$. Crosses: direct integration of the Vlasov equations. Solid line: integration of eq. (5.17). All quantities are dimensionless.

Numerical integration gives $T_{S,f}/M_B \approx 0.751$, in excellent agreement with the data reported in fig. 5.4. In the general case ($\Delta p_S \neq 0$), $e \propto \Delta p_S^2$. The scaling suggested by eq. (5.25) implies that $\Delta p$ scales as $\sqrt{M_B}$.

Consistently with the above scaling arguments, we plot in fig. 5.4 $(T_{S,f} - T_{S,i})/M_B$ as a function of the rescaled width of the initial water-bag $\Delta p_S/\sqrt{M_B}$, for different values of the big subsystem magnetization and kinetic temperature. The data refer to the direct integration of the (constrained) Vlasov equations (5.5) and of eqs. (5.17). In all cases, the data collapse nicely on a single master curve, which confirms the validity of our reasoning. An analytical calculation of $(T_{S,f} - T_{S,i})/M_B$ for $\Delta p_S = 0$ yields $(T_{S,f} - T_{S,i})/M_B \approx 0.751$, in excellent agreement with the result of direct integration of eq. (5.17) (see also Ref. [28]). The inset further shows that $N$-body simulations agree with all results obtained in the $N \to \infty$ limit.

## 5.6 Conclusions

We have shown that a small subsystem of a long-range interacting system and in long-range contact with a large one reaches a zero-flux steady state, that we denote as *canonical* quasi-stationary state. These are stationary states of the associated coupled Vlasov equations, and are quasi-stationary solutions of the $N$-body problem. Remarkably, in the explored range of parameters, we find that hotter-than-reservoir subsystems become even hotter in canonical QSS's. In the context of the HMF model, based on simple scaling arguments, we have shown how the system anomalously increases its kinetic temperature as the fraction of its particles trapped in the resonance set by the reservoir magnetization gain energy. The kinetic energy gain is proportional to the value of $M_B$ and independent of the reservoir temperature at the leading order in $\epsilon$.

We stress here, that this observation does not violate any fundamental law of physics. Indeed, the average kinetic energy of the system does not coincide with its thermodynamic temperature. In this respect, our work raises the following central, yet unanswered, question: which is the correct thermodynamic measure of temperature for a system frozen in a QSS? Notice that in the present work, the energy of the thermal bath was chosen to lie in the part of the (microcanonical) phase diagram corresponding to a magnetized QSS. As far as the system is concerned, we have considered initial energies leading to both magnetized and non magnetized (microcanonical) QSS's.

In conclusion, and based on the theoretical analysis that we have carried out, we argue that the results illustrated in this Chapter are general and extend beyond the HMF case-study, whenever the collisionless Vlasov picture is a good description of the dynamics.

# Chapter 6

# Conclusions

This Chapter summarizes the contributions of this Ph.D. work and discusses avenues for future research.

## 6.1 Summary of contributions

This work concerns the study of perturbed $N$-body mean-field interacting systems. Mean-field interactions belong to the general class of long-range interactions and show intriguing equilibrium and out-of-equilibrium features, as discussed in Chapter 1. One of the most peculiar out-of-equilibrium feature is the fact that these systems get trapped in long-living states, called Quasi-Stationary States (QSSs). Their lifetime diverges algebraically with the size of the system, $N$. We are here interested in studying the influence of a small external perturbation acting on a stable QSS.

The time evolution of QSSs is well described in the large $N$ limit by the Vlasov equation, and Chapter 2 is devoted to the presentation of Kinetic Theory for QSSs. In the mean-field limit ($N \to \infty$), Vlasov dynamics fully describes the time evolution of the system, in absence of singular interactions. This equation possesses an infinite number of stationary solutions that can be either homogeneous or inhomogeneous in space. In the last part of Chapter 2 we have focused our analysis on the properties of the Lenard-Balescu equation, which describes the relaxation to equilibrium of homogeneous long-range systems.

We have developed, in Chapter 3, a linear response theory for homogeneous QSSs using Fourier-Laplace techniques, analogous to the ones used in the theory of linear Landau damping. The theory allows us to compute the variation of

any observable when a small perturbing field is added to the Hamiltonian of the system. Both the time dependent and the asymptotic response are accessible to the theory. The Hamiltonian Mean-Field (HMF) model is a paradigmatic model for mean-field and long-range interactions. It describe the motion of particles on a unitary circle which interact all-to-all with an attractive or repulsive potential. Alternatively, the model can be interpreted as representing $XY$ spins with global coupling. Within this interpretation attractive (repulsive) interactions correspond to ferromagnetic (anti-ferromagnetic) couplings. We have shown that when an external field is applied to a stable QSS, magnetization changes as a result of both the variation of the distribution function and of the mean-field. Comparing our theoretical prediction with numerical simulations we have obtained a good agreement at linear order for three different representative QSSs: the Water-Bag, the Fermi-Dirac and the Gaussian QSSs. Second order corrections are also calculable and can affect the variation of the observables.

The theory for homogeneous states can be obtained without taking into account a peculiar feature of the Vlasov equation, the presence of an infinity of conserved quantities, called Casimirs. This fact cannot be neglected when facing the problem of inhomogeneous states. Moreover, inhomogeneity introduces a coupling between the mean-field modes and the modes of the distribution. The treatment of Landau damping for inhomogeneous states is still an open and difficult problem. However, something can be done within our linear response theory approach, discussed in Chapter 4. Indeed, we have developed an "approximate" linear response theory imposing by hand the constancy of a finite number of Casimirs, besides the usual conserved quantities related with symmetries. Other authors have been able to derive an exact linear response theory for integrable systems, including the HMF model when restricted to stationary states. In order to check the validity of our approximate linear response theory we compare our result for the response of an observable to the exact result obtained using this second type of linear response theory. Overall, the agreement between the two theories is good. However, close to the phase transition of the second order of the HMF model, the disagreement can become quite sharp, because the presence of additional conserved quantities here plays a crucial role. This is why our approximate theory in unable to produce the correct values of the critical exponents, which we instead have obtained using the exact integrable theory in the last part of Chapter 4. It is interesting to remark that the exponent in the inhomogeneous phase is not the "classical" mean-field exponent, but depends on the chosen class of distribution, here the one of Jeans' states.

Our perturbative approach can also be used to discuss the mean-field interaction between a small system and a big one, considered as a reservoir in canonical ensemble theory. In Chapter 5 we have studied in particular how a kinetically-defined temperature changes by this contact and found a non-trivial result that a hotter system can become even hotter by the contact.

## 6.2 Directions for future work

The study of linear response theory of the Vlasov equation results to be important for different areas of physics. For instance, such a linear theory is fundamental for kinetic equations that rule the time evolution of many-particle systems towards Boltzmann equilibrium. In Chapter 2 we have shown how the linear theory for homogeneous states, together with the Markovian hypothesis, brings to the Lenard-Balescu equation, which describes the relaxation of homogeneous state to equilibrium and when the interaction is long-range and non singular. The analogue of this equation for inhomogeneous states is known only for integrable interactions. Indeed, here it becomes interesting to obtain a kinetic equation using the "approximate" linear response theory, developed in Chapter 4, but valid for more general interactions.

Actually, it is relevant to study the validity of the approximate linear response theory and to characterize the importance of the infinite number of conserved quantities in relation to the time evolution of the state. Models with dimension higher than one and non-integrable interactions are also fundamental in plasma physics and astrophysics. For example, the study of the behavior of gravitational systems, which are intrinsically inhomogeneous, is a big challenge for galactic dynamics and cosmology and, nowadays, it is far from been completed.

Although the linear response theory for homogeneous states of Chapter 3 is more developed, there are however open directions also in this field. An intriguing problem is the one of characterizing the time evolution of the response; for instance for the Gaussian distribution in momenta, for which the dielectric function has an infinity of zeros in the lower half complex frequency plane. Moreover, time dependence can be imposed by hand when the external field depends itself on time in a non-trivial way. Indeed, one can study the action of impulsive perturbations on some frequencies and wavelength in order to characterize the energy cascade, in analogy with what has been done for turbulence.

Finally, an interesting direction for future work results from the perturbation theory developed in Chapter 5. Following an analogy with short-range interacting systems, one can evaluate whether a relation of that theory with Lynden-Bell theory exists. In the affirmative case, one can study the Legendre-Fenchel transform of Lynden-Bell entropy in analogy with what is done within the canonical ensemble in equilibrium statistical mechanics.

# Appendix A

This appendix is devoted to some mathematical results that we use in the Kinetic Theory of long-range systems, discussed in Chapter 2.

## A.1 BBGKY Hierarchy

The BBGKY hierarchy of equations (2.10) is obtained integrating by parts. Therefore, it depends on the boundary conditions. For the sake of simplicity we consider periodic boundary conditions in space and that the distribution vanishes when momenta reach infinity in modulus.

The time variation of the $s$-reduced distribution function (2.9) depends on the time variation of the solution $f_N$ of the Liouville equation by the following relation

$$\partial_t f_s \sim \int \prod_{i=s}^{N} dx_i \partial_t f_N = \int \prod_{i=s}^{N} dx_i \mathcal{L}_N f_N, \tag{A.1}$$

where $\mathcal{L}_N$ is the Liouville operator (2.5). This linear operator can be separated in different terms: the first one reads

$$\int \prod_{i=s}^{N} dx_i \sum_{j=1}^{N} p_j \partial_{q_j} f_N = \sum_{j=1}^{s} p_j \partial_{q_j} f_s, \tag{A.2}$$

and is called the *inertial* part of the Liouville equation. All the coordinates from 1 to $s$ are integrated and give a zero contribution thanks to the boundary conditions.

The second term of Eq. (2.4) is the one containing the two-body potential and can be separated in two different contributions. The first contribution is

given by the interaction between two particles of the $s$ set, hence one gets

$$\frac{1}{N}\sum_{j=1}^{s}\partial_{q_j}V(q_i-q_j)\partial_{p_j}f_s. \tag{A.3}$$

Again, integration of the variables in the set $\{(q_i,p_i)|i=1,\ldots,s\}$ is zero due to the boundary conditions. The second contribution is given by the interaction between a particle of the $s$ set and a particle outside this set. The associated operator reads

$$\sum_{j=1}^{s}\partial_{q_j}\int dx_3 V(q_i-q_3)\partial_{p_j}f_{s+1}. \tag{A.4}$$

This last term gives the non-linearity which relates the $s$ particle distribution function with to $s+1$ distribution function, and takes care of the long-range nature of the interaction.

## A.2 Fourier and Laplace transform

### Fourier Transform

The *Fourier transform* of a generic function $f\in L^1$, is defined by the formula

$$\tilde{f}_k=\tilde{f}(k)=\frac{1}{\sqrt{2\pi}}\mathcal{F}[f]_k=\int_{\mathbb{R}}dx f(x)e_k(x), \tag{A.5}$$

where we consider

$$e_k(x)=e^{\imath kx},\quad e_k^*(x)=e^{-\imath kx}. \tag{A.6}$$

The Fourier transform $\tilde{f}(k)$ is also called the $k$-th mode in the text.

The *inverse* transform is given by

$$\mathcal{F}^{-1}[\tilde{f}]_x=\frac{1}{\sqrt{2\pi}}\int_{\mathbb{R}}dk\tilde{f}(k)e_k^*(x). \tag{A.7}$$

The Fourier transform has some useful properties: first of all it is a linear transformation. Moreover, the Fourier transform of the convolution of two functions is the product of the Fourier transforms

$$\mathcal{F}[f*g]_k=\tilde{f}(k)\tilde{g}(k). \tag{A.8}$$

This formula is very useful in many problem of Kinetic theory, where the mean-field potential is a convolution between the two-body potential and the distribution. Therefore, the Fourier transform of the integral of two distributions is an integral itself

$$\mathcal{F}\left[\int dx f(x)g(x)\right] = \int dk \tilde{f}(k)\tilde{g}^*(-k), \tag{A.9}$$

which is called the Plemelj formula.

A third property is that the Fourier transform of a real and even function, is itself real and even.

### Laplace Transform

The *Laplace transform* is defined in two different ways, one for "Mathematician" and the other one for "Physicists". They are related by a rotation of the complex plane. Mathematicians write the transform as

$$\hat{f}_m(s) = \mathcal{L}[f]_s = \int_{0^+}^{\infty} e^{-st} f(t)dt, \quad s \in \mathbb{R}^+, \tag{A.10}$$

where $s \in \mathbb{R}^*$. On the other hand, for Physicists the transform is

$$\begin{aligned} \hat{f}(\omega) &= \mathcal{L}[f]_\omega = \int_{0^+}^{\infty} e^{\imath\omega t} f(t)dt = \hat{f}_m(-\imath\omega), & \text{(A.11)} \\ &= \int_{\mathbb{R}} \Theta(t) e^{\imath\omega t} f(t)dt, \quad Im\{\omega\} > 0, & \text{(A.12)} \end{aligned}$$

where $\Theta(t)$ is the Heaviside step function and $Im\{\omega\} > 0$ in order to have a convergent integral. We use in the text the formalism of Physicists.

The *inverse* of the Laplace transform is more complicated compared to the Fourier transform. Formally, it is defined by the formula

$$f(t) = \mathcal{L}_\Gamma^{-1}[\hat{f}](t) = \int_\Gamma e^{\imath\omega t}\hat{f}(\omega), \tag{A.13}$$

where $\Gamma$ is the *Bromwich* contour which pass over all the poles or singularities of the function $\hat{f}(\omega)$ (see Figure A.1). Defining $\gamma$ a real value such that $\imath\gamma$ is above all the singularities of the integrand $\hat{f}(\omega)$, the inverse transform reads

$$f_\gamma(t) = \int_{\imath\gamma-\infty}^{\imath\gamma+\infty} \hat{f}(\omega)e^{-\imath\omega t}d\omega. \tag{A.14}$$

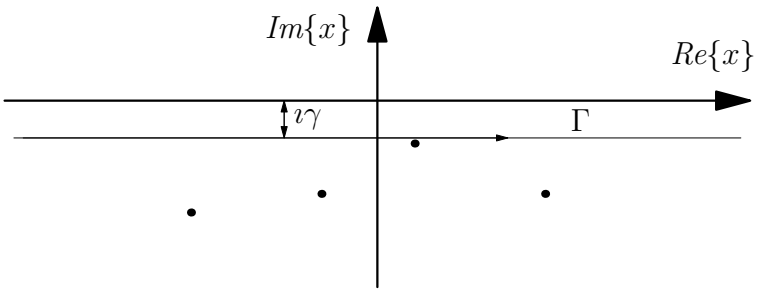


Figure A.1: The scheme of the Bromwich contour used to calculate the inverse Laplace transform.

It is clear now that the inverse transform is well defined only in the case in which the function $f_\gamma$ does not depend on $\gamma$ itself. For example, this is true for holomorphic functions that go to zero at large values of $\omega$, because the integral is equal to the sum of the residues at each singularity.

The Laplace transform has many properties:

- **Derivative:** the LT of a derivative of a function gives

$$\mathcal{L}[f'](\omega) = i\omega\mathcal{L}[f](\omega) - f(t=0). \tag{A.15}$$

- **Convolution:** the LT of the convolution of two functions gives

$$\mathcal{L}[f * g](\omega) = \mathcal{L}[f](\omega)\mathcal{L}[g](\omega). \tag{A.16}$$

- **Limit theorems:** whenever the limits on the l.h.s and on the r.h.s of the following expressions exist, then

$$\lim_{t\to\infty} f(t) = \lim_{s\to 0} s\hat{f}(s), \tag{A.17}$$

$$\lim_{t\to 0} f(t) = \lim_{s\to\infty} s\hat{f}(s). \tag{A.18}$$

## A.3 Riemann-Lebesgue lemma

The *Riemann-Lebesgue theorem* states that the $k$-th mode of the Fourier transform of a differentiable function $f$ goes to zero in the limit $|k| \to \infty$.

However, the way in which the modes go to zero depends crucially on the analyticity properties of the function. When $f \in L^1$ we have

$$\lim_{|k|\to\infty} \tilde{f}(k) = \lim_{|k|\to\infty} \int dx e_k(x) f(x) = \lim_{|k|\to\infty} \frac{1}{\imath k} \int dx e_k(x) \frac{d}{dx} f(x), \tag{A.19}$$

$$\lim_{|k|\to\infty} |\tilde{f}(k)| \leq \lim_{|k|\to\infty} \frac{1}{|k|} \int \Big| \frac{d}{dx} f(x) \Big| dx. \tag{A.20}$$

Then higher modes go to zero at least as $k^{-1}$. Also the Laplace transform is endowed with the same property when the integrand is an even function.

Moreover, we can invert the reasoning: the regularity of a given function $f$ results from the asymptotic behavior of its Fourier transform. For example, consider a distribution $f \in L^1$ well defined in $x = 0$. Its continuity assures that

$$f(0) = \int dk \tilde{f}(k) = \lim_{\eta\to 0} \int dk \frac{e^{-\imath k y}}{\eta} \tilde{f}(k/\eta), \quad \forall y, \tag{A.21}$$

and the same is true for its derivative

$$f^{(n)}(0) = \int dk k^n \tilde{f}(k) = \lim_{\eta\to 0} \int dk k^n \frac{e^{-\imath k y}}{\eta^{n+1}} \tilde{f}(k/\eta), \quad \forall y. \tag{A.22}$$

Therefore, for analytic functions, that are infinitely differentiable, Fourier modes go to zero faster then each power, hence exponentially.

### A.3.1 Analytic functions

Let us now give a more rigorous statement about the behavior of the modes of analytic functions. When a function $f(x)$ is analytic on the real axis it is analytic in a strip in the complex plane around the real axis. The width of this strip is the smallest radius of convergence of the analytic function, and it is not zero by assumption. This radius correspond to the imaginary part of the nearest singularity to the real axis of the function in the complex plane (the smallest imaginary part of the singularities) and we call it $\lambda < 0$. Let us consider a closed rectangular contour $\Gamma$ as in figure A.2 defined by

- $\Gamma_1$ is $x \in [-R, R]$
- $\Gamma_3$ is $x \in [-R + \imath\gamma, R + \imath\gamma]$
- $\Gamma_2$ is $x \in [R, R + \imath\gamma]$

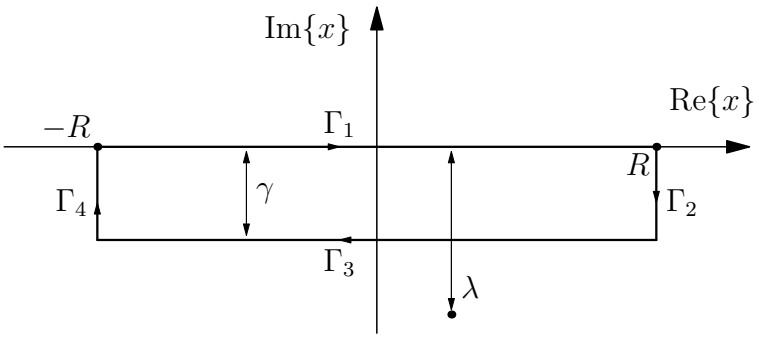


Figure A.2: The path $\Gamma$ that shows the exponential damping for Fourier modes of analytic functions

- $\Gamma_4$ is $x \in [-R, -R + \imath\gamma]$

and $\lambda < \gamma < 0$. Since there are no singularities inside the closed path $\Gamma$ and the function $f$ is analytic, the integral is zero for the Cauchy theorem. The two integrals along the paths parallel to the imaginary axis are

$$\int_{\Gamma_2} f(x)e^{\imath kx}dx = e^{\imath kR}\int_0^{\lambda} f(R+\imath y)e^{-ky}dy, \tag{A.23}$$

$$\int_{\Gamma_4} f(x)e^{\imath kx}dx = e^{-\imath kR}\int_{\lambda}^{0} f(-R+\imath y)e^{-ky}dy, \tag{A.24}$$

$$= -e^{\imath kR}\int_0^{\lambda} f(-R-\imath y)e^{ky}dy. \tag{A.25}$$

We have extracted in both the integrals the oscillating part due to the term with $R$. In the limit of $R \to \infty$ the function $f$ goes to zero distributionally since both integrals are defined on a compact domain. The integrals along the two paths $\Gamma_1$ and $\Gamma_3$ read

$$\int_{\Gamma_1} f(x)e^{\imath kx} = \int_{-R}^{R} f(x)e^{\imath kx}, \tag{A.26}$$

$$\int_{\Gamma_3} f(x)e^{\imath kx} = e^{-k\gamma}\int_{R}^{-R} f(x+\imath\gamma)e^{\imath kx}, \tag{A.27}$$

and are equal in modulus. In the integral along $\Gamma_3$ we have extracted the constant term $e^{-\gamma k}$. In the limit of $R \to \infty$ the first integral along $\Gamma_1$ is the Fourier transform of $f$, while the other is bounded by analyticity.

This result states that for any analytic functions the Fourier mode $k$ goes to zero exponentially and the wave-length scale is given by the nearest singularity to the real axis of $f$ in the complex plane.

## A.4 Principal Value integral

The following divergent integral

$$\int dx \frac{f(x)}{x-y}, \tag{A.28}$$

appears many times in the study of Laplace and Fourier transforms. Let us define the Cauchy principal value part

$$⨍ = \lim_{a\to 0}\left(\int_{-\infty}^{-a} + \int_{a}^{\infty}\right) = \mathrm{P}\int, \tag{A.29}$$

which corresponds to the non singular part of such integral. Therefore, we define the *Plemelj formula*

$$\lim_{a\to 0^+} \frac{1}{x \pm \imath a} = \mathrm{P}\frac{1}{x} \mp \imath\pi\delta(x), \tag{A.30}$$

used to evaluate the integral above in a distributional sense.

# Appendix B

This appendix is devoted to some mathematical results that we use for the Fermi-Dirac distribution in Chapter 3.

## B.1 Normalization, energy density, and stability criterion for the Fermi-Dirac distribution (3.7)

Normalization: Consider the distribution (3.7). The normalization $A$ satisfies

$$A\int_{-\infty}^{\infty}\frac{dp}{1+e^{\beta(p^2-\mu)}}=1. \tag{B.1}$$

Changing variables and doing an integration by parts, we get

$$2\beta A\int_{0}^{\infty}dx\ \frac{\sqrt{x}\ e^{\beta(x-\mu)}}{\Big[1+e^{\beta(x-\mu)}\Big]^2}=1. \tag{B.2}$$

The left hand side may be written in terms of the derivative $\partial f_{\rm FD}(x)/\partial x$ of the Fermi-Dirac-like function $f_{\rm FD}(x)=1/[1+e^{\beta(x-\mu)}]$. We get

$$2A\int_{0}^{\infty}dx\ \sqrt{x}\Big(\frac{-\partial f_{\rm FD}(x)}{\partial x}\Big)=1. \tag{B.3}$$

In the limit of large $\beta$, the derivative $\partial f_{\rm FD}(x)/\partial x$ approaches the Delta function: $\lim_{\beta\to\infty}\partial f_{\rm FD}(x)/\partial x=-\delta(x-\mu)$. In this limit, we may expand $\sqrt{x}$ in a Taylor series about $\mu$,

$$\sqrt{x}=\sqrt{\mu}+\frac{x-\mu}{2\sqrt{\mu}}-\frac{(x-\mu)^2}{8\mu^{3/2}}+\ldots, \tag{B.4}$$

which on substituting in Eq. (B.3) gives

$$A\Big(2\sqrt{\mu}I_0 + \frac{1}{\beta\sqrt{\mu}}\mathcal{I}_1 - \frac{1}{4\beta^2\mu^{3/2}}\mathcal{I}_2 + \dots\Big) = 1. \tag{B.5}$$

Here,

$$\begin{aligned}
\mathcal{I}_0 &= \int_0^\infty dx\ \Big(\frac{-\partial f_{\rm FD}(x)}{\partial x}\Big) \\
&= \int_{-\beta\mu}^\infty dy\ \frac{e^y}{(1+e^y)^2} \\
&\overset{\beta\to\infty}{\longrightarrow} \int_{-\infty}^\infty dy\ \frac{e^y}{(1+e^y)^2} = 1,
\end{aligned} \tag{B.6}$$

$$\begin{aligned}
\mathcal{I}_1 &= \beta\int_0^\infty dx\ (x-\mu)\Big(\frac{-\partial f_{\rm FD}(x)}{\partial x}\Big) \\
&= \int_{-\beta\mu}^\infty dy\ \frac{ye^y}{(1+e^y)^2} \\
&\overset{\beta\to\infty}{\longrightarrow} \int_{-\infty}^\infty dy\ \frac{ye^y}{(1+e^y)^2} = 0,
\end{aligned} \tag{B.7}$$

$$\begin{aligned}
\mathcal{I}_2 &= \beta^2\int_0^\infty dx\ (x-\mu)^2\Big(\frac{-\partial f_{\rm FD}(x)}{\partial x}\Big) \\
&= \int_{-\beta\mu}^\infty dy\ \frac{y^2e^2}{(1+e^y)^2} \\
&\overset{\beta\to\infty}{\longrightarrow} \int_{-\infty}^\infty dy\ \frac{y^2e^y}{(1+e^y)^2} = \frac{\pi^2}{3}.
\end{aligned} \tag{B.8}$$

Thus, to order $1/\beta^2$, we find from Eq. (B.5) that

$$A\Big(2\sqrt{\mu} - \frac{\pi^2}{12\beta^2\mu^{3/2}}\Big) = 1, \tag{B.9}$$

which gives

$$A = \frac{1}{2\sqrt{\mu}}\Big(1 + \frac{\pi^2}{24\beta^2\mu^2}\Big). \tag{B.10}$$

Average energy: The average energy density is obtained from Eq. (??) as

$$e = A\int_{-\infty}^\infty dp\ \frac{p^2/2}{1+e^{\beta(p^2-\mu)}} + \frac{1}{2}. \tag{B.11}$$

Changing variables and doing an integration by parts, we get

$$e = \frac{A}{3}\int_0^\infty dx\ x^{3/2}\Big(\frac{-\partial f_{\rm FD}(x)}{\partial x}\Big) + \frac{1}{2}. \tag{B.12}$$

Expanding $x^{3/2}$ in a Taylor series about $\mu$ and substituting in Eq. (B.12) gives

$$\begin{aligned} e &= \frac{A}{3}\Big(\mu^{3/2}\mathcal{I}_0 + \frac{3}{2\beta}\sqrt{\mu}\mathcal{I}_1 + \frac{3}{8\beta^2\sqrt{\mu}}\mathcal{I}_2 + \dots\Big) + \frac{1}{2} \\ &= \frac{A\mu^{3/2}}{3}\Big(1 + \frac{\pi^2}{8\beta^2\mu^2}\Big) + \frac{1}{2}. \end{aligned} \tag{B.13}$$

Using Eq. (B.10), we find that to $O(1/\beta^2)$, the energy density is

$$e = \frac{\mu}{6}\Big(1 + \frac{\pi^2}{6\beta^2\mu^2}\Big) + \frac{1}{2}. \tag{B.14}$$

Dielectric function: Using Eqs. (3.7) and (2.48), we get

$$\epsilon(1,0) = 1 - A\int_0^\infty dx\ \frac{1}{\sqrt{x}}\Big(\frac{-\partial f_{\rm FD}(x)}{\partial x}\Big). \tag{B.15}$$

Expanding $1/\sqrt{x}$ in a Taylor series about $\mu$, and substituting in Eq. (B.15) gives

$$\epsilon(1,0) = 1 - A\Big(\frac{\mathcal{I}_0}{\sqrt{\mu}} - \frac{\mathcal{I}_1}{2\beta\mu^{3/2}} + \frac{3\mathcal{I}_2}{8\beta^2\mu^{5/2}} + \dots\Big), \tag{B.16}$$

so that to $O(1/\beta^2)$, we get

$$\epsilon(1,0) = 1 - \frac{1}{2\mu}\Big(1 + \frac{\pi^2}{6\beta^2\mu^2}\Big), \tag{B.17}$$

where we have used Eq. (B.10).

# Appendix C

This appendix is devoted to a discussion about some approximations that we use in the study of linear response theory of inhomogeneous states in Chapter 4.

## C.1 Asymptotic time limit of $J_\omega$

We have to evaluate the integral (4.19) in the limit $\omega \to 0$. The idea is that the limit is not trivially zero, but is determined by terms arising from any singularity in manifolds where the Liouville operator is zero.

The motion of a particle in an external potential $\psi(x)$ can be bounded or unbounded. One of the main differences between this two kind of motion comes from the spectral properties of the generator of the dynamics. For instance, the manifold in which the motion changes from bounded to unbounded could show a "zero" dynamics, i.e. the Liouville operator constrained to such manifold is strictly zero. Therefore, the limit of equation (4.19) gets a divergence on such manifolds and could introduces a new term in the eigenvalue equation. For example, the dynamics of the unperturbed HMF system is the dynamics of the pendulum which shows stable and unstable points generating the separatrix between bounded and unbounded motion. Along the separatrix the frequency of the bounded motion diverges and the Liouville operator is zero.

We have to evaluate the following integral

$$\mathcal{J}_\omega = \int dxdv f_0'(\mathcal{H}_0)\varphi(x)\frac{\omega}{\omega - \imath\mathcal{L}_0}e^{\imath kx}, \tag{C.1}$$

in the $\omega \to 0$ limit, while the operator

$$\mathcal{L}_0 g(x,v) = -v\partial_x g + m\partial_x\psi(x)\partial_v g. \tag{C.2}$$

is the Liouville operator of the unperturbed dynamics. The parameter $m$ is the size of the unperturbed mean-field potential, in analogy with the modulus of the magnetization of the HMF model. First of all, we separate the two regions of positive and negative velocities. The Liouville operator in the two regions has the symmetry property

$$\mathcal{L}_0^+ = -\mathcal{L}_0^-. \tag{C.3}$$

Let us now introduce the following transformation of coordinates

$$(x, v) \to (x, E), \qquad mE = \frac{v^2}{2} - m\psi(x). \tag{C.4}$$

The Liouville operator becomes

$$\mathcal{L}_0^+ = \sqrt{m}\sqrt{2(E+\psi)}\partial_x\psi\partial_E. \tag{C.5}$$

The integral (C.1) becomes

$$\mathcal{J}_\omega = \sqrt{m}\int dxdE \frac{f_0'(E+2\psi)}{\sqrt{2(E+\psi)}}\varphi(x)\frac{\omega^2}{\omega^2+\mathcal{L}_0^2}e^{\imath kx}. \tag{C.6}$$

The square of the operator acting on a function $g(x)$ of the spatial variable $x$ gives

$$\mathcal{L}_0 g(x) = 0, \qquad \mathcal{L}_0^2 g(x) = m(\partial_x\psi(x))^2 g(x), \tag{C.7}$$

and, consequently, the integral looses its operatorial form

$$\mathcal{J}_\omega = \sqrt{m}\int dx \frac{\varphi(x)e^{\imath kx}}{1+m\left(\frac{\partial_x\psi}{\omega}\right)^2}\int dE \frac{f_0'(m(E+2\psi))}{\sqrt{2(E+\psi)}}. \tag{C.8}$$

This integral does not depend on $\omega$ only in the manifold where the derivative of the mean-field potential $\partial_x\psi$ is zero. When the Lebesgue measure of that manifold is not zero, integral (C.1) gives a contribution to the eigenvalue equation.

For instance, in the homogeneous case the mean-field potential is zero and the integral above converges to zero in the limit of vanishing frequencies, because the manifold of vanishing mean-field force is of zero measure. This is consistent with the results shown in Chapter 4.3.

## C.2 Energy-Casimir considerations

The theory of Casimirs allows one to obtain stationary solutions of the Vlasov equation from a variational principle [31,57,82,91]. It is also useful to compare the functional form of different distributions.

Calling $c(y)$ a generic invertible and differentiable function, the Casimir functional is

$$\mathcal{C}[f] = \int c(f(x,v))dxdv, \tag{C.9}$$

The function $c$ is referred to the generator of the Casimir. The Vlasov equation describes isolated systems, therefore, it conserves both energy and mass. Thereby, it is possible to write the variational equation

$$\max_f \Big\{ \mathcal{C}[f] \Big| \int f(x,v)\mathrm{E}(x,v) = E, \int f(x,v) = 1 \Big\}, \tag{C.10}$$

and its extremal distribution

$$f(q,p) = (c')^{-1}(\sigma H(q,p)). \tag{C.11}$$

The function $c'$ is the first derivative of the function and the label $-1$ stands for the inverse. Distribution (C.11) is stationary as stated by Jeans, because it depends only on functions such as the Hamiltonian. The value of the Casimir can be written as a function of the distribution

$$\mathcal{C}[f_0] = \sigma\langle H_0\rangle_0 + \langle \int_{z^*}^{\sigma H_0} \frac{f_0(y)}{f_0(\sigma H_0)} dy\rangle_0 \tag{C.12}$$

where $f(z^*) = 0$. This variational approach, in analogy with the thermodynamic one, is related to a form of stability analysis because the solution must maximize the Casimir functional [82].

Inverting this procedure, we consider a known *initial* distribution function $f_0$ which can be generated by a Casimir with generator $c(y)$. Moreover, let us consider that the *final* state satisfies the Casimir variational principle but with a different generator $t(y)$. Linear response theory requires that in the limit of vanishing perturbation $h \to 0$ the Casimirs coincide, hence we develop the Casimir $\mathcal{T}$ around the unperturbed state $f_0$

$$\mathcal{T}[f] \to \int c(f_0) + h \int c'(f_0)\delta f + h \int g(f_0) + \mathcal{O}(h^2). \tag{C.13}$$

The function $g$ represents the variation of the generating function of the Casimir due to the perturbation. Using equation (C.11), the first part of that variation is the variation of the Hamiltonian $\int H_0 \delta f$ and it is zero when the system conserves the energy constraint. Therefore, the variation of the Casimir depends only on the function $g$, which corresponds to a variation of the generator of the Casimis induced by the perturbation. Indeed, the presence of a variation of the generator implies a different functional form of the final state compared to the initial one. The corresponding equation arising from the variational principle reads

$$\delta f c''(f_0) - \delta\sigma H_0 - \sigma\delta H - \delta M + g(f_0) = 0. \tag{C.14}$$

This equation relates the variation of the distribution function $\delta f$ to the variation of the Hamiltonian and corresponds to the Duhamel formula at infinite times.

From a numerical point of view a variation of the generator of the Casimir generator induces a variation in the value of the Casimir in time as can be easily checked.

Moreover, the variation of the energy in perturbed systems, when the perturbation is instantaneously switched on, is zero. In analogy, the variation of the generator of the Casimir is zero with perturbations instantaneously switched on.

# Bibliography


[1] Alexandre, R. . C. Villani: *On the Boltzmann equation for long-range interactions*. Communications on Pure and Applied Mathematics, 55(1):30–70, 2002.

[2] Anteneodo, C. . C. Tsallis: *Breakdown of Exponential Sensitivity to Initial Conditions: Role of the Range of Interactions*. Physical Review Letters, 80(24):5313–5316, . 1998.

[3] Antoni, M. . S. Ruffo: *Clustering and relaxation in Hamiltonian long-range dynamics*. Physical Review E, 52(3), 1995.

[4] Antoniazzi, A., F. Califano, D. Fanelli . S. Ruffo: *Exploring the Thermodynamic Limit of Hamiltonian Models: Convergence to the Vlasov Equation*. Physical Review Letters, 98(15):150602, . 2007.

[5] Antoniazzi, A., D. Fanelli, S. Ruffo . Y. Y. Yamaguchi: *Nonequilibrium Tricritical Point in a System with Long-Range Interactions*. Physical Review Letters, 99(4):040601, . 2007.

[6] Arnold, V. I.: *Mathematical Methods of Classical Mechanics*. Springer-Verlag, 1989.

[7] Baalrud, S. D., J. D. Callen . C. C. Hegna: *A kinetic equation for unstable plasmas in a finite space-time domain*. Physics of Plasmas, 15(9):092111, 2008.

[8] Bachelard, R., T. Dauxois, G. De Ninno, S. Ruffo . F. Staniscia: *Vlasov equation for long-range interactions on a lattice*. Physical Review E, 83(6):061132, . 2011.

[9] Baldovin, F., P.-H. Chavanis . E. Orlandini: *Microcanonical quasistationarity of long-range interacting systems in contact with a heat bath*. Physical Review E, 79(1):011102, . 2009.

[10] Baldovin, F. . E. Orlandini: *Hamiltonian Dynamics Reveals the Existence of Quasistationary States for Long-Range Systems in Contact with a Reservoir*. Physical Review Letters, 96(24):240602, . 2006.

[11] Balescu, R.: *Irreversible processes in ionized gases*. Physics of Fluids, (3):52, 1960.

[12] Balescu, R.: *Statistical dynamics: matter out of equilibrium*. Imperial College Press, 1997.

[13] Barré, J., F. Bouchet, T. Dauxois . S. Ruffo: *Out-of-Equilibrium States as Statistical Equilibria of an Effective Dynamics in a System with Long-Range Interactions*. Physical Review Letters, 89(11):110601, . 2002.

[14] Barré, J., A. Olivetti . Y. Y. Yamaguchi: *Dynamics of perturbations around inhomogeneous backgrounds in the HMF model*. Journal of Statistical Mechanics: Theory and Experiment, P08002, 2010.

[15] Barré, J., A. Olivetti . Y. Y. Yamaguchi: *Algebraic damping in the one-dimensional Vlasov equation*. Journal of Physics A: Mathematical and Theoretical, 44(405502):24, 2011.

[16] Benetti, F. P. D. C., T. N. Teles, R. Pakter . Y. Levin: *Ergodicity Breaking and Parametric Resonances in Systems with Long-Range Interactions*. Physical Review Letters, 108(14):140601, . 2012.

[17] Binney, J. . S. Tremaine: *Galactic dynamics*. Princeton University Press, 1987.

[18] Bogoliubov, N. N.: *Problems of a dynamical theory in statistical physics*, . Section 11. 1946.

[19] Bonifacio, R. . L. De Salvo: *Collective atomic recoil laser (CARL) optical gain without inversion by collective atomic recoil and self-bunching of two-level atoms*. Nuclear Instruments and Methods in Physics ..., 341:360–362, 1994.

[20] Bonifacio, R., C. Pellegrini . L. Narducci: *Collective instabilities and high-gain regime in a free electron laser*. Optics Communications, 50(6):373–378, 1984.

[21] Bouchet, F. . J. Barré: *Classification of phase transitions and ensemble inequivalence, in systems with long range interactions*. Journal of Statistical Physics, 118(516):1073–1105, 2005.

[22] Bouchet, F. . T. Dauxois: *Kinetics of anomalous transport and algebraic correlations in a long-range interacting system.*. Journal of Physics: Conference Series 7, . 34–47, 2005.

[23] Bouchet, F. . T. Dauxois: *Prediction of anomalous diffusion and algebraic relaxations for long-range interacting systems, using classical statistical mechanics*. Physical Review E, 72(045103 (R)), 2005.

[24] Bouchet, F. . A. Venaille: *Statistical mechanics of two-dimensional and geophysical flows*. Physics Reports, 515:227–295, 2012.

[25] Braun, W. . K. Hepp: *The Vlasov dynamics and its fluctuations in the 1/N limit of interacting classical particles*. Communication in Mathematical Physics, 56:125–146, 1977.

[26] Buyl, P. de: *Numerical resolution of the Vlasov equation for the Hamiltonian Mean-Field model*. Communications in Nonlinear Science and Numerical Simulation, 15(8):2133–2139, . 2010.

[27] Buyl, P. de, G. De Ninno, D. Fanelli, C. Nardini, A. Patelli, F. Piazza . Y. Y. Yamaguchi: *Absence of thermalization for systems with long-range interactions coupled to a thermal bath*. Physical Review E, 87(042110), . 2013.

[28] Buyl, P. de, D. Mukamel . S. Ruffo: *Self-consistent inhomogeneous steady states in Hamiltonian mean-field dynamics*. Physical Review E, 84(6):061151, . 2011.

[29] Caglioti, E. . F. Rousset: *Quasi-stationary states for particle systems in the mean-field limit*. Journal of Statistical Physics, 129:241–263, 2007.

[30] Caglioti, E. . F. Rousset: *Long Time Estimates in the Mean Field Limit*. Archive for Rational Mechanics and Analysis, 190:517–547, 2008.

[31] Campa, A. . P.-H. Chavanis: *A dynamical stability criterion for inhomogeneous quasi-stationary states in long-range systems*. Journal of Statistical Mechanics: Theory and Experiment, P06001, 2010.

[32] Campa, A., T. Dauxois . S. Ruffo: *Statistical mechanics and dynamics of solvable models with long-range interactions*. Physics Reports, 480:57–159, 2009.

[33] Campa, A., A. Giansanti . G. Morelli: *Long-time behavior of quasistationary states of the Hamiltonian mean-field model*. Physical Review E, 76(4):041117, . 2007.

[34] Chappell, W. R.: *Microscopic approach to kinetic theory*. Journal of Mathematical Physics, 8:268–305, 1967.

[35] Chavanis, P.-H.: *Hamiltonian and Brownian systems with long-range interactions: III. The BBGKY hierarchy for spatially inhomogeneous systems*. Physica A: Statistical Mechanics and its Applications, 387(4):787–805, . 2008.

[36] Chavanis, P.-H.: *Kinetic theory of spatially homogeneous systems with long-range interactions: III. Application to power-law potentials, plasmas, stellar systems, and to the HMF model*. arXiv preprint arXiv:1303.1004, . 1–25, 2013.

[37] Chavanis, P.-H.: *Linear response theory for hydrodynamic and kinetic equations with long-range interactions*. The European Physical Journal Plus, 128(4):38, . 2013.

[38] Chavanis, P.-H., F. Baldovin . E. Orlandini: *Noise-induced dynamical phase transitions in long-range systems*. Physical Review E, 83(4):040101, . 2011.

[39] Colson, W.: *Theory of a free electron laser*. Physics Letters A, 59(3):187–190, 1976.

[40] Crawford, J. D.: *Amplitude equations for electrostatic waves: Universal singular behavior in the limit of weak instability*. Physics of Plasmas, 2(1):97, 1995.

[41] Crawford, J. D. . P. D. Hislop: *Vlasov equation on a symplectic leaf*. Physics letter A, 134(1):19–24, 1988.

[42] Crawford, J. D. . P. D. Hislop: *Application of the method of spectral deformation to the Vlasov-poisson system*. Annals of Physics, 189(2):265–317, . 1989.

[43] Dauxois, T., V. Latora . A. Rapisarda: *The Hamiltonian Mean Field Model: from Dynamics to Statistical Mechanics and back*. Lecture Notes in Physics, 602:458–488, 2002.

[44] Dauxois, T., S. Ruffo, E. Arimondo . M. Wilkens: *Dynamics and Thermodynamics of Systems with Long-Range Interactions*. Springer, Lecture No ., 2002.

[45] Dawson, J. M.: *Thermal Relaxation in a One-Species, One-Dimensional Plasma*. Physics of Fluids, 7(3):419, 1964.

[46] Dobrushin, R. L.: *Vlasov equation*. Functional Analysis and Its Applications, 13(2):115–123, 1979.

[47] Dyson, F. J.: *Existence of a phase-transition in a one-dimensional Ising ferromagnet*. Communication in Mathematical Physics, 12:91–107, 1969.

[48] Elskend, Y. . D. Escande: *Microscopic dynamics of plasmas and chaos*. Series in plasma physics. Institute of Physics Publishing, 2003.

[49] Ettoumi, W. . M.-C. Firpo: *Action diffusion and lifetimes of quasistationary states in the Hamiltonian mean-field model*. Physical Review E, 87(3):030102, . 2013.

[50] Feix, M. R. . P. Bertrand: *A Universal Model: The Vlasov Equation*. Transport Theory and Statistical Physics, 34(1-2):7–62, 2005.

[51] Figueiredo, A. . R. T. Filho: *Scaling of the dynamics of homogeneous states of one-dimensional long-range interacting systems*. arXiv preprint arXiv:1305.4417v2, cond-mat.s:1–14, 2013.

[52] Fisher, M. E., S. Ma . B. G. Nickel: *Critical exponent for long-range interactions*. Physical Review Letters, 29(14):917–920, 1972.

[53] Fried, B. D. . S. D. Conte: *The Plasma Dispersion Function*. Academic Press, New York, 1961.

[54] Gabrielli, A., M. Joyce . B. Marcos: *Quasistationary states and the range of pair interactions*. Physical Review Letters, 105(210602), 2010.

[55] Heyvaerts, J.: *A Balescu-Lenard-type kinetic equation for the collisional evolution of stable self-gravitations systems*. Montly Notices of the Royal Astronomical Society, 407:355–372, 2010.

[56] Hislop, P. D. . J. D. Crawford: *Application of the method of spectral deformation to the Vlasov-Poisson system II Mathematical results*. Journal of Mathematical Physics, 30:2819–2837, 1989.

[57] Holm, D. D., J. E. Marsden, T. Ratiu . A. Weinstein: *Nonlinear stability of fluid and plasma equilibria*. Physics Reports, 2, 1984.

[58] Hubbard, J.: *Calculation of partition functions*. Physical Review Letters, 3(2):77, 1959.

[59] Inagaki S. . T. Konishi: *Dynamical stability of a simple model similar to self-gravitating systems*. Publication of the astronomical society of Japan, 45:733–635, 1993.

[60] Ivanov, A.: *Critical dynamics under the vlassov-poisson equations : critical exponents and scaling of the distribution function near the point of a marginal stability*. The Astrophysical Journal, 1:622–634, 2001.

[61] Ivanov, A. V., I. H. Cairns . P. a. Robinson: *Wave damping as a critical phenomenon*. Physics of Plasmas, 11(10):4649, 2004.

[62] Jain, K., F. Bouchet . D. Mukamel: *Relaxation times of unstable states in systems with long range interactions*. Journal of Statistical Mechanics: Theory and Experiment, 2007(11):P11008–P11008, . 2007.

[63] Jeans, J. H.: *Problems of Cosmogony and Stellar Dynamics*. Cambridge University Press, 1919.

[64] Joyce, M. . T. Worrakitpoonpon: *Quasistationary states in the self-gravitating sheet model*. Physical Review E, 84(1):011139, . 2011.

[65] Kac, M.: *On the partition function of a one-dimensional gas*. Physics of Fluids, 2(1):8–12, 1959.

[66] Kac, M., G. E. Uhlenbeck . P. C. Hemmer: *On the Van der Waals theory of the vapor-liquid equilibrium. I. Discussion of a one-dimensional model*. Journal of Mathematical Physics, 4(2):216–228, 1963.

[67] Kato, T.: *Perturbation Theory for Linear Operators*. Springer-Verlag, New York, 1980.

[68] Khintchin, A. I.: *Mathematical foundations of statistical mechanics*. Dover Publications, 1949.

[69] Kiessling, M. K.: *A complementary thermodynamic limit for classical Coulomb matter*. Journal of Statistical Physics, 59(5/6):1157–1186, 1990.

[70] Kubo, R.: *The fluctuation-dissipation theorem*. Reports on Progress in Physics, 29:255–284, 1966.

[71] Landau, L. D.: *On the vibration of the electronic plasma*. Journal of Physics USSR, 10(25):445, 1946.

[72] Landau, L. D. . E. M. Lifshitz: *Physical kinetic*, . 10 . *Course of theoretical physics*. Pergamon International Library, 1981.

[73] Lenard, A.: *On Bogoliubov's kinetic equation for a spatially homogeneous plasma*. Annals of Physics, 10(3):390–400, 1960.

[74] Liboff, R. L.: *Correlation functions in statistical mechanics and astrophysics*. Physical Review A, 39(8):4098–4102, 1989.

[75] Liboff, R. L.: *Kinetic theory: classical, quantum and relativistic descriptions, third edition*. Springer, 2003.

[76] Lynden-Bell, D.: *Statistical mechanics of violent relaxation in stellar systems*. Montly Notices of the Royal Astronomical Society, 136:101–121, 1967.

[77] Lynden-Bell, D.: *Negative specific heat in Astronomy, Physics and Chemistry*. Physica A, 263:293–304, 1999.

[78] McLachlan, R. I. . P. Atea: *The accuracy of symplectic integrators*. Nonlinearity, 5:541–562, 1992.

[79] Mori, T.: *Microcanonical analysis of exactness of the mean-field theory in long-range Interacting systems*. Journal of Statistical Physics, 147:1020–1040, 2012.

[80] Mori, T.: *Phase transitions in systems with non-additive long-range interactions*. Journal of Statistical Mechanics: Theory and Experiment, 2013(10):P10003, . 2013.

[81] Morrison, P. J.: *The Maxwell-Vlasov equations as a continuous Hamiltonian system*. Physics Letters, 80A(5,6), 1980.

[82] Morrison, P. J.: *Variational principle and stability of nonmonotonic Vlasov–Poisson equilibria*. Zeitschrift für Naturforschung, 42a:1115–1123, 1987.

[83] Mouhot, C. . C. Villani: *Landau damping*. Journal of Mathematical Physics, 51(15204), 2010.

[84] Mukamel, D., S. Ruffo . N. Schreiber: *Breaking of Ergodicity and Long Relaxation Times in Systems with Long-Range Interactions*. Physical Review Letters, 95(24):240604, . 2005.

[85] Mynick, H. E.: *The generalized Balescu-Lenard collision operator*. Journal of Plasma Physics, 39(2):303–317, 1988.

[86] Nardini, C., S. Gupta, S. Ruffo, T. Dauxois . F. Bouchet: *Kinetic theory for non-equilibrium stationary states in long-range interacting systems*. Journal of Statistical Mechanics: Theory and Experiment, L01002, 2012.

[87] Neunzert, H.: *An introduction to the nonlinear Boltzmann-Vlasov equation*. . *Kinetic Theories and the Boltzmann Equation*, . 60–110. Springer, Lecture No ., 1984.

[88] Nicholson, D. R.: *Introduction to plasma theory*. Wiley series in plasma physics. John Wiley and Sons, 1983.

[89] Niiyama, T., Y. Shimizu, T. Kobayashi, T. Okushima . K. Ikeda: *Inhomogeneity of Local Temperature in Small Clusters in Microcanonical Equilibrium*. Physical Review Letters, 99(1):014102, . 2007.

[90] Nityananda, R.: *The gravitational dynamics of galaxies*. Pramana, 73(1):193–214, . 2009.

[91] Ogawa, S.: *Spectral and formal stability criteria of spatially inhomogeneous stationary solutions to the Vlasov equation for the Hamiltonian mean-field model*. Physical Review E, 87(6):062107, . 2013.

[92] Ogawa, S., A. Patelli . Y. Y. Yamaguchi: *Non-mean-field Critical Exponent in a Mean-field Model: Dynamics versus Statistical Mechanics*. arXiv preprint arXiv:1304.2982, 1:1–5, 2013.

[93] Ogawa, S. . Y. Y. Yamaguchi: *Linear response theory in the Vlasov equation for homogeneous and for inhomogeneous quasistationary states*. Physical Review E, 85(061115), 2012.

[94] Padmanabhan, T.: *Statistical mechanics of gravitating systems*. Physics Reports, 5(5):285–362, 1990.

[95] Pakter, R. . Y. Levin: *Core-Halo Distribution in the Hamiltonian Mean-Field Model*. Physical Review Letters, 106(200603), 2011.

[96] Patelli, A., S. Gupta, C. Nardini . S. Ruffo: *Linear response theory for long-range interacting systems in quasistationary states.*. Physical Review E, 85(021133), . 2012.

[97] Patelli, A. . S. Ruffo: *Statistical mechanics and dynamics of long-range interacting systems*. Rivista di Matematica della Università di Parma, 4:345–396, 2013.

[98] Penrose, O.: *Electrostatic instability of a non-Maxwellian plasma*. Physics of Fluids, 3:258–265, 1960.

[99] Penrose, O. . J. L. Lebowitz: *Rigorous treatment of metastable states in the van der Waals-Maxwell theory*. Journal of Statistical Physics, 3(2):211–236, 1971.

[100] Reed, M. . B. Simon: *Methods of modern mathematical physics II: Fourier analysics, self-adjointness*, . 2. Academic Press, 1975.

[101] Rostoker, N. . M. N. Rosenbluth: *Test Particles in a Completely Ionized Plasma*. Physics of Fluids, 3(1):1, 1960.

[102] Rouet, J. L. . M. R. Feix: *Relaxation for one-dimensional plasma: Test particles versus global distribution behavior*. Physics of Fluids B: Plasma Physics, 3(8):1830, 1991.

[103] Ruelle, D.: *Statistical mechanics of a one-dimensional lattice gas*. Communication in Mathematical Physics, 9:267–278, 1968.

[104] Simon, A. . M. N. Rosenbluth: *Single-mode saturation of the bump-on-tail instability: Immobile ions*. Physics of Fluids, 19(10):1567, 1976.

[105] Spohn, H.: *Kinetic equations from Haniiltonian dynamics : Markovian limits*. 613(3):569–615, 1980.

[106] Spohn, H.: *On the Vlasov Hierarchy*. Mathematical Methods in the Applied Sciences, 3(1):445–455, . 1981.

[107] Springel, V., S. D. M. White, A. Jenkins, C. S. Frenk, N. Yoshida, L. Gao, J. Navarro, R. Thacker, D. Croton, J. Helly, J. a. Peacock, S. Cole, P. Thomas, H. Couchman, A. Evrard, J. Colberg . F. Pearce: *Simulations of the formation, evolution and clustering of galaxies and quasars.*. Nature, 435(7042):629–36, . 2005.

[108] Suzuki, M.: *Ergodicity, constants of motion, and bounds for susceptibilities*. Physica, 51(2):277–291, . 1971.

[109] Tabor, M. . Y. M. Treve (.): *Poisson brackets for fluids and plasmas*, . 88. AIP conference, 1982.

[110] Thiffeault, J. . P. J. Morrison: *Classification and Casimir invariants of Lie-Poisson brackets*. Physica D, 136:205–244, 2000.

[111] Touchette, H.: *When is a quantity additive, and when is it extensive?*. Physica A, 305(1-2):84–88, . 2002.

[112] Touchette, H.: *The large deviation approach to statistical mechanics*. Physics Reports, 478:1–69, 2009.

[113] Touchette, H., R. S. Ellis . B. Turkington: *An introduction to the thermodynamic and macrostate levels of nonequivalent ensembles*. Physica A: Statistical Mechanics and its Applications, 340(1-3):138–146, . 2004.

[114] Vlasov, A. A.: *On vibration properties of electron gas*. Journal of Experimental and Theoretical Physics, 8(3):291, 2938.

[115] Vollmayr-Lee, B. P. . E. Luijten: *A Kac-potential treatment of nonintegrable interactions*. Physical Review E, 63(031108), 2001.

[116] Whittaker, E. T. . G. N. Watson: *A course of modern analysis*. Cambridge University Press, Cambridge, Mathematic ., 1996.

[117] Yamaguchi, Y. Y., J. Barré, F. Bouchet, T. Dauxois . S. Ruffo: *Stability criteria of the Vlasov equation and quasi-stationary states of the HMF model*. Physica A, 337:36–66, 2004.

[118] Zanette, D. . M. Montemurro: *Dynamics and nonequilibrium states in the Hamiltonian mean-field model: A closer look*. Physical Review E, 67(3):031105, . 2003.